THE *STAPHYLOCOCCUS AUREUS* SER/THR KINASE STK1 SPECIFICALLY PHOSPHORYLATES GRAR, A TRANSCRIPTION FACTOR INVOLVED IN GLOBAL SIGNAL TRANSDUCTION

MICHAEL FRIDMAN

A THESIS SUBMITTED TO
THE FACULTY OF GRADUATE STUDIES
IN PARTIAL FULFILLMENT OF THE REQUIREMENTS
FOR THE DEGREE OF
MASTER OF SCIENCE

GRADUATE PROGRAM IN BIOLOGY
YORK UNIVERSITY
TORONTO, ONTARIO

SEPTEMBER 2013

ABSTRACT

Staphylococcus aureus coordinates gene expression at appropriate times throughout its life cycle. The work herein demonstrates *S. aureus* serine-threonine kinase (Stk1) can phosphorylate the response regulator GraR *in vitro*. Phosphorylation was confirmed by mass spectrometry and specifically occurs at the DNA-binding domain at three threonine positions: Thr128, 130 and 149. Stk1 could not phosphorylate BceR, a GraR homolog with 56% sequence similarity. We have also discovered, through *in vivo* work, novel phenotypes of an *S. aureus* Δ*graR* knockout. It is shown that GraR plays a role in proper cell growth, division and wall teichoic acid maintenance. Δ*graR* mutant complemented with ectopically expressed GraR-WT reverts phenotypes to normal, whereas GraR-D51N does not. Collectively our data suggest a novel, more global, regulatory role for the GraSR system. Understanding signaling and post-translational modification networks and their downstream effects is essential in order to rationally develop new strategies to treat *S. aureus* infections.

ACKNOWLEDGMENTS

The pursuit of greater knowledge is no solo venture. I am truly thankful to all who shaped my development both personally and academically. Often forgotten are the pioneers of the field who challenged the status quo and ventured in the face of uncertainty.

It has been a pleasure to work in the laboratory of Dr.Golemi-Kotra, where my academic roots have been established. Her door was always open, and many times led to insightful conversations where many new ideas were born. I could not have asked for a better lab, to train and grow. Thank you to my committee members, Dr. Hudak, Dr. Audette and Dr. McDermott who took the time and effort to dissect this work.

My parents, Eugene and Olga, instilled within me the aspiration to understand the world and become the best person I could possibly be. This thesis would not be possible without their love and support.

Michele, I would like to express my heartfelt gratitude for always being there, no matter the circumstance. Through it all we stand together.

An extended thank you to my friends Lorin, Endri and Sherry. To listen, drink (coffee) and console.

Anatoli, to you I dedicate this thesis.

Science, my lad, is made up of mistakes, but they are mistakes which it is useful to make, because they lead little by little to the truth.
-Jules Verne

TABLE OF CONTENTS

LIST OF TABLES

LIST OF FIGURES

Chapter one

Chapter two

Chapter three

Chapter four

LIST OF ABBREVIATIONS

Ala – Alanine
Asp – Aspartic acid
CFU – colony forming units
CRA – Congo Red agar
Da – Daltons
DTT – Dithiothreitol
FPLC – Fast protein liquid chromatography
GlcNAc – N-Acetylglucosamine
His – Histidine
IPTG – Isopropyl ß-D-thiogalactopyranoside
MES – 2-(N-morpholino)ethanesulfonic acid
MIC – Minimum inhibitory concentration
Ni-NTA – Nickel-nitrilotriacetic acid
NMR – Nuclear magnetic resonance
PASTA - Penicillin-binding protein and serine/threonine kinase associated domains
PB – Phosphorylation buffer
PBS – Phosphate buffered saline
PCR – Polymerase chain reaction
poly-RboP – polyribitol phosphate
PTM – Post-translational modification
RPM – rotations per minute
SDS – Sodium dodecyl sulfate
SDS-PAGE – Sodium dodecyl sulfate-polyacrylamide gel electrophoresis
STK – Serine/Threonine kinase
STP – Serine/Threonine phosphatase
Subsp – Subspecies
TA – teichoic acid
TCA – Trichloroacetic acid
TCS – Two-component system
TEM – Transmission electron microscopy
Thr – Threonine
TSB – Tryptic soy broth
WT – Wild type
WTA – Wall teichoic acid

CHAPTER ONE

INTRODUCTION

1.1 *Staphylococcus aureus*

1.1.1 A brief history

In 1882 the Scottish surgeon Alexander Ogston examined pus under the microscope and based on morphology termed the bacteria *Staphylococci*, which is derived from the Greek words "staphyle," meaning bunch of grapes, and "kokkos," for berry (implying round) (Ogston, 1984). Two years later the German surgeon Anton Rosenbach isolated a strain of *Staphylococci* and based on colony appearance defined its species name: *aureus*, in Latin *aurum* means gold (Baird-Parker, 1990). Taken together the name *Staphylococcus aureus* literally means "bunch of golden, round grapes," which accurately describes both morphology and appearance.

S. aureus is a Gram-positive facultative anaerobic bacterium that can survive in the presence or absence of oxygen. It is nonmotile, does not form spores and typically contains both catalase and coagulase enzymes. The catalase and coagulase tests are widely used to identify *S. aureus* and distinguish it from *Enterococci* and *Streptococci.* However, it should be stressed that *S. aureus* catalase- and coagulase- negative strains have been identified and caution should be exercised when using these tests to identify between organisms (Over et al., 2000; Thylefors et al., 1998).

1.1.2 Prevalence and pathogenesis

S. aureus is ubiquitous and can be found everywhere in nature, from soil samples to livestock. It can also be found on inanimate medical objects such as prosthetics and catheters, which is why it is one of the most common causes of nosocomial infections (Deurenberg and Stobberingh, 2008). In the context of human health it is considered an opportunistic pathogen often associated with asymptomatic colonization of skin and mucosal surfaces. Although no global statistics exist, a large-scale study in the United States from 2003 - 2004 found that 28.6 % of the population was colonized in the nose with *S. aureus* (Gorwitz et al., 2008).

In many cases pathogenesis of *S. aureus* involves colonization and local infections, resulting in mild-skin infections such as boils and pimples. However, if the bacterium gets into the blood it can cause metastatic infections resulting in life-threating complications such as meningitis, pneumonia and septic shock (Archer, 1998). This pathogen can infect nearly every organ and tissue in the body, in part due to its extensive arsenal of immune evasion molecules and virulence factors (Kobayashi and DeLeo, 2009; Liu, 2009). Surprisingly, *S. aureus* maintains fine control over these genes and regulates them as required. Although a topic of debate, a recent study proposed that *S. aureus* might be able to survive intracellularly within neutrophils, which in turn act as Trojan Horses to spread the infection into distant parts of the body (Thwaites and Gant, 2011). This work sheds light on why some cases involving persistent bacteremia are difficult to treat, despite the presence of highly active, bactericidal antibiotics.

1.2 Antibiotics and drug-resistant *Staphylococcus aureus*

1.2.1 Antibiotics

Perhaps the greatest medical advance of the past-century, and arguably the greatest of all time, was the discovery that fungi produce toxins capable of killing bacteria that cause human diseases. In the 1890's French physician Ernest Duchesne demonstrated interaction between *Penicillium glaucum*, a mold, and the common intestinal bacterium *Escherichia coli*. He also showed that rats treated with a combination of *P. glaucum* and lethal doses of *Salmonella typhi* survived. Unfortunately, the researcher himself did not, and died of tuberculosis before fully completing his research. Sir Alexnader Fleming rediscovered this phenomenon by noting that bacteria in his petri dishes would not grow properly in the vicinity of the *Penicillium* mold. He published his findings in 1929 and handed the world its first antibiotic: penicillin (Fleming, 1980).

The proceeding twenty years, referred to as "the Golden Age of antibiotic discovery," would supply modern medicine with roughly half of all the antibacterial drugs used today (Davies, 2006) and combined with increased public health measures mortality rates from infectious diseases dropped significantly. Before the introduction of antibiotics in the 1940's, the mortality rate for staphylococcal bacteremia was estimated to be 70 % (Spink, 1954). This rate dropped to 25 % as a result of penicillin. Unfortunately from the moment an antibiotic is introduced into the clinic, its usefulness lifetime begins to shorten as resistant strains arise and by 1954 mortality rates rose back

up to 45 %. In the late 1950's, methicillin, a synthetic penicillin, was introduced to treat infections caused by penicillin-resistant *S. aureus* and within only two years methicillin-resistant *S. aureus* (MRSA) strains were observed (Barber, 1961). This pattern of antibiotic introduction and resistance is demonstrated in Fig. 1.2.1.

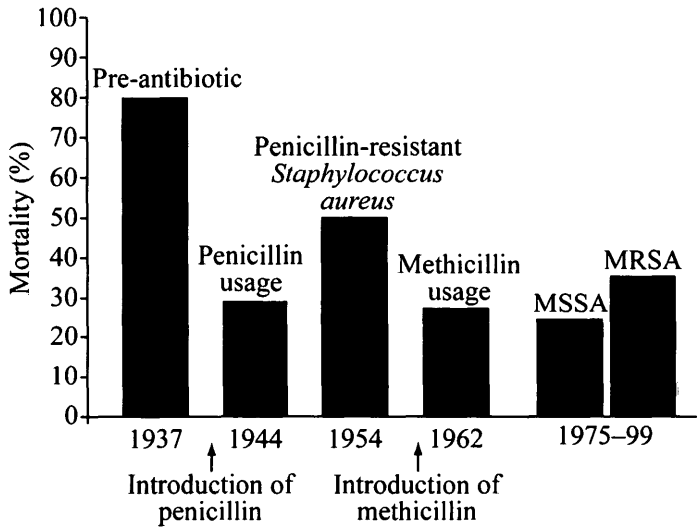

Figure 1.2.1 Mortality rates of staphylococcal bacteremia over time, adapted from (Dancer, 2008).
Despite their effectiveness, as soon as an antibiotic is introduced into the clinic its usefulness declines with time and mortality rates rise.

Antibiotics are chemical warfare agents that have been shaped through billions of years of evolution in bacteria and fungi. Therefore drug resistance is inevitable because after a billion years of making errors, most of the drug-resistant genes are out there somewhere. As a matter of fact, several years before the widespread use of penicillin as a therapeutic a group of scientists discovered a bacterial penicillinase in *E. coli* (Abraham

and Chain, 1988).

Drug resistance is not necessarily a man-made artifact. Yes, misuse and abuse of antibiotics in the clinical setting has been a catalyst in facilitating the problem, but from the start we had a grossly unfair handicap in the arms race. Bacteria can evolve as much in a day as we can in a thousand years, which means mutations within the genetic material that bestow resistance arise spontaneously. Hence the problem with drug resistance is both the emergence of new genes in old germs and the convening of old genes with new hosts.

To make matters worse the methods of discovering antibiotics are outdated and all the low-hanging fruit has already been picked, which explains why the rate of antibiotic discovery is declining (Nathan, 2004). As observed in Fig. 1.2.2 there exists an innovation gap, between the launch of quinolones in 1962 and the approval of lipopeptides in 2003, in which no new antibiotic classes made it to the clinic (Schriever et al., 2005; Walsh, 2003). There are several novel classes of antibiotics currently in human clinical trials and many more could be developed through better understanding of bacterial systems (Moir et al., 2012; Schneider and Sahl, 2010).

1.2.2 MRSA, VISA and VRSA overview

The struggle to keep MRSA infections at bay persisted beyond the 1960's. Within two decades MRSA was prevalent in hospital settings around the world (Schaefler et al., 1981) and to make matters worse this organism started to present itself in the community, termed community-associated MRSA (CA-MRSA) (Saravolatz et al., 1982a; Saravolatz

et al., 1982b). This was alarming because not only was this pathogen resistant to methicillin, but it was capable of infecting young healthy people in the community such as prisoners, athletes and those living in crowded areas with no connection to the health care setting. For example, between 1990 and 1995 the prevalence of CA-MRSA in a Chicago hospital increased from 10 to over 250 per 100,000 admissions (Herold et al., 1998).

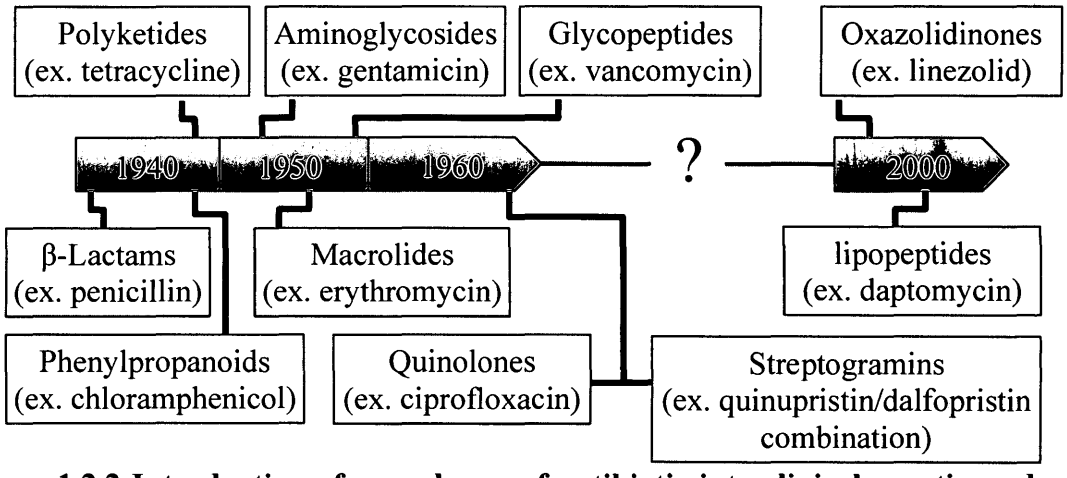

Figure 1.2.2 Introduction of new classes of antibiotic into clinical practice, adopted from (Walsh, 2003) with updated information
Note the "golden age of antibiotic discovery" between 1940 and 1960 and the innovation gap between 1960 and 2003.

Genetic analysis revealed that CA-MRSA strains, such as USA300 and USA400, contain the staphylococcal chromosomal cassette (SCC) *mec* IV that renders them resistant to beta-lactams, such as penicillin and methicillin. However, the SCC *mec* cassette found in CA-MRSA is smaller than those found in hospital-associated MRSA (HA-MRSA) and thus provides less resistance than the larger SCCs (Hiramatsu et al., 2001). But CA-MRSA tends to be more virulent than HA-MRSA and has been shown to

cause rapidly progressive, highly invasive life-threatening diseases (Adem et al., 2005; Mongkolrattanothai et al., 2003).

Almost all CA-MRSA strains carry the Panton-Valentine-Leukocidin (PVL) gene, a virulence factor that is a key differentiator between HA- and CA- MRSA strains. This gene codes for an exotoxin that causes leukocyte destruction and tissue necrosis and has been suggested to be the main player in bestowing virulence characteristics to CA-MRSA (Boyle-Vavra and Daum, 2007; Etienne, 2005).

The rise of MRSA in the 80's and 90's led to a dramatic revival of vancomycin, with a >100-fold increase occurring over the next two decades (Kirst et al., 1998). It didn't take long for *S. aureus* strains to surface with reduced susceptibility towards vancomycin and other glycopeptides. In 1996 the first MRSA strain, termed MU50, was identified in Japan (Hiramatsu et al., 1997). This strain had a vancomycin minimum inhibitory concentration (MIC) of 8 μg/mL, and thus designated as vancomycin-intermediate *S. aureus* (VISA). According to the National Committee for Clinical Laboratory Standards if an *S. aureus* strain has a vancomycin MIC $\leq$ 2μg/mL it is susceptible (VSSA), 4 – 8 μg/mL it is intermediate (VISA) and $\geq$ 16 μg/mL it is resistant (VRSA) (NCCLS, 2012). Although VISA and VRSA infections have been identified all over the world, their prevalence remains quite low (Howden et al., 2010). Nonetheless there is lingering concern that our early victories have accelerated the pace of drug resistance and the war on germs is an uphill battle in which our foes are showing strong signs of pulling ahead. Vancomycin, once considered the antibiotic of last resort, needs a

new substitute.

1.3 First line of defense: the cell wall

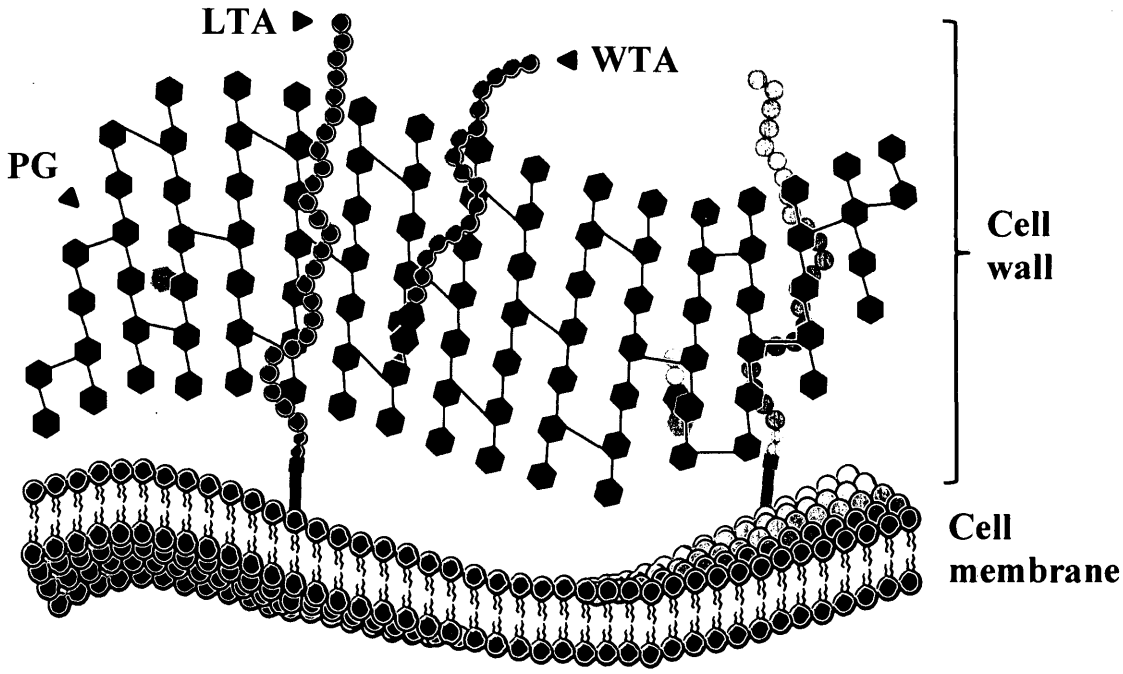

Figure 1.3.1 Diagram of the *S. aureus* cell wall
The *S. aureus* cell wall is composed of a thick, multilayered peptidoglycan (PG) on the exterior of the cytoplasm. The shorter fragments are wall teichoic acids (WTA) and are covalently embedded in peptidoglycan. The longer fragments are lipoteichoic acids (LTA) and are anchored to the cytoplasmic membrane.

The cell membrane of *S. aureus* alone is not sufficient to provide the rigidity that a free-living organism requires. A thick single layer of peptidoglycan maintains the shape and integrity of the cell, as well as provides a protective interface for interaction with the external environment (Fig. 1.3.1). It should be stressed that glycopolymers and proteins, both of which have highly variable and strain-specific roles, govern the composition of

bacterial cell walls (Clarke and Foster, 2006; Weidenmaier and Peschel, 2008). The bacterial cell wall is an ideal target for antimicrobial targets because no comparable structure exists in humans. Drugs that target these structures are typically very effective and have low toxicity.

1.3.1 Peptidoglycan and its role in MRSA, VISA and VRSA

Peptidoglycan (PG), also called murein, is composed of two alternating sugar derivatives, N-acetylglucosamine (GlcNAc) and N-acetylmuramic acid (MurNAc), linked via a β-(1-4)-glycosidic bond (Fig.1.3.2). This is the bond that lysozyme, an antimicrobial enzyme that is part of the human innate immune system, can specifically recognize and enzymatically cleave. Unfortunately *S. aureus* is extremely resistant to lysozyme because the C-6 position of every second MurNAc residue is O-acetylated (Bera et al., 2005). It has also been observed that high degree of PG cross-linking and wall teichoic acid (WTA) contributes to lysozyme resistance (Bera et al., 2007).

In *S. aureus* the MurNAc residue is attached to a peptide stem made up of $_{L}$-Ala-$_{D}$-Glu-$_{L}$-Lys-$_{D}$-Ala-$_{D}$-Ala. The terminal $_{D}$-Ala residue gets cleaved in the maturation process and the penultimate $_{D}$-Ala gets attached to an $_{L}$-Lys residue of a different MurNAc-GlcNAc unit via a pentaglycine bridge (Vollmer et al., 2008). Interestingly, this transpeptidation reaction is inhibited by β-lactam antibiotics, such as penicillin, whereby the antibiotic acts as a suicide substrate to irreversibly bind the transpeptidase active site of penicillin binding proteins. This mode of action prevents cells from forming pentaglycine bridges, which leads to loss of cell wall integrity and ultimately death. *S.*

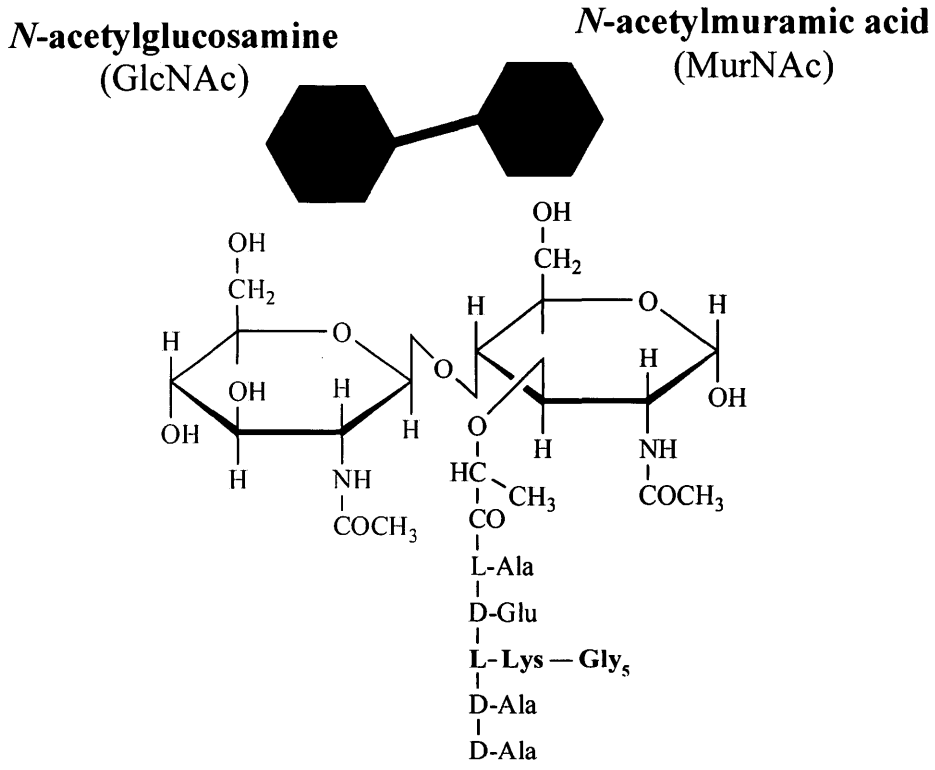

Figure 1.3.2 Chemical structure of *S. aureus* peptidoglycan
General peptidoglycan (PG) monomer composed of two sugars: N-acetylglucosamine and N-acetylmuramic acid. Polymers are linked via the pentaglycine interbridge from $_{L}$-Lys to $_{D}$-Ala. Note terminal $_{D}$-Ala gets cleaved in the mature PG.

aureus employs two β-lactam resistance mechanisms: expression of blaZ, a β-lactamase enzyme that hydrolyzes β-lactam antibiotic and PBP2a, a penicillin binding protein that has very low affinity towards β-lactams and thus its transpeptidase domain remains active. The latter is encoded by the *mecA* gene, which is part of the SCC *mec* cassette and provides resistance against all β-lactam antibiotics in MRSA strains (Katayama et al., 2000).

Another important antibiotic that acts on the cell wall biosynthesis pathway is

vancomycin. Unlike β-lactams, which bind penicillin-binding proteins and inactivate their active sites, vancomycin binds the terminal $_{D}$-Ala-$_{D}$-Ala of nascent PG precursors (Perkins, 1969; Watanakunakorn, 1984). This binding prevents access of penicillin-binding proteins to their natural substrates, and thus carboxypeptidase activity, which precedes transpeptidation, is inhibited. Although vancomycin and β-lactams have completely different substrates and modes of action the end result is the same, cells are unable to carry out cell wall synthesis.

Unlike β-lactam resistance, intermediate vancomycin resistance is not due to the acquisition of new genes but more so the gradual alteration of PG biosynthesis. Several proteins, such as the global regulator Agr (Sakoulas et al., 2005) and the two-component system VraSR (Kuroda et al., 2004), have been suggested to play an important role in resistance. Based on clinical isolates, it was observed that all VISA strains have abnormally thickened cell walls. This phenotype is suggested to be the result of increased cell wall biosynthesis (Cui et al., 2003; Hiramatsu, 2001) and/or lower degree of PG crosslinking (Sieradzki and Tomasz, 1997). Increased cell wall biosynthesis, likely due to Agr and VraSR and their corresponding genes, increases cell wall thickness and thus prevents vancomycin from reaching its target. Decreased PG crosslinking, on the other hand, leads to an increase in mature PG and thus increased $_{D}$-Ala-$_{D}$-Ala residues. Although vancomycin can bind mature $_{D}$-Ala-$_{D}$-Ala, these act as decoys to trap vancomycin and prevent it from acting on its true target. Both of these defense strategies make it difficult for vancomycin to reach terminal $_{D}$-Ala-$_{D}$-Ala of nascent PG.

VRSA strains, in addition to the above mentioned resistance mechanisms, employ yet another layer of defense against vancomycin. It should be noted that this is not a novel mechanism; high levels of vancomycin resistance were reported in 1988, in clinical isolates of *Enterococcus* species (Leclercq et al., 1988; Uttley et al., 1988). Furthermore in 1992 a British researcher demonstrated *in vitro* that vancomycin resistance can travel from *Enterococcus* to *Staphylococcus* (Noble et al., 1992). The scientific community hoped incompatibility would prevent the dreaded mating from ever occurring outside the test tube. Unfortunately in hospitals these two organisms often share close living quarters and it took only a decade for nature to reproduce the above-mentioned laboratory experiment. In 2002 the first VRSA strain was isolated with a vancomycin MIC of 1,024 μg/mL (Centers for Disease and Prevention, 2002), in comparison a VSSA has a vancomycin MIC of 1 μg/mL.

Genetic analysis revealed that VRSA strains contain an alternative pathway for nascent PG biosynthesis (Clark et al., 2005). The genes encoded in Tn1546, a transposon carried on a plasmid, replace the carboxy $_{D}$-Ala-$_{D}$-Ala of nascent PG with $_{D}$-Ala-$_{D}$-Lac. Proper binding is facilitated by hydrogen bonds between vancomycin and $_{D}$-Ala-$_{D}$-Ala; however, altering the structure to $_{D}$-Ala-$_{D}$-Lac prevents the substrate from fitting in the binding pocket of vancomycin. The analogy most often mentioned is that of a lock and key, where the lock, or the substrate, is altered so the key, vancomycin, no longer fits. Affinity of vancomycin to $_{D}$-Ala-$_{D}$-Lac is decreased by a factor of 1000 (Bugg et al., 1991). There are other mechanisms by which the cell wall, specifically PG, contributes to

antibiotic resistance. But due to the clinical relevance of MRSA, specifically CA-MRSA, and VISA/VRSA much attention has been focused on β-lactams and glycopeptides.

1.3.2 Teichoic acids

The *S. aureus* cell wall consists of two structural components: peptidoglycan, described above, and cell wall glycopolymers. These glycopolymers will be referred to as wall teichoic acids (WTA) (Fig.1.3.3A), those covalently attached to PG, and lipoteichoic acids (LTA) (Fig 1.3.3B), which are anchored to the cytoplasmic membrane. WTAs are attached to MurNAc of the PG backbone via a linkage unit consisting of GlcNAc, MurNAc and two or three glycerolphosphate residues. The WTA repeating unit is composed of ribitolphosphate (RboP) that differs profoundly in length between subspecies and even individual strains, and has been shown to reach lengths of up to 40 repeating units (Endl et al., 1983). LTAs are attached to the cytoplasmic membrane by a diacylglycerol, which itself is attached to a disaccharide. The LTA repeating unit is composed of glycerolphosphate and is on average ~23 units in length (Fischer, 1994).

Previous studies have shown that WTA (Weidenmaier et al., 2004) is dispensable for viability whereas LTA is not (Grundling and Schneewind, 2007). An important modification of teichoic acids, which occurs in almost all strains, is the incorporation of $_{D}$-Ala. It should be noted that WTA Poly-RboP, in addition to $_{D}$-alanylation, can also be glycosylated with either α- or β- GlcNAc. Work by Brown *et al.* has demonstrated that glycosylation may be a contributor to methicillin resistance (Brown et al., 2012).

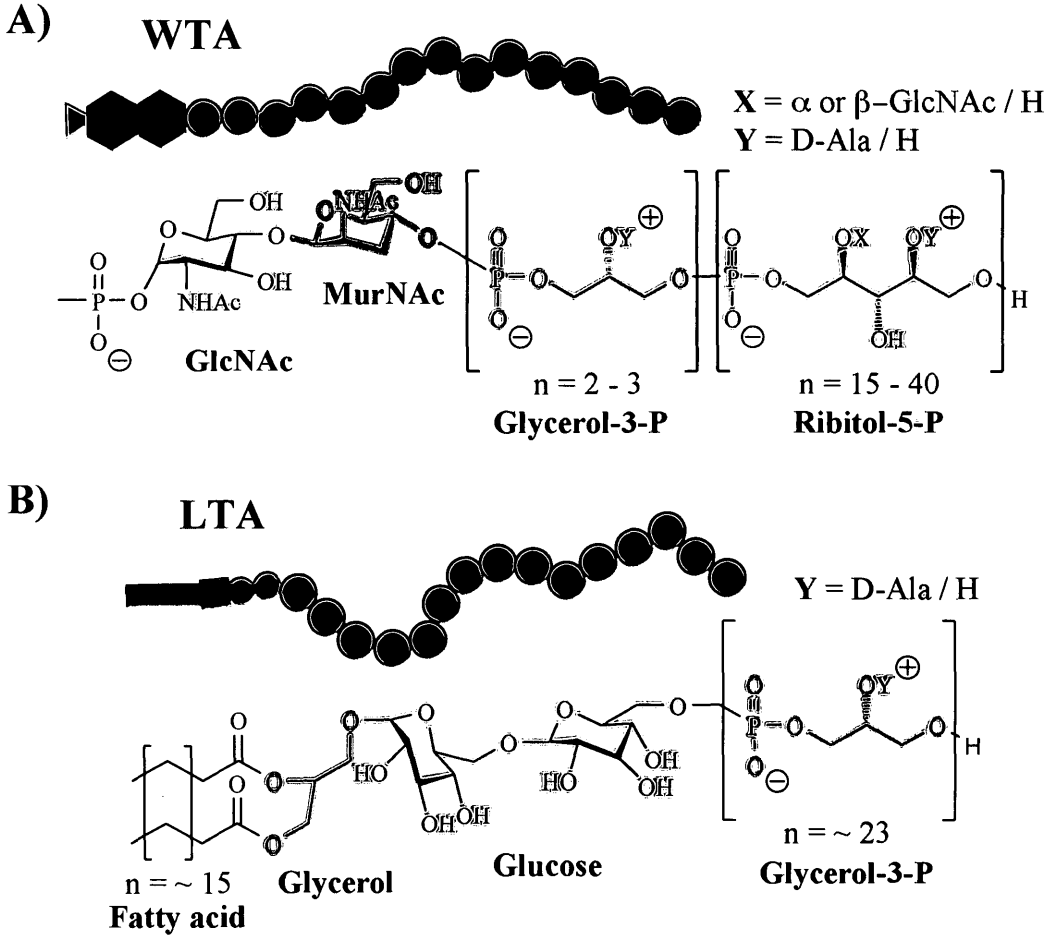

Figure 1.3.3 Chemical structure of *S. aureus* teichoic acids
A) Wall teichoic acid (WTA) linkage unit is composed of N-acetylglucosamine (GlcNAc) and N-acetylmuramic acid (MurNAc) followed by two to three D-alanylated glycerol phosphate residues. The WTA backbone on average ranges from 15 - 40 units of ribitol phosphates (substituted with D-Ala and/or α- or β- GlcNAc). B) Lipoteichoic acid (LTA) linkage unit is composed of a diacylglycerol connected to disaccharide. The LTA backbone on average is ~23 units of glycerolphosphates (substituted mainly with D-Ala).

Glycosylation of WTA is an emerging field and it remains to be seen what the physiological relevance is. Thus the remainder of this discussion will focus on D-alanylation of teichoic acids, which has been extensively studied and reviewed

(Weidenmaier and Peschel, 2008).

Teichoic acid net charge is profoundly altered when D-Ala groups are attached, resulting in a more positive charge (Neuhaus and Baddiley, 2003). This is especially important because the majority of antimicrobial molecules the cell encounters are positively charged and thus D-Ala decoration can repel these molecules. Accordingly, lack of D-alanylation has been shown to sensitize *S. aureus* towards antimicrobial peptides (Peschel et al., 1999). Furthermore, this modification has been implicated in adherence to host cells (Weidenmaier et al., 2005), biofilm formation (Gross et al., 2001), regulation of autolysis (Peschel et al., 2000) and cell growth (Tabuchi et al., 2010).

The *dltABCD* genes, constituting the *dlt* operon, are responsible for D-Ala incorporation into WTA and LTA. This operon is exclusively under the regulation of the two-component system GraSR, also known as ApsSR (Li et al., 2007). It is beyond the scope of this work to go into detail regarding the specific genes and subsequent biosynthesis pathways of teichoic acids and their corresponding modifications. It is, however, important to understand that *S. aureus* commits vast amounts of genetic information, resources and energy to synthesize and maintain teichoic acids and their corresponding modifications. Given the importance of teichoic acids they remain a lucrative target for future drug development.

1.4 Two-component systems

S. aureus is able to adapt quickly to changes in its immediate environment, such

as variations in nutrient availability, osmolality, pH, temperature and antibiotic presence. Signal transduction mechanisms are responsible for sensing and responding to the above changes in the form of differential gene expression. In *S. aureus*, and many other prokaryotic organisms, this is accomplished by two-component systems (TCS), also known as sensor kinase/response regulator systems. A typical TCS is made up of a histidine kinase, a cytoplasmic membrane protein capable of autophosphorylation (at a histidine residue) following an external stimulus and a response regulator protein that is capable of receiving this "message" in the form of phosphorylation (at an aspartic acid residue) and conveying it in the form of gene regulation (Stock et al., 2000). For a more up-to-date review of the field refer to the following papers (Capra and Laub, 2012; Casino et al., 2010; Laub and Goulian, 2007).

According to the latest Microbial Signal Transduction database, MiST 2.1, in 1,420 completed genomes analyzed to date, approximately 87,173 genes encode for TCS (Ulrich and Zhulin, 2010). The number and function of TCSs differs enormously from species to species, and this is likely the result of adaptation to the many environmental niches bacteria inhabit. According to MiST 2.1 there are 16 classical TCSs systems in the *S. aureus* 8325 genome and 17 in the MRSA strain MU50. Some of these TCSs have been extensively studied and well characterized, such as VraSR (Belcheva and Golemi-Kotra, 2008), WalKR (Dubrac et al., 2008) and GraSR (Falord et al., 2012). Others are hypothetical and remain to be investigated. Given the proceeding chapters focus on the response regulator GraR, a brief introduction to the GraSR TCS will be presented.

1.4.1 The GraSR two-component system

The GraSR, glycopeptide resistance associated, system is made up of GraS, the histidine kinase, and the response regulator GraR. In the literature this system was originally termed ApsSR, for antimicrobial peptide sensor (Li et al., 2007) based on homology with *Staphylococcus epidermidis*, but later renamed to GraSR. The GraS protein is presumed to function as a sensor kinase that possess a short-terminal sensing domain, and two transmembrane helices separated by a short loop that is buried in the cytoplasmic membrane. GraR, on the other hand, belongs to the OmpR subfamily of response regulators, which are categorized by a unique C-terminal winged helix-turn-helix domain (Martinez-Hackert and Stock, 1997).

It is presumed that GraS, following autophosphorylation, is capable of phosphorylating the aspartic acid residue at position 51 of the cognate response regulator GraR. Phosphorylation of GraR likely alters its binding affinity to DNA through conformational changes within the protein (Johnson and Barford, 1993). Neither phosphorylation of GraR nor DNA-binding has been reported *in vitro.* However, through microarray analysis and *in vivo* examination of knockout strains it was determined that GraSR regulates *mprF*, *vraFG* and the *dlt* operon (Cui et al., 2005; Falord et al., 2011).

In section 1.3.2 it was demonstrated that regulation of the *dlt* operon, by GraSR, is responsible for $_{D}$-alanylation of TAs that maintains an overall positive surface charge to repel antimicrobials. The *mprF* gene is a lysyl-phosphatidylglycerol synthase that also contributes to an overall positive surface charge by adding lysine to phosphatidylglycerol

within the cell membrane (Oku et al., 2004). The *VraFG* genes code for an ABC transporter, which is suggested to sense antimicrobial peptides, however characterization of this system is in its infancy (Falord et al., 2012). Numerous studies have observed that point mutations within the GraSR system can lead to VISA and VRSA phenotypes (Cui et al., 2009; Neoh et al., 2008; Yoo et al., 2013), which is likely explained through increased expression of *mprF* and *dlt* operon.

Despite the importance of GraSR in conferring resistance to antimicrobial peptides, a recent study has suggests a more global role for this system that is not limited to the expression *mprF*, *vraFG* and the *dlt* operon (Falord et al., 2011). Microarray analysis revealed that 424 genes are differentially expressed in the *S. aureus* Δ*graSR* mutant strain. Furthermore *in silico* genome scanning uncovered 26 novel potential GraR-binding sites. Taken together this study demonstrates for the first time novel links to the virulence, stress response and cell wall signal transduction pathways (Falord et al., 2011).

1.5 Signal transduction by Ser/Thr protein kinases

It was previously assumed that Ser/Thr kinases (STKs) were exclusive to eukaryotic systems and the predominant signaling pathways in prokaryotes were those of TCSs. However, in the 90's the first prokaryotic Ser/Thr kinase was discovered in *Myxocuccus xanthus* (Munoz-Dorado et al., 1991; Zhang et al., 1992). In the following two decades it became obvious that Ser/Thr kinases are key players in bacterial signal transduction, and was summarized well by the title: "No longer an **exclusive club**:

eukaryotic signalling domains in bacteria" (Bakal and Davies, 2000), which also happens to be an excellent review paper. For an up-to-date review the reader is advised to consult the following papers (Burnside and Rajagopal, 2012; Pereira et al., 2011). A recent Global Ocean Sampling dataset, led by the J. Craig Venter, reveled that Ser/Thr kinases are just as ubiquitous as histidine kinases and may be equally important in regulating prokaryotic behavior (Kannan et al., 2007).

1.5.1 *S. aureus* Ser/Thr Kinase and Phosphatase

The *S. aureus* genome contains one major Ser/Thr kinase and phosphatase, termed Stk1 and Stp1, respectively. These proteins are cotranscribed and thus work together to regulate substrates (Beltramini et al., 2009). It should be noted that a subset of MRSA strains, such as MU50, MW2 and N315, contain a soluble Ser/Thr kinase, termed Stk2. To date the function of Stk2 is unknown. Stk1 is a transmembrane protein that contains three repeating penicillin-binding protein and serine/threonine kinase associated domains (PASTA) at the extracellular surface and a cytoplasmic kinase domain (A schematic is presented in Section 2.1, Fig. 2.1.1). The intracellular kinase domain belongs to the Hanks-type structural family of kinases first descried in eukaryotes (Hanks et al., 1988), which is why prokaryotic STKs are sometimes referred to as "eukaryotic-like." The structure of the Stk1 kinase domain was recently solved, unfortunately the protein crystalized in an inactive form, autoinhibited state (Rakette et al., 2012). The three-dimensional structure of the PASTA domains was also solved (Paracuellos et al., 2010; Ruggiero et al., 2011) and studies suggest these domains may bind PG (Shah et al., 2008;

Squeglia et al., 2011).

It is yet unknown which molecules activate Stk1 and whether these interactions facilitate autophosphorylation. However, in *B. subtilis* it was demonstrated PrkC, a homologue of Stk1, contains an arginine residue in the PASTA domain capable of interacting with the negatively charged *meso*-diaminopimelic acid (DAP) side chain of PG (Squeglia et al., 2011). The PG of *S. aureus* is Lys-type, and is unable to bind to the PrkC PASTA domain, vice versa the DAP-type PG cannot bind Stk1 PASTA domain (Shah et al., 2008). It is suggested that throughout bacterial evolution and divergence the STK proteins were conserved but acquired new roles depending on, for example, the physical environment or niche the organism inhabited.

Although the stimuli sensed by Stk1 are almost completely unknown, a number of phosphorylation targets have been identified. Known substrates of Stk1 to date include SarA (Didier et al., 2010; Sun et al., 2012), MgrA (Truong-Bolduc et al., 2008), LuxS (Cluzel et al., 2010), PurA (Donat et al., 2009), CcpA (Leiba et al., 2012), enzymes of the central metabolism (Lomas-Lopez et al., 2007) and a human transcription factor (Miller et al., 2010). Along with *in vivo* studies Stk1/Stp1 are suggested to be important in growth, virulence, antibiotic resistance and secondary metabolite production through the phosphorylation of the above-mentioned, and yet to be determined, substrates. This central role makes Stk1 a suitable target for future drug development.

1.6 Aims of this work

In the context of human health pathogenic bacteria with antibiotic resistance are a public threat. There is a challenge to develop safe drugs that target bacterial pathways and not those of the host organism. Therefore identifying targets such as Stk1, and understanding their biological roles, is essential for the development of novel antibacterial molecules. Whether these are essential targets of the bacteria or not, the combination of a number of drugs can act synergistically to decrease virulence and fundamental processes with a lower chance of developing resistance.

Hence the aim of this work was to biochemically characterize Stk1 and its cognate Stp1 partner *in vitro* with an emphasis on discovering novel phosphorylation targets. The second part focused on translating our findings *in vivo*. The third part of this work questions whether GraR-regulated genes are solely responsible for antimicrobial peptide resistance, or whether these genes are simply required for proper cell function and as a byproduct are able to confer resistance? For example, GraSR regulates many genes, some of which make the overall surface charge positive. But is positive surface charge only elicited in the presence of antimicrobial peptides or is surface charge an intrinsic mechanism that governs the normal activity of proteins and other factors? It will be argued that GraSR in fact plays a global role in the cell, and some of the genes previously believed to be responsible for antimicrobial peptide resistance are required under non-stress conditions for proper cell function.

References

Abraham, E.P., and Chain, E. (1988). An enzyme from bacteria able to destroy penicillin. 1940. Rev Infect Dis *10*, 677-678.

Adem, P.V., Montgomery, C.P., Husain, A.N., Koogler, T.K., Arangelovich, V., Humilier, M., Boyle-Vavra, S., and Daum, R.S. (2005). Staphylococcus aureus sepsis and the Waterhouse-Friderichsen syndrome in children. N Engl J Med *353*, 1245-1251.

Archer, G.L. (1998). Staphylococcus aureus: a well-armed pathogen. Clin Infect Dis *26*, 1179-1181.

Baird-Parker, A.C. (1990). The staphylococci: an introduction. Soc Appl Bacteriol Symp Ser *19*, 1S-8S.

Bakal, C.J., and Davies, J.E. (2000). No longer an exclusive club: eukaryotic signalling domains in bacteria. Trends Cell Biol *10*, 32-38.

Barber, M. (1961). Methicillin-resistant staphylococci. J Clin Pathol *14*, 385-393.

Belcheva, A., and Golemi-Kotra, D. (2008). A close-up view of the VraSR two-component system. A mediator of Staphylococcus aureus response to cell wall damage. J Biol Chem *283*, 12354-12364.

Beltramini, A.M., Mukhopadhyay, C.D., and Pancholi, V. (2009). Modulation of cell wall structure and antimicrobial susceptibility by a Staphylococcus aureus eukaryote-like serine/threonine kinase and phosphatase. Infect Immun *77*, 1406-1416.

Bera, A., Biswas, R., Herbert, S., Kulauzovic, E., Weidenmaier, C., Peschel, A., and Gotz, F. (2007). Influence of wall teichoic acid on lysozyme resistance in Staphylococcus aureus. J Bacteriol *189*, 280-283.

Bera, A., Herbert, S., Jakob, A., Vollmer, W., and Gotz, F. (2005). Why are pathogenic staphylococci so lysozyme resistant? The peptidoglycan O-acetyltransferase OatA is the major determinant for lysozyme resistance of Staphylococcus aureus. Mol Microbiol *55*, 778-787.

Boyle-Vavra, S., and Daum, R.S. (2007). Community-acquired methicillin-resistant Staphylococcus aureus: the role of Panton-Valentine leukocidin. Lab Invest *87*, 3-9.

Brown, S., Xia, G., Luhachack, L.G., Campbell, J., Meredith, T.C., Chen, C., Winstel, V., Gekeler, C., Irazoqui, J.E., Peschel, A., *et al.* (2012). Methicillin resistance in Staphylococcus aureus requires glycosylated wall teichoic acids. Proc Natl Acad Sci U S A *109*, 18909-18914.

Bugg, T.D., Wright, G.D., Dutka-Malen, S., Arthur, M., Courvalin, P., and Walsh, C.T. (1991). Molecular basis for vancomycin resistance in Enterococcus faecium BM4147: biosynthesis of a depsipeptide peptidoglycan precursor by vancomycin resistance proteins VanH and VanA. Biochemistry *30*, 10408-10415.

Burnside, K., and Rajagopal, L. (2012). Regulation of prokaryotic gene expression by eukaryotic-like enzymes. Curr Opin Microbiol *15*, 125-131.

Capra, E.J., and Laub, M.T. (2012). Evolution of two-component signal transduction systems. Annu Rev Microbiol *66*, 325-347.

Casino, P., Rubio, V., and Marina, A. (2010). The mechanism of signal transduction by two-component systems. Curr Opin Struct Biol *20*, 763-771.

Centers for Disease, C., and Prevention (2002). Staphylococcus aureus resistant to vancomycin--United States, 2002. MMWR Morb Mortal Wkly Rep *51*, 565-567.

Clark, N.C., Weigel, L.M., Patel, J.B., and Tenover, F.C. (2005). Comparison of Tn1546-like elements in vancomycin-resistant Staphylococcus aureus isolates from Michigan and Pennsylvania. Antimicrob Agents Chemother *49*, 470-472.

Clarke, S.R., and Foster, S.J. (2006). Surface adhesins of Staphylococcus aureus. Adv Microb Physiol *51*, 187-224.

Cluzel, M.E., Zanella-Cleon, I., Cozzone, A.J., Futterer, K., Duclos, B., and Molle, V. (2010). The Staphylococcus aureus autoinducer-2 synthase LuxS is regulated by Ser/Thr phosphorylation. J Bacteriol *192*, 6295-6301.

Cui, L., Lian, J.Q., Neoh, H.M., Reyes, E., and Hiramatsu, K. (2005). DNA microarray-based identification of genes associated with glycopeptide resistance in Staphylococcus aureus. Antimicrob Agents Chemother *49*, 3404-3413.

Cui, L., Ma, X., Sato, K., Okuma, K., Tenover, F.C., Mamizuka, E.M., Gemmell, C.G., Kim, M.N., Ploy, M.C., El-Solh, N., *et al.* (2003). Cell wall thickening is a common feature of vancomycin resistance in Staphylococcus aureus. J Clin Microbiol *41*, 5-14.

Cui, L., Neoh, H.M., Shoji, M., and Hiramatsu, K. (2009). Contribution of vraSR and graSR point mutations to vancomycin resistance in vancomycin-intermediate Staphylococcus aureus. Antimicrob Agents Chemother *53*, 1231-1234.

Dancer, S.J. (2008). The effect of antibiotics on methicillin-resistant Staphylococcus aureus. J Antimicrob Chemother *61*, 246-253.

Davies, J. (2006). Where have All the Antibiotics Gone? Can J Infect Dis Med Microbiol *17*, 287-290.

Deurenberg, R.H., and Stobberingh, E.E. (2008). The evolution of Staphylococcus aureus. Infect Genet Evol *8*, 747-763.

Didier, J.P., Cozzone, A.J., and Duclos, B. (2010). Phosphorylation of the virulence regulator SarA modulates its ability to bind DNA in Staphylococcus aureus. FEMS Microbiol Lett *306*, 30-36.

Donat, S., Streker, K., Schirmeister, T., Rakette, S., Stehle, T., Liebeke, M., Lalk, M., and Ohlsen, K. (2009). Transcriptome and functional analysis of the eukaryotic-type serine/threonine kinase PknB in Staphylococcus aureus. J Bacteriol *191*, 4056-4069.

Dubrac, S., Bisicchia, P., Devine, K.M., and Msadek, T. (2008). A matter of life and death: cell wall homeostasis and the WalKR (YycGF) essential signal transduction pathway. Mol Microbiol *70*, 1307-1322.

Endl, J., Seidl, H.P., Fiedler, F., and Schleifer, K.H. (1983). Chemical composition and structure of cell wall teichoic acids of staphylococci. Arch Microbiol *135*, 215-223.

Etienne, J. (2005). Panton-Valentine leukocidin: a marker of severity for Staphylococcus aureus infection? Clin Infect Dis *41*, 591-593.

Falord, M., Karimova, G., Hiron, A., and Msadek, T. (2012). GraXSR proteins interact with the VraFG ABC transporter to form a five-component system required for cationic antimicrobial peptide sensing and resistance in Staphylococcus aureus. Antimicrob Agents Chemother *56*, 1047-1058.

Falord, M., Mader, U., Hiron, A., Debarbouille, M., and Msadek, T. (2011). Investigation of the Staphylococcus aureus GraSR regulon reveals novel links to virulence, stress response and cell wall signal transduction pathways. PLoS One *6*, e21323.

Fischer, W. (1994). Lipoteichoic acid and lipids in the membrane of Staphylococcus aureus. Med Microbiol Immunol *183*, 61-76.

Fleming, A. (1980). Classics in infectious diseases: on the antibacterial action of cultures of a penicillium, with special reference to their use in the isolation of B. influenzae by Alexander Fleming, Reprinted from the British Journal of Experimental Pathology 10:226-236, 1929. Rev Infect Dis *2*, 129-139.

Gorwitz, R.J., Kruszon-Moran, D., McAllister, S.K., McQuillan, G., McDougal, L.K., Fosheim, G.E., Jensen, B.J., Killgore, G., Tenover, F.C., and Kuehnert, M.J. (2008). Changes in the prevalence of nasal colonization with Staphylococcus aureus in the United States, 2001-2004. J Infect Dis *197*, 1226-1234.

Gross, M., Cramton, S.E., Gotz, F., and Peschel, A. (2001). Key role of teichoic acid net charge in Staphylococcus aureus colonization of artificial surfaces. Infect Immun *69*, 3423-3426.

Grundling, A., and Schneewind, O. (2007). Synthesis of glycerol phosphate lipoteichoic acid in Staphylococcus aureus. Proc Natl Acad Sci U S A *104*, 8478-8483.

Hanks, S.K., Quinn, A.M., and Hunter, T. (1988). The protein kinase family: conserved features and deduced phylogeny of the catalytic domains. Science *241*, 42-52.

Herold, B.C., Immergluck, L.C., Maranan, M.C., Lauderdale, D.S., Gaskin, R.E., Boyle-Vavra, S., Leitch, C.D., and Daum, R.S. (1998). Community-acquired methicillin-resistant Staphylococcus aureus in children with no identified predisposing risk. JAMA *279*, 593-598.

Hiramatsu, K. (2001). Vancomycin-resistant Staphylococcus aureus: a new model of antibiotic resistance. Lancet Infect Dis *1*, 147-155.

Hiramatsu, K., Cui, L., Kuroda, M., and Ito, T. (2001). The emergence and evolution of methicillin-resistant Staphylococcus aureus. Trends Microbiol *9*, 486-493.

Hiramatsu, K., Hanaki, H., Ino, T., Yabuta, K., Oguri, T., and Tenover, F.C. (1997). Methicillin-resistant Staphylococcus aureus clinical strain with reduced vancomycin susceptibility. J Antimicrob Chemother *40*, 135-136.

Howden, B.P., Davies, J.K., Johnson, P.D., Stinear, T.P., and Grayson, M.L. (2010). Reduced vancomycin susceptibility in Staphylococcus aureus, including vancomycin-intermediate and heterogeneous vancomycin-intermediate strains: resistance mechanisms, laboratory detection, and clinical implications. Clin Microbiol Rev *23*, 99-139.

Johnson, L.N., and Barford, D. (1993). The effects of phosphorylation on the structure and function of proteins. Annu Rev Biophys Biomol Struct *22*, 199-232.

Kannan, N., Taylor, S.S., Zhai, Y., Venter, J.C., and Manning, G. (2007). Structural and functional diversity of the microbial kinome. PLoS Biol *5*, e17.

Katayama, Y., Ito, T., and Hiramatsu, K. (2000). A new class of genetic element, staphylococcus cassette chromosome mec, encodes methicillin resistance in Staphylococcus aureus. Antimicrob Agents Chemother *44*, 1549-1555.

Kirst, H.A., Thompson, D.G., and Nicas, T.I. (1998). Historical yearly usage of vancomycin. Antimicrob Agents Chemother *42*, 1303-1304.

Kobayashi, S.D., and DeLeo, F.R. (2009). An update on community-associated MRSA virulence. Curr Opin Pharmacol *9*, 545-551.

Kuroda, M., Kuroda, H., Oshima, T., Takeuchi, F., Mori, H., and Hiramatsu, K. (2004). Two-component system VraSR positively modulates the regulation of cell-wall biosynthesis pathway in Staphylococcus aureus. Molecular Microbiology *49*, 807-821.

Laub, M.T., and Goulian, M. (2007). Specificity in two-component signal transduction pathways. Annu Rev Genet *41*, 121-145.

Leclercq, R., Derlot, E., Duval, J., and Courvalin, P. (1988). Plasmid-mediated resistance to vancomycin and teicoplanin in Enterococcus faecium. N Engl J Med *319*, 157-161.

Leiba, J., Hartmann, T., Cluzel, M.E., Cohen-Gonsaud, M., Delolme, F., Bischoff, M., and Molle, V. (2012). A Novel Mode of Regulation of the Staphylococcus aureus Catabolite Control Protein A (CcpA) Mediated by Stk1 Protein Phosphorylation. J Biol Chem *287*, 43607-43619.

Li, M., Cha, D.J., Lai, Y., Villaruz, A.E., Sturdevant, D.E., and Otto, M. (2007). The antimicrobial peptide-sensing system aps of Staphylococcus aureus. Mol Microbiol *66*, 1136-1147.

Liu, G.Y. (2009). Molecular pathogenesis of Staphylococcus aureus infection. Pediatr Res *65*, 71R-77R.

Lomas-Lopez, R., Paracuellos, P., Riberty, M., Cozzone, A.J., and Duclos, B. (2007). Several enzymes of the central metabolism are phosphorylated in Staphylococcus aureus. FEMS Microbiol Lett *272*, 35-42.

Martinez-Hackert, E., and Stock, A.M. (1997). Structural relationships in the OmpR family of winged-helix transcription factors. J Mol Biol *269*, 301-312.

Miller, M., Donat, S., Rakette, S., Stehle, T., Kouwen, T.R., Diks, S.H., Dreisbach, A., Reilman, E., Gronau, K., Becher, D., *et al.* (2010). Staphylococcal PknB as the first prokaryotic representative of the proline-directed kinases. PLoS One *5*, e9057.

Moir, D.T., Opperman, T.J., Butler, M.M., and Bowlin, T.L. (2012). New classes of antibiotics. Curr Opin Pharmacol *12*, 535-544.

Mongkolrattanothai, K., Boyle, S., Kahana, M.D., and Daum, R.S. (2003). Severe Staphylococcus aureus infections caused by clonally related community-acquired methicillin-susceptible and methicillin-resistant isolates. Clin Infect Dis *37*, 1050-1058.

Munoz-Dorado, J., Inouye, S., and Inouye, M. (1991). A gene encoding a protein serine/threonine kinase is required for normal development of M. xanthus, a gram-negative bacterium. Cell *67*, 995-1006.

Nathan, C. (2004). Antibiotics at the crossroads. Nature *431*, 899-902.

NCCLS (2012). Performance standards for antimicrobial susceptibility testing; Twenty-Second Informational Supplement M100-S22. The National Committee for Clinical Laboratory Standards *32:3*.

Neoh, H.M., Cui, L., Yuzawa, H., Takeuchi, F., Matsuo, M., and Hiramatsu, K. (2008). Mutated response regulator graR is responsible for phenotypic conversion of Staphylococcus aureus from heterogeneous vancomycin-intermediate resistance to vancomycin-intermediate resistance. Antimicrob Agents Chemother *52*, 45-53.

Neuhaus, F.C., and Baddiley, J. (2003). A continuum of anionic charge: structures and functions of D-alanyl-teichoic acids in gram-positive bacteria. Microbiol Mol Biol Rev *67*, 686-723.

Noble, W.C., Virani, Z., and Cree, R.G. (1992). Co-transfer of vancomycin and other resistance genes from Enterococcus faecalis NCTC 12201 to Staphylococcus aureus. FEMS Microbiol Lett *72*, 195-198.

Ogston, A. (1984). Classics in infectious diseases. "On abscesses". Alexander Ogston (1844-1929). Rev Infect Dis *6*, 122-128.

Oku, Y., Kurokawa, K., Ichihashi, N., and Sekimizu, K. (2004). Characterization of the Staphylococcus aureus mprF gene, involved in lysinylation of phosphatidylglycerol. Microbiology *150*, 45-51.

Over, U., Tuc, Y., and Soyletir, G. (2000). Catalase-negative Staphylococcus aureus: a rare isolate of human infection. Clin Microbiol Infect *6*, 681-682.

Paracuellos, P., Ballandras, A., Robert, X., Kahn, R., Herve, M., Mengin-Lecreulx, D., Cozzone, A.J., Duclos, B., and Gouet, P. (2010). The extended conformation of the 2.9-A crystal structure of the three-PASTA domain of a Ser/Thr kinase from the human pathogen Staphylococcus aureus. J Mol Biol *404*, 847-858.

Pereira, S.F., Goss, L., and Dworkin, J. (2011). Eukaryote-like serine/threonine kinases and phosphatases in bacteria. Microbiol Mol Biol Rev *75*, 192-212.

Perkins, H.R. (1969). Specificity of combination between mucopeptide precursors and vancomycin or ristocetin. Biochem J *111*, 195-205.

Peschel, A., Otto, M., Jack, R.W., Kalbacher, H., Jung, G., and Gotz, F. (1999). Inactivation of the dlt operon in Staphylococcus aureus confers sensitivity to defensins, protegrins, and other antimicrobial peptides. J Biol Chem *274*, 8405-8410.

Peschel, A., Vuong, C., Otto, M., and Gotz, F. (2000). The D-alanine residues of Staphylococcus aureus teichoic acids alter the susceptibility to vancomycin and the activity of autolytic enzymes. Antimicrob Agents Chemother *44*, 2845-2847.

Rakette, S., Donat, S., Ohlsen, K., and Stehle, T. (2012). Structural analysis of Staphylococcus aureus serine/threonine kinase PknB. PLoS One *7*, e39136.

Ruggiero, A., Squeglia, F., Marasco, D., Marchetti, R., Molinaro, A., and Berisio, R. (2011). X-ray structural studies of the entire extracellular region of the serine/threonine kinase PrkC from Staphylococcus aureus. Biochem J *435*, 33-41.

Sakoulas, G., Eliopoulos, G.M., Fowler, V.G., Jr., Moellering, R.C., Jr., Novick, R.P., Lucindo, N., Yeaman, M.R., and Bayer, A.S. (2005). Reduced susceptibility of Staphylococcus aureus to vancomycin and platelet microbicidal protein correlates with defective autolysis and loss of accessory gene regulator (agr) function. Antimicrob Agents Chemother *49*, 2687-2692.

Saravolatz, L.D., Markowitz, N., Arking, L., Pohlod, D., and Fisher, E. (1982a). Methicillin-resistant Staphylococcus aureus. Epidemiologic observations during a community-acquired outbreak. Ann Intern Med *96*, 11-16.

Saravolatz, L.D., Pohlod, D.J., and Arking, L.M. (1982b). Community-acquired methicillin-resistant Staphylococcus aureus infections: a new source for nosocomial outbreaks. Ann Intern Med *97*, 325-329.

Schaefler, S., Jones, D., Perry, W., Ruvinskaya, L., Baradet, T., Mayr, E., and Wilson, M.E. (1981). Emergence of gentamicin- and methicillin-resistant Staphylococcus aureus strains in New York City hospitals. J Clin Microbiol *13*, 754-759.

Schneider, T., and Sahl, H.G. (2010). An oldie but a goodie - cell wall biosynthesis as antibiotic target pathway. Int J Med Microbiol *300*, 161-169.

Schriever, C.A., Fernandez, C., Rodvold, K.A., and Danziger, L.H. (2005). Daptomycin: a novel cyclic lipopeptide antimicrobial. Am J Health Syst Pharm *62*, 1145-1158.

Shah, I.M., Laaberki, M.H., Popham, D.L., and Dworkin, J. (2008). A eukaryotic-like Ser/Thr kinase signals bacteria to exit dormancy in response to peptidoglycan fragments. Cell *135*, 486-496.

Sieradzki, K., and Tomasz, A. (1997). Inhibition of cell wall turnover and autolysis by vancomycin in a highly vancomycin-resistant mutant of Staphylococcus aureus. J Bacteriol *179*, 2557-2566.

Spink, W.W. (1954). Staphylococcal infections and the problem of antibiotic-resistant staphylococci. AMA Arch Intern Med *94*, 167-196.

Squeglia, F., Marchetti, R., Ruggiero, A., Lanzetta, R., Marasco, D., Dworkin, J., Petoukhov, M., Molinaro, A., Berisio, R., and Silipo, A. (2011). Chemical basis of peptidoglycan discrimination by PrkC, a key kinase involved in bacterial resuscitation from dormancy. J Am Chem Soc *133*, 20676-20679.

Stock, A.M., Robinson, V.L., and Goudreau, P.N. (2000). Two-component signal transduction. Annu Rev Biochem *69*, 183-215.

Sun, F., Ding, Y., Ji, Q., Liang, Z., Deng, X., Wong, C.C., Yi, C., Zhang, L., Xie, S., Alvarez, S., *et al.* (2012). Protein cysteine phosphorylation of SarA/MgrA family transcriptional regulators mediates bacterial virulence and antibiotic resistance. Proc Natl Acad Sci U S A *109*, 15461-15466.

Tabuchi, Y., Shiratsuchi, A., Kurokawa, K., Gong, J.H., Sekimizu, K., Lee, B.L., and Nakanishi, Y. (2010). Inhibitory role for D-alanylation of wall teichoic acid in activation of insect Toll pathway by peptidoglycan of Staphylococcus aureus. J Immunol *185*, 2424-2431.

Thwaites, G.E., and Gant, V. (2011). Are bloodstream leukocytes Trojan Horses for the metastasis of Staphylococcus aureus? Nat Rev Microbiol *9*, 215-222.

Thylefors, J.D., Harbarth, S., and Pittet, D. (1998). Increasing bacteremia due to coagulase-negative staphylococci: fiction or reality? Infect Control Hosp Epidemiol *19*, 581-589.

Truong-Bolduc, Q.C., Ding, Y., and Hooper, D.C. (2008). Posttranslational modification influences the effects of MgrA on norA expression in Staphylococcus aureus. J Bacteriol *190*, 7375-7381.

Ulrich, L.E., and Zhulin, I.B. (2010). The MiST2 database: a comprehensive genomics resource on microbial signal transduction. Nucleic Acids Res *38*, D401-407.

Uttley, A.H., Collins, C.H., Naidoo, J., and George, R.C. (1988). Vancomycin-resistant enterococci. Lancet *1*, 57-58.

Vollmer, W., Blanot, D., and de Pedro, M.A. (2008). Peptidoglycan structure and architecture. FEMS Microbiol Rev *32*, 149-167.

Walsh, C. (2003). Where will new antibiotics come from? Nat Rev Microbiol *1*, 65-70.

Watanakunakorn, C. (1984). Mode of action and in-vitro activity of vancomycin. J Antimicrob Chemother *14 Suppl D*, 7-18.

Weidenmaier, C., Kokai-Kun, J.F., Kristian, S.A., Chanturiya, T., Kalbacher, H., Gross, M., Nicholson, G., Neumeister, B., Mond, J.J., and Peschel, A. (2004). Role of teichoic acids in Staphylococcus aureus nasal colonization, a major risk factor in nosocomial infections. Nat Med *10*, 243-245.

Weidenmaier, C., and Peschel, A. (2008). Teichoic acids and related cell-wall glycopolymers in Gram-positive physiology and host interactions. Nat Rev Microbiol *6*, 276-287.

Weidenmaier, C., Peschel, A., Xiong, Y.Q., Kristian, S.A., Dietz, K., Yeaman, M.R., and Bayer, A.S. (2005). Lack of wall teichoic acids in Staphylococcus aureus leads to reduced interactions with endothelial cells and to attenuated virulence in a rabbit model of endocarditis. J Infect Dis *191*, 1771-1777.

Yoo, J.I., Kim, J.W., Kang, G.S., Kim, H.S., Yoo, J.S., and Lee, Y.S. (2013). Prevalence of amino acid changes in the yvqF, vraSR, graSR, and tcaRAB genes from vancomycin intermediate resistant Staphylococcus aureus. J Microbiol *51*, 160-165.

Zhang, W., Munoz-Dorado, J., Inouye, M., and Inouye, S. (1992). Identification of a putative eukaryotic-like protein kinase family in the developmental bacterium Myxococcus xanthus. J Bacteriol *174*, 5450-5453.

CHAPTER TWO

IN VITRO CHARACTERIZATION OF THE *S. AUREUS* STK1/STP1 PROTEINS AND THEIR POTENTIAL TARGETS

2.1 Introduction

Bacterial survival hinges on the ability to coordinate gene expression at appropriate times throughout its life cycle. Furthermore, the ability to sense and respond to external cues, such as natural perturbations in the cell wall or antibiotic stress, is equally important. In *S. aureus*, and other prokaryotic organisms, this coordination has been attributed to pairs of proteins commonly referred to as a two-component system (TCS).

There have been 16 TCSs systems identified in the *S. aureus* genome (Ito et al., 1999; Kuroda et al., 2001). Briefly, a TCS is composed of a histidine kinase, a cytoplasmic membrane protein that undergoes autophosphorylation (at a histidine residue) following a stimulus and a response regulator, typically a transcription factor, which gets phosphorylated (at an aspartic acid residue) to ultimately control gene expression (Chang and Stewart, 1998; Laub and Goulian, 2007; Stock et al., 2000). In *S. aureus* these systems have been found to be involved in a number of biological processes such as, but not limited to, autolysis (Brunskill and Bayles, 1996), production of toxins and virulence factors (Ventura et al., 2010; Yarwood et al., 2001), biofilm formation

(Sharma-Kuinkel et al., 2009), cell wall synthesis (Belcheva and Golemi-Kotra, 2008; Kuroda et al., 2004) and resistance to antimicrobial peptides (Falord et al., 2012; Yang et al., 2012).

In light of these findings, a growing body of literature supports another post-translational modification involving serine/threonine, and to a lesser extant tyrosine phosphorylation (Bakal and Davies, 2000; Munoz-Dorado et al., 1991; Zhang et al., 1992). The discovery of serine/threonine kinases (STK) and phosphatases (STP) has diversified our understanding of how cells sense and coordinate gene expression. Prokaryotic STKs and STPs, much like TCS, are linked to many processes such as sporulation (Shah et al., 2008), antibiotic resistance (Tamber et al., 2010), biofilm formation (Liu et al., 2011) and virulence (Cheung and Duclos, 2012).

The *S. aureus* MU50 genome contains two highly conserved genes, *sav1219* and *sav1220*, designated Stp1 (744bp/247aa) and Stk1 (1995bp/664aa), respectively. Other aliases of the Stk1 protein in the literature include PknB and PrkC, but it will be referred to as Stk1 in this study. The domain organization of these proteins is presented in Fig. 2.1.1. The N-terminal, or catalytic region, of Stk1 is cytoplasmic and harbors the regulatory elements involved in activation and specificity of the protein. The catalytic region is attached to a single α-helix which transverses the cytoplasmic membrane and connects to three extracellular penicillin-binding protein and serine/threonine kinase associated domains (PASTA). The Stp1 protein is a cytoplasmic protein.

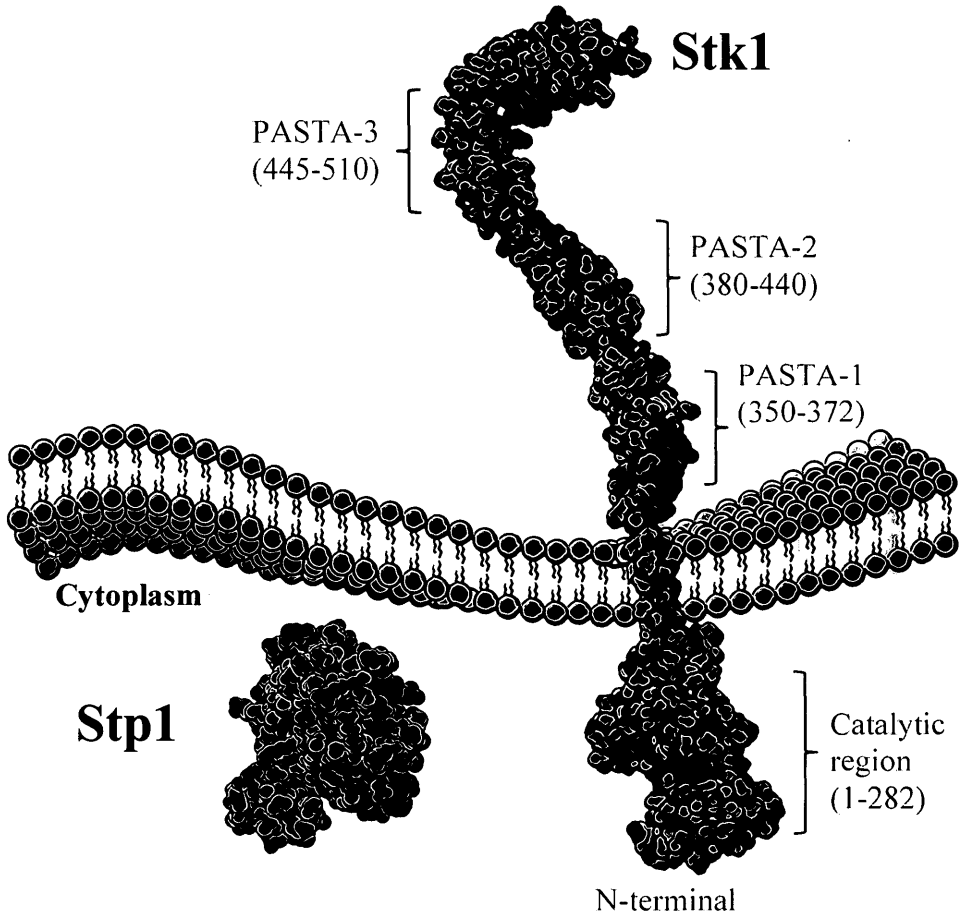

Figure 2.1.1 Domain organization of Stk1 and Stp1
The kinase, Stk1 (shown in blue), contains a cytoplasmic catalytic (N-terminal) region connected to three extracellular PASTA domains by a single transmembrane α-helix. The phosphatase, Stp1 (shown in orange), is a cytoplasmic protein. Stp1 depicted as *M. tuberculosis* PP2C-Family Ser/Thr Protein Phosphatase (retrieved from Protein Data Bank (PDB) with accession code: 1TXO (Pullen et al., 2004)) and Stk1 constructed from accession codes: 4EQM (Rakette et al., 2012) and 3M9G (Paracuellos et al., 2010). Figure prepared using UCSF Chimera 1.8 and Photoshop/Illustrator CS6 (Adobe®).

The precise role of Stk1, and its cotranscribing Stp1, has not been established given the varying functions these proteins appear to be involved in. Early studies demonstrated that Stk1 and Stp1 are involved in proper cell wall architecture and antimicrobial resistance (Beltramini et al., 2009), as well as carbohydrate metabolism

(Lomas-Lopez et al., 2007) and efflux pump regulation (Truong-Bolduc et al., 2008). However, subsequent work suggested a more diverse role for Stk1/Stp1 system as a result of a transcriptome analysis on *S. aureus* Stk1 knockout (ΔStk1) strain that revealed high regulatory impacts on a large variety of genes (Donat et al., 2009).

The above-mentioned studies probing Stk1 function were predominantly *in vivo* based. These studies established important phenotypes of ΔStk1 and/or ΔStp1, but failed to demonstrate the molecular mechanism by which Stk1 exerts its function. Put differently, Stk1 is a kinase protein that does not directly regulate genes, but does so via phosphorylation of substrates that themselves are directly or indirectly involved in gene regulation. The identification of substrates Stk1 phosphorylates aids in bridging the gap between observed ΔStk1 phenotypes and molecular mechanisms governing these phenotypes.

To date, studies have reported that Stk1 is capable of phosphorylating the substrates SarA (Didier et al., 2010; Sun et al., 2012), MgrA (Truong-Bolduc et al., 2008), LuxS (Cluzel et al., 2010), PurA (Donat et al., 2009), CcpA (Leiba et al., 2012), enzymes of the central metabolism (Lomas-Lopez et al., 2007) and a human transcription factor (Miller et al., 2010). For the purpose of this study, it is irrelevant to understand in detail the roles of these enzymes, however, one should appreciate the diversity of proteins that are phosphorylated by Stk1. Hence the study herein aims to further investigate the functional role of Stk1/Stp1 *in vitro*, with an emphasis on discovering new phosphorylation targets of Stk1.

2.2 Materials and Methods

2.2.1 Materials and chemicals

The Champion pET Directional TOPO Expression Kit was purchased from Invitrogen. Chemicals and growth media were purchased from Sigma (Oakville, Canada) or Thermo-Fisher (Whitby, Canada), unless otherwise stated. All resins for purification were purchased from Qiagen or GE Healthcare (Quebec, Canada). All primers were purchased from Sigma (Oakville, Canada). Cold ATP and restriction enzymes were purchased from New England Biolabs (Pickering, Canada). The DNA polymerases PfuTurbo® and Phusion® High-fidelity were purchased from Agilent Technologies and Thermo-Fisher (Whitby, Canada), respectively. Radioactive γ-^{32}P-ATP with specificity of 10 Ci/mmol was purchased from PerkinElmer LAS Canada Inc. (Toronto, Canada). The Trypsin Profile IGD kit was obtained from Sigma-Aldrich.

2.2.2 Expression and purification of His-Stk1

The *sav1220* gene, Stk1, was amplified from *S. aureus* MU50 genome and cloned directly into pET151/D-TOPO with primer set Dir 5'- CACCATGATAGGTAAA ATAATAAATGAAC and Rev 5'- TTATTAAATATCATCATAGCTGACTTC. The 6xHis tag is located on the N-terminal of the protein. The resulting plasmid was used to transform NovaBlue cells, which were sequenced (T7 and T7term primers) for the correct insert (York University, Department of Biology, Core Facility). The plasmid was ultimately transformed into BL21(DE3) cells.

A 1 mL overnight seed culture of *E. coli* BL21(DE3) containing pET151/D-TOPO-His-Stk1 was used to inoculate 800 mL of Terrific Broth medium supplemented with ampicillin (100 μg/mL). The inoculated medium was grown at 37°C, 200 rpm, until OD_{600} reached 0.6-0.8, at which time protein expression was induced by addition of Isopropyl ß-$_D$-thiogalactopyranoside (IPTG) at a final concentration of 1 mM for 18 hours at 10°C, 100 rpm. Cells were harvested at 8, 230 xg for 15 min at 4°C. Resulting pellets, aliquoted to 1.5 g, were frozen at -80°C if subsequent purification steps were not carried out on same day. All parts of the purification protocol were carried out at 4°C on a fast protein liquid chromatography (FPLC) instrument (Amersham Biosciences). Harvested pellets were resuspended in 10 mL of 50 mM $NaPO_4$, 300 mM NaCl, and 10 mM imidazole, pH 7.5 containing Triton-X100 (0.5% final). Sonication (3 min of 20 sec on, 20 off; 20% amplitude) was used to liberate the protein and centrifugation at 18,138 xg for 60 min was carried out to rid of cell debris. Supernatant was loaded onto a 5 mL Ni-NTA self-packed column (Generon). Elution was carried out at 3 mL/min with a step gradient of 10%, 30%, 50% and 100% elution buffer (50 mM $NaPO_4$, 300 mM NaCl, and 300 mM imidazole, pH 7.5) and 10 mL fractions were collected. Fractions containing protein of interest were pooled and concentrated using centrifugal filter Ultracel-30K (Amicon, Millipore). Protein homogeneity was assessed using 12.5% SDS-PAGE and stained with Coomassie Blue.

2.2.3 Expression and purification of Stp1

The *sav1219* gene, Stp1, was amplified from *S. aureus* MU50 genome and

cloned into pET26b(+) with primer set Dir 5'- GGAATTCCATATGCTAGAGG CACAATTTTTTAC and Rev 5'-AAGGAATTCCTCATCATCATACTTTATCA CCTTCAATAG. Restriction cut sites *NdeI* (Dir primer) and *EcoRI* (Rev primer) are underlined. The resulting plasmid was used to transform NovaBlue cells, which were sequenced (T7 and T7term) for the correct insert (York University, Department of Biology, Core Facility). The plasmid was ultimately transformed into BL21(DE3) cells.

A 1 mL overnight seed culture of *E. coli* BL21(DE3) containing pET26b(+)-Stp1 was used to inoculate 800 mL of Terrific Broth medium supplemented with kanamycin (30 μg/mL). The inoculated medium was grown at 37°C, 200 rpm, until OD_{600} reached 0.6-0.8, at which time protein expression was induced by addition of IPTG at a final concentration of 0.5 mM. Expression was carried out for 12 hours at 25°C, 120 rpm. Cells were harvested at 8, 230 xg for 15 min at 4°C. Resulting pellets, aliquoted to 3 g, were frozen at -80°C if subsequent purification steps were not carried out on same day. All parts of the purification protocol were carried out at 4°C by FPLC. Harvested pellets were resuspended in loading buffer (20 mM Tris buffer, pH 7.0, supplemented with 5 mM $MgCl_2$). Sonication (3 min of 30 sec on, 30 off; 20% amplitude) was used to liberate the protein and centrifugation at 18,138 xg for 60 min was carried out to remove cell debris. The resulting supernatant was applied to a DEAE cellulose-Sepharose Fast Flow self-packed column (Econo-Column, 2.5 x 20 cm, 80 mL column volume, Bio-Rad) pre-equilibrated in loading buffer. Elution was carried out at 4 mL/min with a 480 mL linear gradient from loading buffer to elution buffer (500 mM Tris buffer, pH 7.0, 5 mM

$MgCl_2$), and 10 mL fractions were collected. Fractions containing protein of interest were pooled and concentrated using centrifugal filter Ultracel-10K (Amicon, Millipore). The concentrated sample was re-applied to a similar DEAE cellulose-Sepharose Fast Flow self-packed column (C column 16/20, 40 mL column volumes, GE Healthcare). Fractions containing protein of interest were pooled and concentrated using new centrifugal filter Ultracel-10K (Amicon, Millipore). Protein homogeneity was assessed using a 15% SDS-PAGE and stained with Coomassie Blue.

2.2.4 Purification of GraR, BceR, VraR, WalR, FmtA, PBP4 and PBP2a

All proteins were purified by FPLC at 4°C. The purification of BceR and WalR was similar to previously described VraR protein (Belcheva and Golemi-Kotra, 2008). GraR was purified similarly with minor modifications. Briefly, for the final polishing step the GraR protein was passed through a HiPrep 26/60 Sephacryl S-200 HR size exclusion column (GE Healthcare). PBP4 was purified similarly to previously described FmtA protein (Fan et al., 2007). PBP2a was purified by passing supernatant through Q-Sepharose column; the fractions containing protein of interest were collected, desalted and further passed through S-Support column.

2.2.5 His-Stk1 identification by mass spectrometry

His-Stk1 (10 μM) was separated by 12.5% SDS-PAGE and stained with Coomassie Blue; the band of interest was cut from the gel and an in-gel tryptic digestion was carried out with the Trypsin Profile IGD Kit (Sigma Aldrich). The sample was

analyzed by liquid chromatography-mass spectrometry (LC-MS/MS) at the Advanced Protein Technology Centre, The Hospital for Sick Children (Toronto, Canada).

2.2.6 His-Stk1 phosphorylation assays

2.2.6.1 Autophosphorylation of His-Stk1

His-Stk1 (2 μM) was incubated with 20 μM [γ-^{32}P]-ATP (10 Ci/mmol) in phosphorylation buffer (PB), 25 mM Tris-HCl (pH 7.5), 1 mM DTT, and 10 mM $MgCl_2$ at room temperature. The reactions were quenched at various time intervals by the addition of 5x SDS Gel-loading buffer. Quenched reactions were separated by 12.5% SDS-PAGE. Radioactive SDS-PAGE gel was exposed to autoradiography cassette, which was scanned using TYPHOON Trio$^+$ (GE Healthcare), and then stained by Coomassie blue.

2.2.6.2 Effects of divalent ions on the autophosphorylation of His-Stk1

His-Stk1 (5 μM) was incubated with 20 μM [γ-^{32}P]-ATP (10 Ci/mmol) in 25 mM Tris-HCl, pH 7.5, 1 mM DTT and varying concentrations of either $MgCl_2$ or $MnCl_2$ for 30 min at room temperature. The reactions were quenched with 5x SDS Gel-loading buffer and separated by 12.5% SDS-PAGE. Radioactive SDS-PAGE gel was exposed to autoradiography cassette, which was scanned using TYPHOON Trio$^+$ (GE Healthcare), and then stained by Coomassie blue.

2.2.6.3 Stability of His-Stk1 following autophosphorylation

His-Stk1 (20 μM) was autophosphorylated with 20 μM [γ-^{32}P]-ATP (10

Ci/mmol) in PB, described above, for 30 min. The master mixture was desalted to remove excess [γ-^{32}P]-ATP with desalting column (Pierce Zeba^{TM}, Thermo Scientific) and further incubated at room temperature. Sample was removed from master mixture at defined time intervals and quenched with 5x SDS Gel-loading buffer. Quenched reactions were separated by 12.5% SDS-PAGE. Radioactive SDS-PAGE gel was exposed to autoradiography cassette, which was scanned using TYPHOON Trio^{+} (GE Healthcare).

2.2.7 Dephosphorylation of His-Stk1 by Stp1

His-Stk1 (25 μM) was autophosphorylated, as in section 2.2.6.2, either on its own or in the presence of Stp1 (20 μM) for 30 min at room temperature. Reactions were quenched with 5x SDS Gel-loading buffer and separated by 12.5% SDS-PAGE. Radioactive SDS-PAGE gel was exposed to autoradiography cassette, which was scanned using TYPHOON Trio^{+} (GE Healthcare), and then stained by Coomassie blue.

2.2.8 Phosphorylation of potential His-Stk1 substrates

2.2.8.1 Probing phosphorylation of response regulators

His-Stk1 (5 μM) was incubated with the response regulators GraR (10 μM), BceR (10 μM), VraR (20 μM) and WalR (10 μM) with 20 μM [γ-^{32}P]-ATP (10 Ci/mmol) in PB at room temperature for 30 min. Proteins were separated by 15% SDS-PAGE, exposed to autoradiography cassette, which was scanned using TYPHOON Trio^{+} (GE Healthcare), and then stained by Coomassie blue.

2.2.8.2 Probing phosphorylation of penicillin-binding proteins

His-Stk1 (10 μM) was incubated with the penicillin-binding proteins PBP2a (10 μM), PBP4 (20 μM) and FmtA (20 μM) with 20 μM [γ-^{32}P]-ATP (10 Ci/mmol) in PB at room temperature for 30 min. GraR (10 μM) was used as a control and phosphorylated under same conditions. Proteins were separated by 12.5% SDS-PAGE, exposed to autoradiography cassette, which was scanned using TYPHOON Trio^{+} (GE Healthcare), and then stained by Coomassie blue.

2.2.9 Assessing phosphorylation of FmtA by His-Stk1 with acidic-native PAGE

His-Stk1 (10 μM) was incubated with FmtA (20 μM), PBP4 (20 μM) and GraR (10 μM) with 20 μM [γ-^{32}P]-ATP (10 Ci/mmol) in PB at both room temperature and 37°C for 30 min. Proteins were separated by 10% acidic-native PAGE, exposed to autoradiography cassette, which was scanned using TYPHOON Trio^{+} (GE Healthcare), and then stained by Coomassie blue.

2.2.10 Closer examination of GraR phosphorylation by His-Stk1

2.2.10.1 Time-dependent phosphorylation of GraR by His-Stk1

A master mixture containing His-Stk1 (5 μM), GraR (10 μM) and 20 μM [γ-^{32}P]-ATP (10 Ci/mmol) in PB was incubated at room temperature. Aliquots of 15 μL were removed and quenched at various time intervals by the addition of 5x SDS Gel-loading buffer. Quenched reactions were separated by 15% SDS-PAGE. Radioactive SDS-PAGE gel was exposed to autoradiography cassette, which was scanned using

TYPHOON Trio^{+} (GE Healthcare), and then stained by Coomassie blue.

2.2.10.2 Phosphorylation of denatured GraR by His-Stk1

His-Stk1 (5 μM) and GraR (25 μM) were incubated with 20 μM [γ-^{32}P]-ATP (10 Ci/mmol) in PB at room temperature for 30 min either together or separately. In a separate reaction proteins were first denatured by boiling for 10 min and subsequently phosphorylated under same conditions. Reactions were separated by 15% SDS-PAGE. Radioactive SDS-PAGE gel was exposed to autoradiography cassette, which was scanned using TYPHOON Trio^{+} (GE Healthcare), and then stained by Coomassie blue.

2.2.10.3 Quantifying phosphorylated GraR by Phos-tag PAGE

His-Stk1 (5 μM) and GraR (either 5 or 10 μM) were incubated with 20 μM [γ-^{32}P]-ATP (10 Ci/mmol) in PB at 37°C for 30 min. Reactions were quenched and loaded to 12% SDS-PAGE and 12% phos-tag PAGE. The phos-tag PAGE method is described in detail (Kinoshita and Kinoshita-Kikuta, 2011; Kinoshita et al., 2006). Briefly, the gel contained 100 μM Mn^{2+}-phos-tag in 12% acrylamide (made from 30% acrylamide, 0.8% bis-acrylamide stock). No SDS was added to the gel. Electrophoresis was carried out in a manner identical to the traditional SDS-PAGE. Radioactive gels were exposed to autoradiography cassette, which were scanned using TYPHOON Trio^{+} (GE Healthcare), and stained by Coomassie blue.

2.2.10.4 Dephosphorylation of GraR by Stp1

Phosphorylation of GraR (10 μM) was carried by the addition of His-Stk1 (5

μM) with 20 μM [γ-^{32}P]-ATP (10 Ci/mmol) in PB at room temperature for 30 min. Subsequently, Stp1 (20 μM) was added and the reaction proceeded for 30 min more. Reactions were separated by 15% SDS-PAGE. The gel was exposed to autoradiography cassette, which was scanned using TYPHOON Trio^{+} (GE Healthcare), and then stained by Coomassie blue.

2.2.11 Investigating the Stk1-mediated phosphorylation sites of GraR

2.2.11.1 Phosphorylation of GraR^{C} and GraR^{N}

His-Stk1 (5 μM) was incubated with 20 μM of GraR C-terminal (GraR^{C}) or GraR-N terminal (GraR^{N}) with 20 μM [γ-^{32}P]-ATP (10 Ci/mmol) in PB at room temperature for 30 min. GarR^{C} was separated with 15% SDS-PAGE. GarR^{N} was separated with 12.5% SDS-PAGE. Both gels were exposed to autoradiography cassette, which was scanned using TYPHOON Trio^{+} (GE Healthcare). Only GarR^{N} gel was stained with Coomassie blue.

2.2.11.2 Identification of phosphorylated GraR sites by mass spectrometry

Phosphorylation of GraR full length (40 μM) or GraR^{C} (40 μM) was achieved by incubating with His-Stk1 (20 μM) in presence of cold ATP (500 μM) in PB at room temperature for 60 min. As a control, GraR proteins and His-Stk1 were incubated together under same conditions without cold ATP. Following phosphorylation GraR full length was directly digested with trypsin (Promega) overnight at 37°C in 100 mM ammonium bicarbonate, whereas GraR-C terminal was separated by 15% SDS-PAGE.

The gel was stained with Coomassie Blue; the band of interest was cut from the gel and an in-gel tryptic digestion was carried out with the Trypsin Profile IGD Kit (Sigma Aldrich). The full length GraR was analyzed by liquid chromatography-mass spectrometry (LC-MS/MS) at the Centre for Research in Mass Spectrometry, York University (Toronto, Canada). The GraR-C terminal was analyzed by liquid chromatography-mass spectrometry (LC-MS/MS) at the Advanced Protein Technology Centre, The Hospital for Sick Children (Toronto, Canada).

2.2.11.3 Site-directed mutagenesis of GraR phosphorylation sites

The pET26b::*graR* contrast was previously prepared in the laboratory. pET26b::*graR* mutants harboring threonine to alanine substitutions at Thr128 (encoded by ACA) , Thr130 (encoded by ACT), Thr149 (encoded by ACG) and a triple mutant containing all three mutations were generated with the QuikChange™ Site-Directed Mutagenesis method (Stratagene). Alanine substitutions are highlighted in bold within the PCR primers. The GraR-T128A mutant was generated with PCR primers Dir 5'-CTGAAGAAAAACGT**GCA**TTGACTTGGCAAG and Rev 5'- CTTGCCAAGTCAA **TGC**ACGTTTTTCTTCAG. The GraR-T130A mutant was generated with PCR primers Dir 5'- GAAAAACGTACATTG**GCT**TGGCAAGATGC and Rev 5'- GCATCTTGCCA **AGC**CAATGTACGTTTTTC. The GraR-T149A mutant was generated with PCR primers Dir 5'-CAAAAAGGTGACGAT**GCG**ATTTTTCTATCC and Rev 5'-GGATAGAAAAAT**CGC**ATCGTCACCTTTTTG. The GraR triple mutant was first generated with Dir 5'- GAAAAACGT**GCA**TTG**GCT**TGGCAAGATGC and Rev 5'-

GCATCTTGCCA**AGC**CAA**TGC**ACGTTTTTC to yield GraR-T128A/T130A, which was further mutated with the same primers used for GraR-T149A to yield GraR-T128A/T130A/T149A.

Following PCR amplification the products were digested with restriction endonuclease *DpnI* to remove original methylated template DNA. Subsequently, *E. coli* NovaBlue cells were transformed with the *DpnI*-digested reactions. Correct mutagenesis was confirmed by DNA sequencing (York University, Department of Biology, Core Facility). The resulting constructs were transformed into *E. coli* BL21(DE3) cells. Expression and purification for GraR single mutants was carried out as previously described for GraR wild-type.

2.2.11.4 Phosphorylation of GraR-T128A, GraR-T130A and GraR-T149A by His-Stk1

His-Stk1 (5 μM) was incubated with GraR-WT (25 μM), GraR-T128A (25 μM), GraR-T130A (10 μM) and GraR-T149A (25 μM) with 20 μM [γ-^{32}P]-ATP (10 Ci/mmol) in PB at room temperature for 30 min. Proteins were separated by 15% SDS-PAGE, exposed to autoradiography cassette, which was scanned using TYPHOON Trio^{+} (GE Healthcare), and then stained by Coomassie blue.

2.2.11.5 Expression of GraR triple mutant (T128A/T130A/T149A)

A 1 mL overnight seed culture of *E. coli* BL21(DE3) containing pET26b(+)-GraR-T128A/T130A/T149A was used to inoculate 800 mL of Terrific Broth medium

supplemented with kanamycin (30 μg/mL). The inoculated medium was grown at 37°C, 200 rpm, until OD_{600} reached 0.6-0.8. Protein expression was induced by addition of IPTG at concentrations of 0.1 or 0.5 mM. Expression was carried out for 12-18 hours at 25°C or 18°C, 120 rpm. Expression tests were separated by 15% SDS-PAGE and stained with Coomassie blue.

2.3 Results

2.3.1 Expression and purification of His-Stk1

The pET151/D-TOPO-His-Stk1 construct, transformed into *E. coli* BL21(DE3) cells, contains an inducible T7 promoter. Following induction with IPTG sufficient amount of soluble His-Stk1 was obtained, as seen in Fig. 2.3.1, for subsequent purification steps.

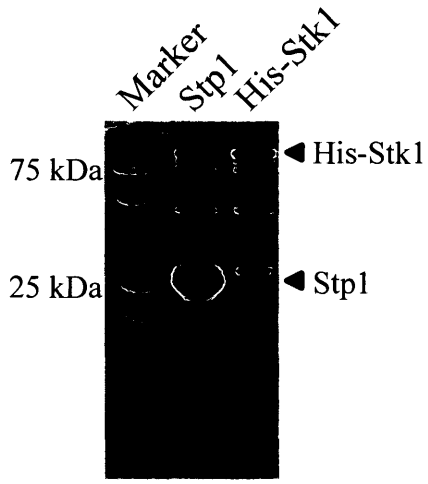

Figure 2.3.1 Expression of Stp1 and His-Stk1 recombinant proteins in BL21(DE3) Expression profile of target proteins analyzed by 15% SDS-polyacrylamide gel, stained with Coomassie blue. Expression of His-Stk1 achieved by addition of 1 mM IPTG for 18 hours at 10 °C. For Stp1 expression, 0.5 mM IPTG added for 16 hours at 25°C.

The theoretical pI of His-Stk1 was calculated to be 5.76 with a calculated molecular weight of 74,377 Da. The calculated molecular weight of the recombinant protein is 78,160 Da and a pI of 5.85 due to the 6xHis-V5 epitope-TEV sequence at the

N-terminus of the protein. His-Stk1 contains a 6xHis tag and to facilitate protein purification the supernatant was passed through a Ni-NTA column connected to an FPLC system. The protein was eluted with step gradients of increasing imidazole concentrations, Fig. 2.3.2A, and protein purity was assessed during purification (Fig. 2.3.2B) and following concentration (Fig. 2.3.2C). Typically 1-1.5 mg of His-Stk1 would be obtained from a 1.5 g cell pellet.

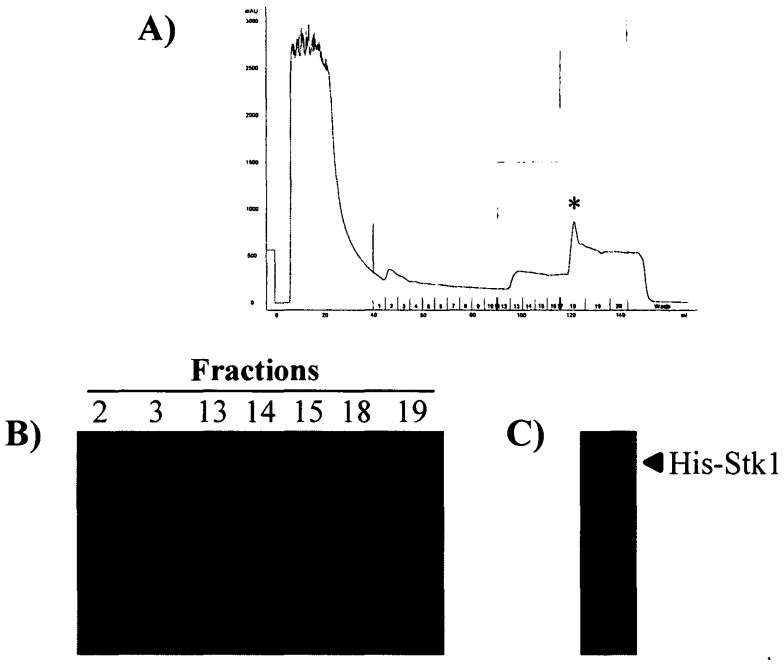

Figure 2.3.2 Purification chromatogram of His-Stk1 following Ni-NTA column analyzed by SDS-PAGE
A) FPLC chromatogram following elution from a Ni-NTA column. Protein elution indicated with asterisk. On chromatogram blue line represents UV at 280nm, green is concentration and in red are the fractions B) A 12.5% SDS-PAGE was loaded with fractions from Ni-NTA column. C) Pure His-Stk1 following concentration separated by 12.5% SDS-PAGE. Gels were stained with Coomassie blue to detect proteins.

Although the protein gets expressed, the amount of expression is much lower than typical expression systems or compared to Stp1 (Figure 2.3.1). Thus to confirm successful His-Stk1, following purification and separation by SDS-PAGE, the band of interest was cut out and sent for analysis by liquid chromatography-mass spectrometry (LC-MS/MS). Data in Appendix A confirms that the band of interest is indeed His-Stk1.

2.3.2 Expression and purification of Stp1

The pET26b(+)-Stp1 construct, transformed into *E. coli* BL21(DE3) cells, contains an inducible T7 promoter. Following induction with IPTG sufficient amount of soluble Stp1 was obtained, Fig. 2.3.1, for subsequent purification steps. The theoretical pI of Stp1 was calculated to be 5.02 with a molecular weight of 27,916 Da (minus first methionine). The purification strategy involved passing the supernatant through a DEAE cellulose-Sepharose column (anion exchange) (Fig. 2.3.3A). The resulting fractions, despite being adequately pure as assessed by 15% SDS-PAGE (Fig. 2.3.3B), were pooled together and passed through a smaller DEAE cellulose-Sepharose column (Fig. 2.3.3C). Resulting fractions (Fig. 2.3.3D) were concentrated and final protein homogeneity (Fig 2.3.3E) was assessed by 15% SDS-PAGE. Typically 20-25 mg of Stp1 was obtained from a 2.5 g pellet.

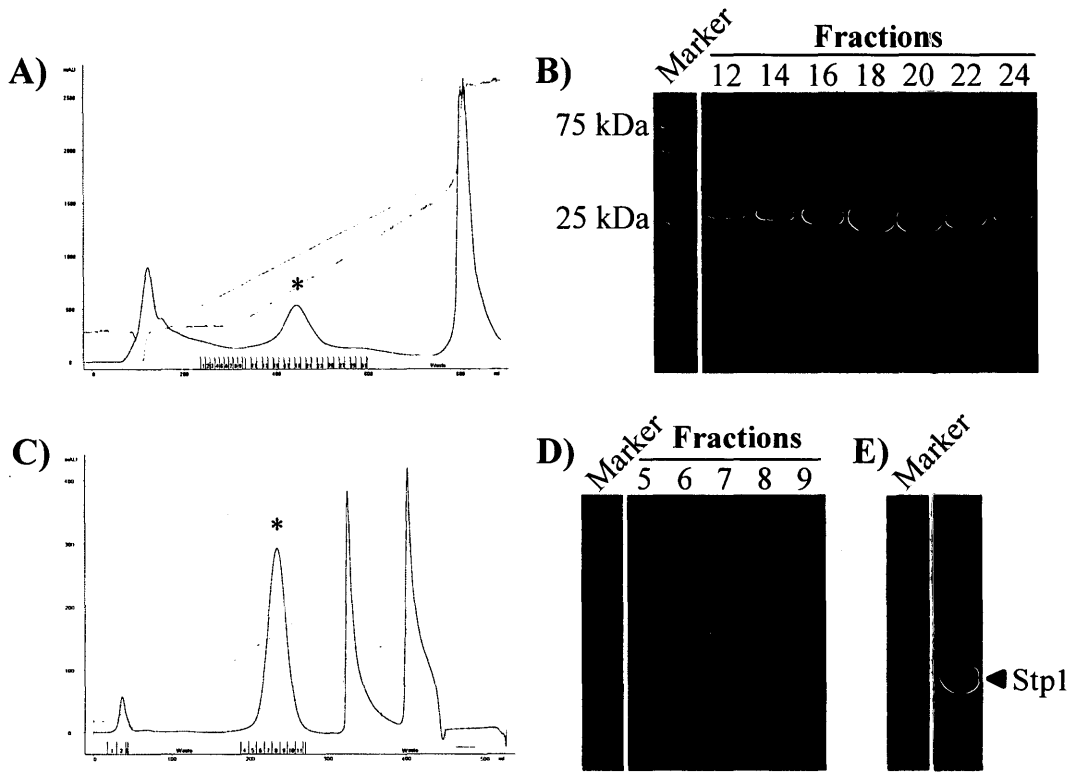

Figure 2.3.3 Purification chromatograms of Stp1 following DEAE columns analyzed by SDS-PAGE

A) FPLC chromatogram following elution from 80 mL DEAE column. B) A 15% SDS-PAGE gel was loaded with fractions from 80 mL DEAE column. C) FPLC chromatogram following elution from 40 mL DEAE column.D) A 15% SDS-PAGE gel was loaded with fractions from 40 mL DEAE column. E) A 12.5% SDS-PAGE gel was loaded with pure Stp1. Gels were stained with Coomassie blue to detect proteins. Markers in each figure coincide with same gel, but different lanes. Protein elutions indicated with asterisks. On chromatograms blue line represents UV at 280nm, green is concentration, teal is conductivity and in red are the fractions.

2.3.3 Enzymatic activity of His-Stk1 and Stp1 *in vitro*

To examine the importance of Stk1 and Stp1 it was necessary to establish that purified recombinant proteins were enzymatically active *in vitro*. This was carried out

with phosphorylation assays involving radioactive ATP. His-Stk1, in the presence of [γ-^{32}P]-ATP undergoes autophosphorylation in a time-dependent manner (Fig. 2.3.4A), where the majority of the kinase is phosphorylated within the first 30 min.

Autophosphorylation of His-Stk1 was achieved with either Mg^{2+} or Mn^{2+} as cofactors (Fig. 2.3.4B). Although this experiment revealed that at higher concentrations of Mn^{2+} less phosphorylation is achieved, as observed by the decrease in signal.

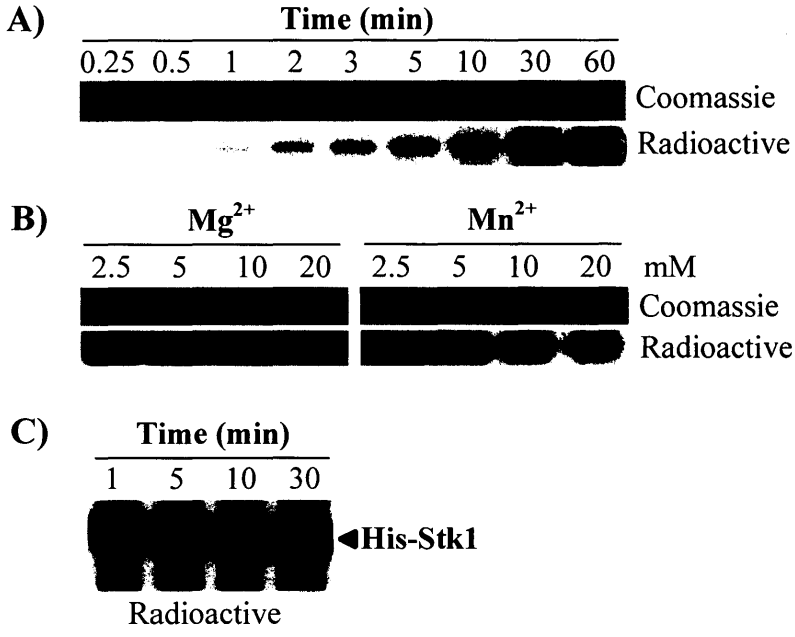

Figure 2.3.4 Enzymatic activity of His-Stk1 *in vitro*
A) Autophosphorylation of His-Stk1. His-Stk1 (2 μM) was incubated with [γ-^{32}P]- ATP (20 μM) at various time intervals in PB at room temperature. Both images are of same gel. B) His-Stk1 (5 μM) was incubated with [γ-^{32}P]-ATP (20 μM) in 25 mM Tris-HCl, pH 7.5, 1 mM DTT and varying concentrations of either $MgCl_2$ or $MnCl_2$ for 30 min at room temperature. Reactions were quenched with 5× SDS Gel-loading buffer. Both images are of same gel. C) His-Stk1 (20 μM) was autophosphorylated, desalted and further incubated at room temperature. Reactions were quenched at indicated time intervals. All reactions resolved with 12.5% SDS-PAGE, exposed to autoradiography cassette, scanned using TYPHOON Trio+ (GE Healthcare). A) and B) were subsequently stained with Coomassie blue.

Following autophosphorylation, and the removal of excess ATP by desalting, it was observed that His-Stk1 signal was stable for at least 30 min at room temperature (Fig. 2.3.4C). This prompted the investigation of the phosphatase activity of Stp1 towards phosphorylated His-Stk1. The results demonstrate that addition of Stp1 to an already phosphorylated His-Stk1 completely removes the signal (Fig. 2.3.5).

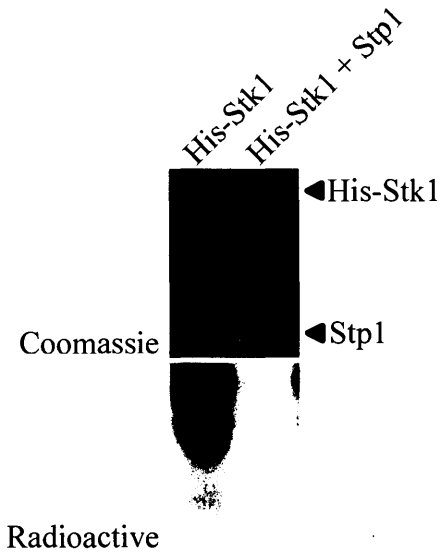

Figure 2.3.5 Phosphatase activity of Stp1 towards phosphorylated His-Stk1
His-Stk1 (5 μM) was autophosphorylated with [γ-^{32}P]- ATP (20 μM) for 30 min in PB at room temperature. Stp1 (20 μM) was added to the mixture and further incubated for 30 min at room temperature . Reactions were quenched and resolved by 12.5% SDS-PAGE. The gel was exposed to an autoradiography cassette, which was scanned using TYPHOON Trio+ (GE Healthcare) and subsequently stained with Coomassie blue.

2.3.4 Phosphorylation of potential *S. aureus* substrates by His-Stk1 *in vitro*

The ultimate goal of this study was to discover novel substrates of His-Stk1 and its cognate Stp1. Both proteins were established to be active *in vitro*, hence we moved on

to probing interaction with various proteins. Previous research has recognized that Stk1 is capable of phosphorylating global regulators of *S. aureus*. To determine whether His-Stk1 can phosphorylate response regulators belonging to TCS, we carried out *in vitro* kinase assays. As shown in Fig. 2.3.6, His-Stk1 is capable of phosphorylating GraR and unable to phosphorylate VraR, BceR or WalR.

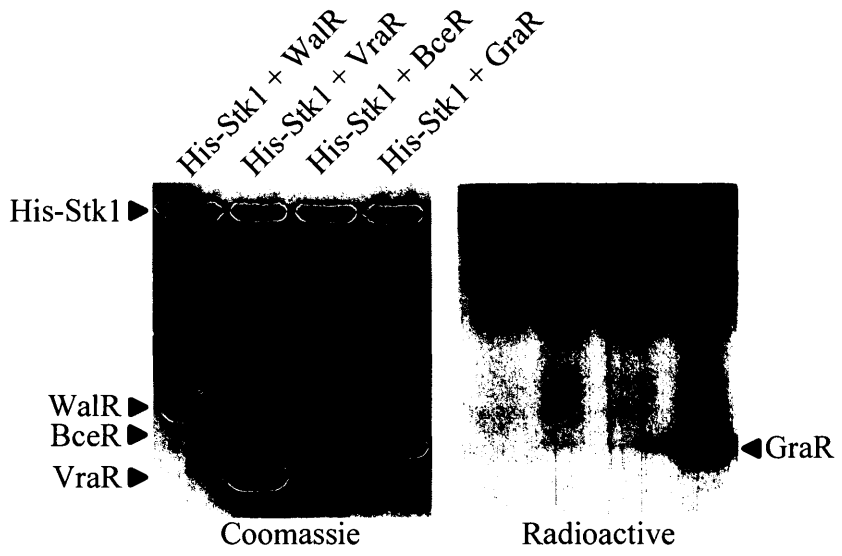

Figure 2.3.6 His-Stk1phosphorylation of response regulators
His-Stk1 (5 μM) was incubated with the response regulators WalR (10 μM), VraR (20 μM), BceR (10 μM) and GarR (10μM) for 30 min in PB at room temperature in the presence of [γ-^{32}P]- ATP (20 μM). Reactions were quenched and resolved by 15% SDS-PAGE. The gel was exposed to an autoradiography cassette, which was scanned using TYPHOON Trio+ (GE Healthcare) and subsequently stained with Coomassie blue.

The observation that His-Stk1 was capable of specifically phosphorylating GraR *in vitro* prompted us to investigate whether other proteins, such as penicillin binding proteins, were capable of undergoing phosphorylation by His-Stk1. In this experiment

PBP2a, PBP4 and FmtA were incubated with and without His-Stk1 in the presence of [γ-^{32}P]- ATP. The GraR protein was used as a control. Under the conditions tested, the results demonstrate His-Stk1 is unabale to phosphorylate PBP2a or PBP4, however a faint band was observed for FmtA (Fig. 2.3.7).

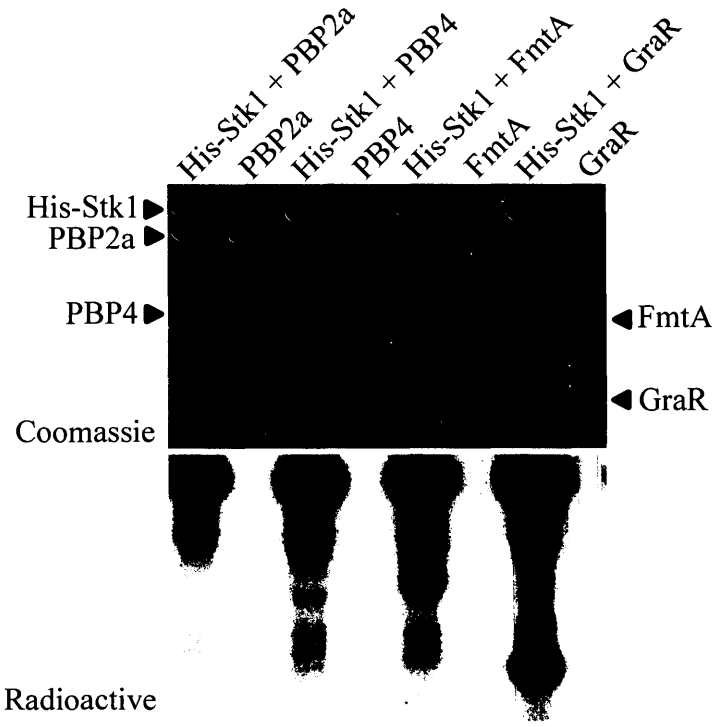

Figure 2.3.7 His-Stk1 phosphorylation of penicillin-binding proteins
The penicillin-binding proteins PBP2a (10 μM), PBP4 (20 μM) and FmtA (20 μM) were incubated either alone or with His-Stk1 (10 μM) in the presence of [γ-^{32}P]- ATP (20 μM) in PB for 30 min at room temeperature. GraR (10 μM) was used as control and subjected to same conditions Reactions were resolved by 12.5% SDS-PAGE. The gel was exposed to an autoradiography cassette, which was scanned using TYPHOON Trio+ (GE Healthcare) and subsequently stained with Coomassie blue.

As can be seen in the coomassie gel the FmtA protein does not form a single crisp band but forms a streak between two bands, hence the phosphorylation signal is

dispersed. In order to obtain a single band FmtA, pI of 9.58, can be seperated by an acidic-native PAGE (gel typically used for basic proteins with pI > 7.0). Based on Fig. 2.3.8 it is suggested that FmtA may be a phosphorylation substrate for His-Stk1. PBP4, pI of 8.89, was used as a negative control. It should be noted that His-Stk1 and GraR both have a pI < 7.0 and cannot enter the gel, this is especially noticeable for His-Stk1 which remains in the stacking portion of the gel.

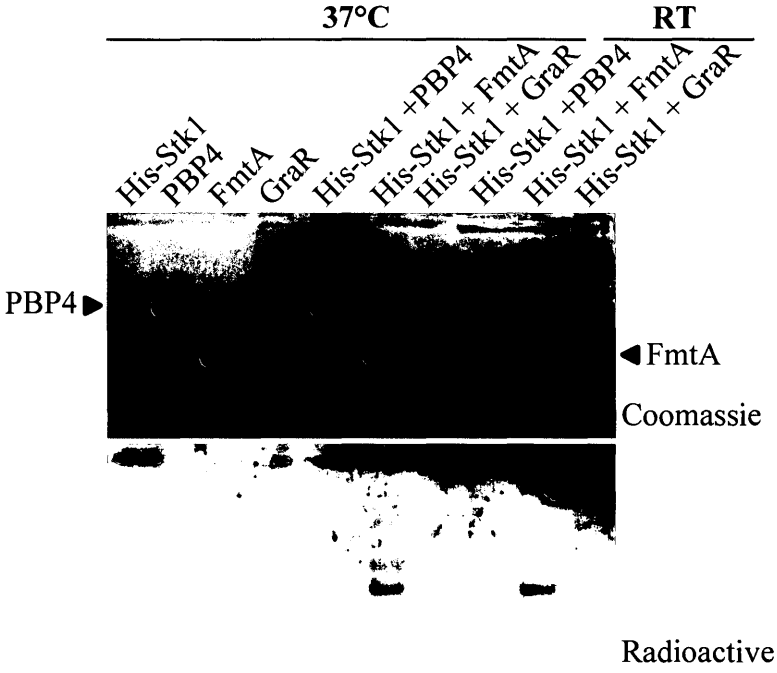

Figure 2.3.8 His-Stk1 phosphorylation of FmtA resolved by acidic-native PAGE
The penicillin-binding protein FmtA (20 μM) was incubated either alone or with His-Stk1 (10 μM) in the presence of [γ-^{32}P]- ATP (20 μM) in PB for 30 min at either 37°C or room temperature. GraR (10 μM) used as positive control and PBP4 (20 μM) used as negative control were subjected to same conditions. Note His-Stk1 and GraR unable to enter gel due to pI. Reactions were resolved by 10% acidic-native PAGE. The gel was exposed to an autoradiography cassette, which was scanned using TYPHOON Trio+ (GE Healthcare) and subsequently stained with Coomassie blue.

2.3.5 Closer examination of GraR phosphorylation by His-Stk1

Despite the identification of two potential substrates (FmtA and GraR), we decided to focus on the phosphorylation of GraR. The kinase assays involving His-Stk1 and response regulators demonstrated specificity towards GraR only. BceR is a response regulator from *Bacillus subtilis* that shares 56% sequence identity to GraR (Fig. 2.3.9), did not undergo phosphorylation by His-Stk1 (Fig.2.3.6).

```
            10        20        30        40        50        60
BceR MFKLLLIEDDESLFHEIKDRLTGWSYDVYGIQDFSQVLQEFAAVNPDCVIIDVQLPKFDG-60
GraR MQI-LLVEDDNTLFQELKKELEQWDFNVAGIEDFGKVMDTFESFNPEIVILDVQLPKYDG-59

BceR FHWCRLIRSRSNVPILFLSSRDHPADMVMSMQLGADDFIQKPFHFDVLIAKIQAMFRRVH-121
GraR FYWCRKMREVSNVPILFLSSRDNPMDQVMSMELGADDYMQKPFYTNVLIAKLQAIYRRVY-119

BceR HYNTEPS-TIKTWCGAAVDAEQNLVSNDKGSVELTKNEMFILKQLIEQKNKIVSREELIR-182
GraR EFTAEEKRTL-TWQDAVVDLSKDSIQKGDDTIFLSKTEMIILEILITKKNQIVSRDTIIT-179
              *  *                  *
BceR SLWNDERFVSDNTLTVNVNRLRKKLDALQLGAYIETKVGQGYIAKEEDKFYD-230
GraR ALWDDEAFVSDNTLTVNVSRLRKKLSEISMDSAIETKVGKGYMAHE-224
```

Figure 2.3.9 Sequence alignment of GraR and BceR
Highlighted in red and green are identical and similar amino acids, respectively. Putative phosphorylation sites of GraR, Thr128, Thr130, and T1hr49, are marked with asterisks.

We further probed whether His-Stk1 phosphorylates GraR in a time-dependent manner. As it can be seen in Fig. 2.3.10, the majority of phosphorylation, determined by the relative intensity of bands (analyzed by ImageJ 1.46q), takes place within the first 30 min. Furthermore, to determine if phosphorylation is structure dependent, we boiled samples and repeated kinase assay. Based on Fig. 2.3.11, it is suggested that His-Stk1 cannot phosphorylate a denatured GraR protein.

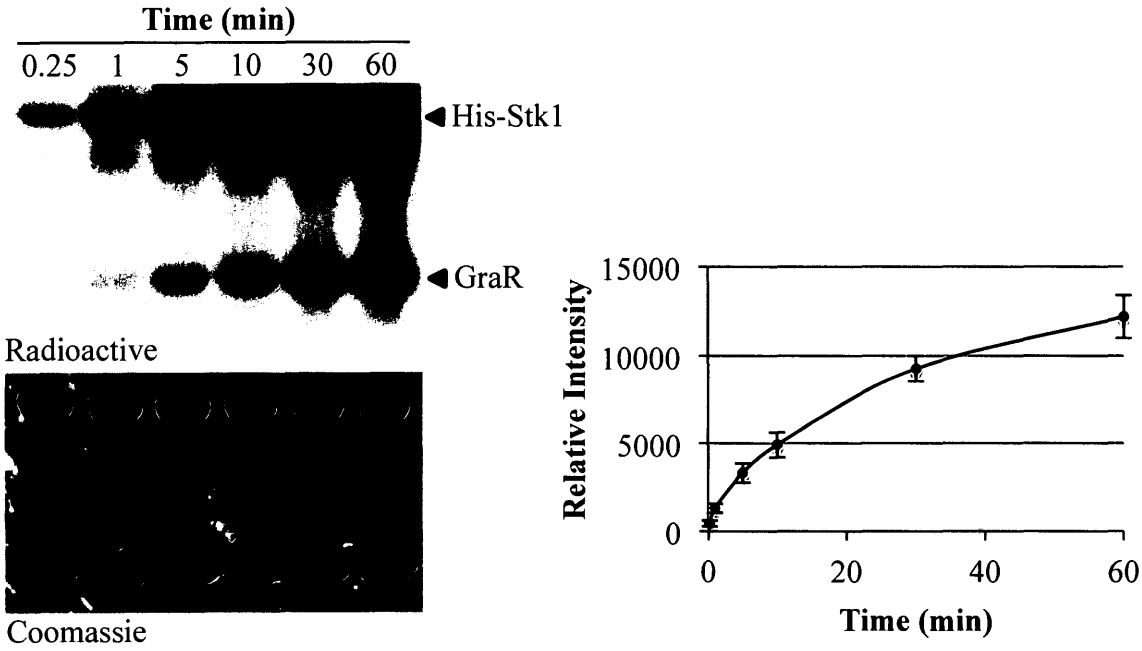

Figure 2.3.10 Time-dependent phosphorylation of GraR by His-Stk1
Time-dependent phosphorylation of GraR (25 μM) by His-Stk1 (20μM) in presence of [γ-^{32}P]-ATP (20 μM) and PB at various time intervals. Reactions were quenched with 5× SDS Gel-loading buffer and resolved with 15% SDS-PAGE. The gel was exposed to autoradiography cassette, scanned using TYPHOON Trio+ (GE Healthcare) and stained with Coomassie blue. Band intensity analyzed by ImageJ 1.46q and plotted against time.

In an attempt to answer how much of the GraR protein undergoes phosphorylation we employed the Phos-tag PAGE method. Briefly, this gel separates phosphorylated species from non-phosphorylated on a PAGE gel that can be analyzed by Coomassie blue staining. Based on Fig. 2.3.12, no phosphorylated GraR was detected by Coomassie blue staining; however, low levels were detected by autoradiography. These results suggest that under these conditions GraR undergoes low-levels, < 5%, of phosphorylation by His-Stk1. As a control the same reactions were also separated by conventional SDS-PAGE.

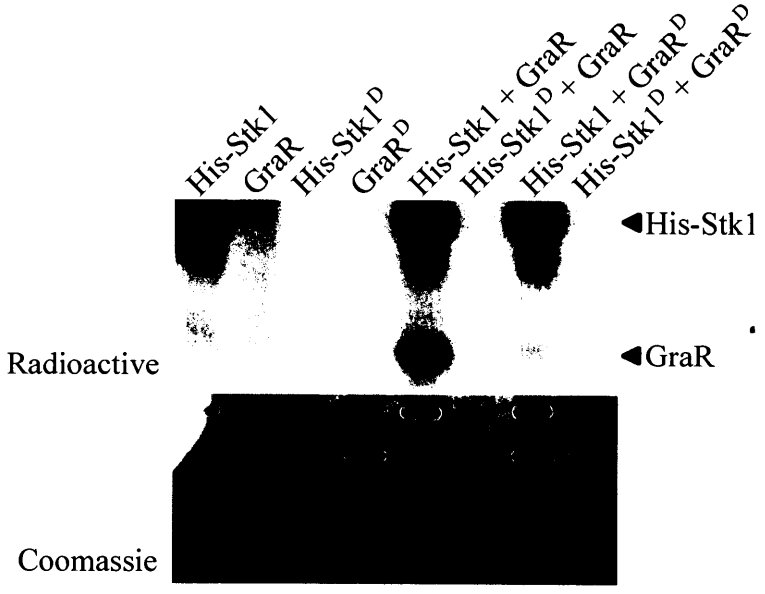

Figure 2.3.11 Phosphorylation of thermo-denatured GraR by His-Stk1
Denatured proteins were boiled for 10 min prior to reaction. 5 μM of native His-Stk1 or denatured His-Stk1 (His-Stk1^{D}) was incubated with native GraR or denatured GraR (GraR^{D}) at 20 μM in presence of [γ-^{32}P]-ATP (20 μM) and PB for 30 min at room temperature. Reactions were resolved with 15% SDS-PAGE. The gel was exposed to autoradiography cassette, scanned using TYPHOON Trio+ (GE Healthcare) and stained with Coomassie blue.

Albeit low levels of phosphorylation the results above indicate specificity towards GraR phosphorylation. Given that Stk1 and Stp1 are cotranscribed, and thus likely work as a pair, it was hypothesized that Stp1 is responsible for removing the phosphate group from GraR. To test this we carried out a phosphorylation assay, where His-Stk1 and GraR were first incubated with [γ-^{32}P]-ATP for 30 min at room temperature. Stp1 was subsequently added and the reaction proceeded for 30 more min. Indeed, as seen in Fig. 2.3.13, Stp1 was capable of dephosphorylation both His-Stk1 and GraR. It should be noted that Stp1 and GraR have similar molecular weights.

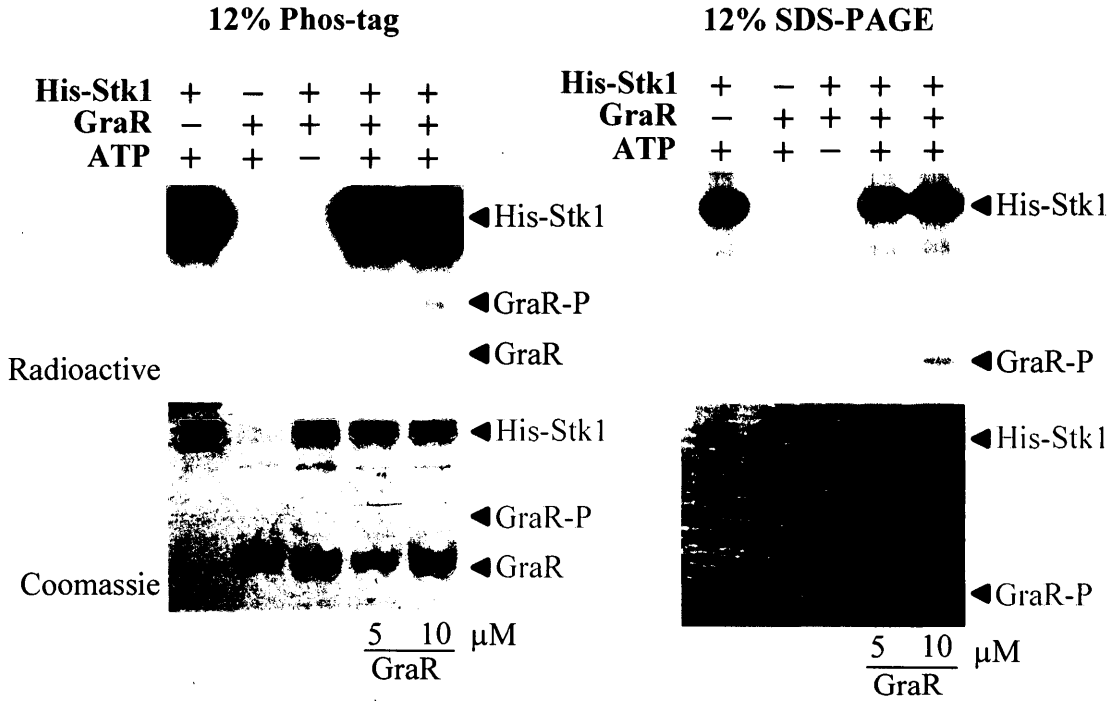

Figure 2.3.12 Quantifying GraR phosphorylation by Phos-tag PAGE
A master mixture of His-Stk1 (5 μM) and GraR (5 or 10 μM) was incubated with [γ-^{32}P]-ATP (20 μM) and PB for 30 min at 37°C. Reactions were quenched and loaded simultaneously to both 12% SDS-PAGE and 12% Phos-tag PAGE (100 μM Mn^{2+}-phos-tag). The gels were exposed to autoradiography cassette, scanned using TYPHOON Trio+ (GE Healthcare) and stained with Coomassie blue.

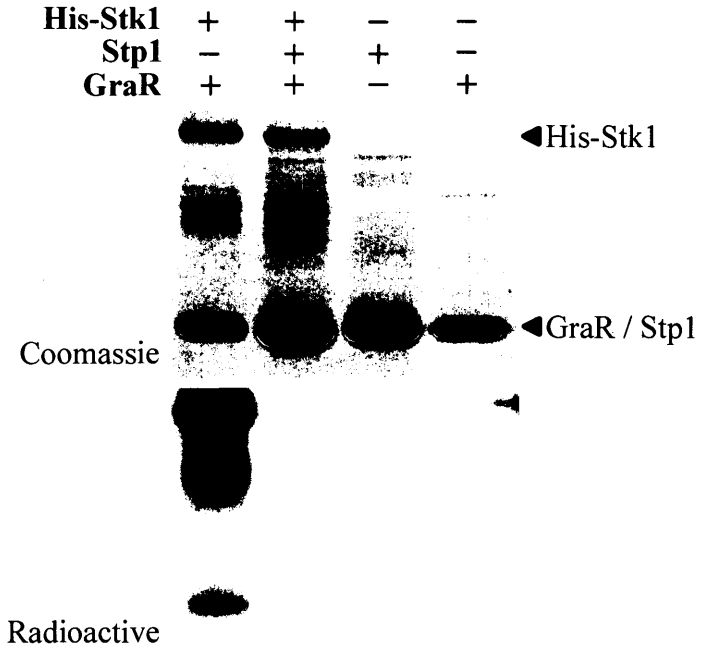

Figure 2.3.13 Phosphatase activity of Stp1 towards phosphorylated GraR
His-Stk1 (5 μM) was incubated with GraR (10 μM) and [γ-^{32}P]-ATP (20 μM) in PB for 30 min at room temperature. Stp1 (20 μM) was subsequently added to the mixture and the reaction proceeded for 30 min. Reactions were resolved with 15% SDS-PAGE. The gel was exposed to autoradiography cassette, scanned using TYPHOON Trio+ (GE Healthcare) and stained with Coomassie blue.

2.3.6 Investigating the Stk1-mediated phosphorylation sites of GraR

GraR is a transcription factor and belongs to the OmpR family of response regulators. This family of proteins is comprised of two clearly defined domains. We investigated which domain of GraR, the N- or the C-terminal, undergoes phosphorylation by His-Stk1. As observed in Fig. 2.3.14A the C-terminal domain of GraR, labeled GraR^{C}, underwent phosphorylation and was suggested to harbor the phosphorylation site/s. The N-terminal, GraR^{N}, did not undergo phosphorylation (Fig. 2.3.14B).

To confirm phosphorylation and establish the number of phosphorylation sites

we opted for mass spectrometry analysis. His-Stk1 and $GraR^C$ were incubated with and without cold ATP. Samples were separated by SDS-PAGE and the band of interest was cut out and trypsin-digested. These peptides were analyzed by liquid chromatography-mass spectrometry (LC-MS/MS) at the Advanced Protein Technology Centre, The Hospital for Sick Children (Toronto, Canada). The results identified threonine 128, 130 and 149 as the Stk1-mediated phosphorylation sites on $GraR^C$ (Fig. 2.3.15B). In the control reaction, His-Stk1 incubated with $GraR^C$ in the absence of ATP, no phosphorylation modifications were observed (2.3.15A).

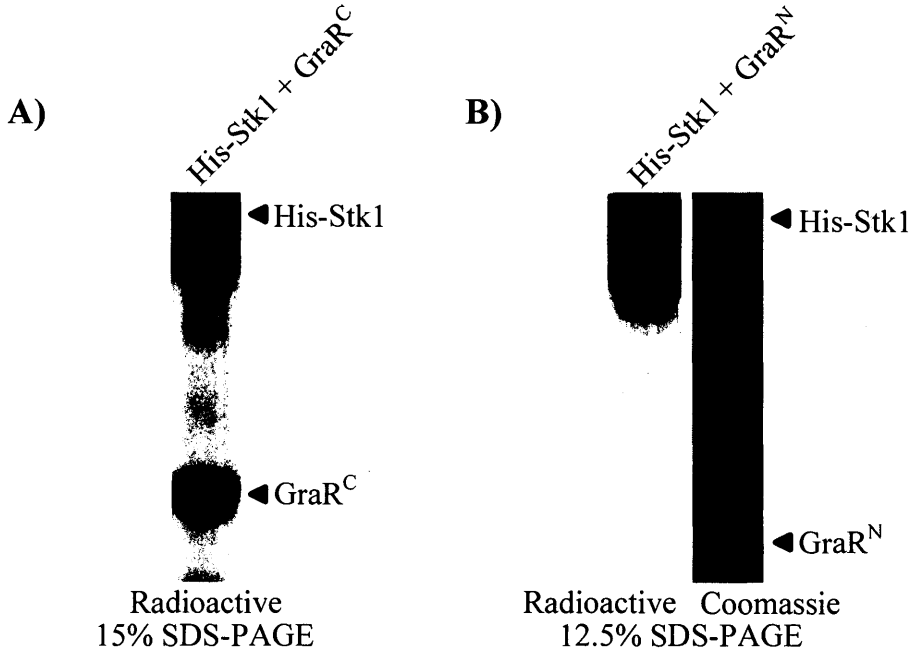

Figure 2.3.14 Phosphorylation of $GraR^C$ and $GraR^N$ terminals by His-Stk1
His-Stk1 (10 μM) and [γ-^{32}P]-ATP (20 μM) was incubated with A) 20 μM GraR-C terminal ($GraR^C$) or B) 20 μM GraR-N terminal ($GraR^N$) in PB for 30 min at room temperature. $GraR^C$ and $GraR^N$ were separated by 15% and 12.5% SDS-PAGE, respectively. Gels were exposed to autoradiography cassette and scanned using TYPHOON Trio+ (GE Healthcare). Only $GarR^N$ gel was further Coomassie stained.

It should be noted that full-length GraR was subjected to the same phosphorylation conditions as described above with cold ATP. The full length GraR was analyzed by liquid chromatography-mass spectrometry (LC-MS/MS) at the Centre for Research in Mass Spectrometry, York University (Toronto, Canada). This group confirmed the phosphorylation sites on the GraR C-terminal domain and ruled out any other phosphorylation sites, including the amino acids that span the GraR N-terminal domain. For ionization spectra refer to Appendix B.

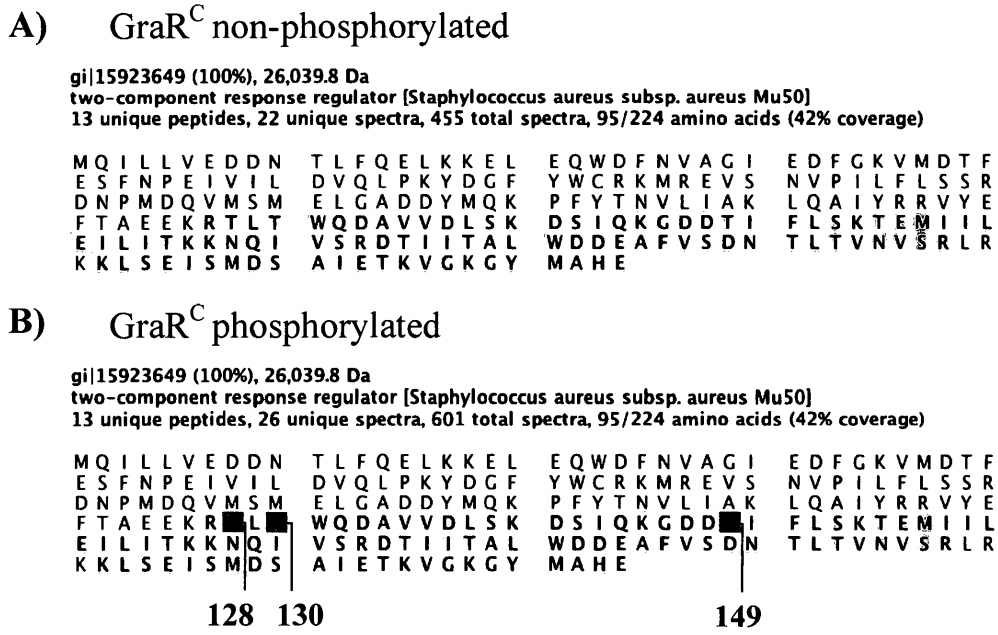

Figure 2.3.15 GraR phosphorylation sites determined by mass spectrometry
His-Stk1 (20 μM) was incubated with GarR^C (40 μM) in PB at room temperature for 60 min either A) without cold ATP or B) with cold ATP (500 μM). The highlighted portion (yellow) refers to amino acids within the unique peptides. Phosphorylation sites indicated in green with respective numbering. Data obtained from Scaffold program. The sequence coverage is 94% (95/101), not 42%, because it is the C-terminal only. For ionization spectra refer to Appendix B.

The identification of the putative phosphorylation sites on GraR allowed us to investigate whether mutating the threonine sites to alanine will have an effect on phosphorylation signal. Alanine residues do not undergo phosphorylation because they lack –OH group needed for substitution with phosphate group. Single GraR mutants where generated by site-directed mutagenesis and sequenced to ensure correct mutations. The results from these experiments suggest that all single mutants are capable of undergoing phosphorylation by His-Stk1 (Fig. 2.3.16). These experiments are not quantitative but there is a slight decrease in phosphorylation signal on the GraR-T149A mutant.

Given that mass spectrometry identified three phosphorylation sites and single mutant proteins were able to undergo phosphorylation, it was hypothesized that all three phosphorylation sites need to be mutated to fully abolish the phosphorylation signal. Following successful cloning of the GraR triple mutant, where all three threonine sites were mutated to alanines, various colonies were selected for expression. As can be seen in Appendix C there is high level of expression, however most, if not all, of the protein is aggregated in the pellet portion. In an attempt to solubilize the protein we carried out expression at lower concentrations of IPTG as well as lower temperature. However, the protein remained in the pellet portion and thus we were unable to purify the protein.

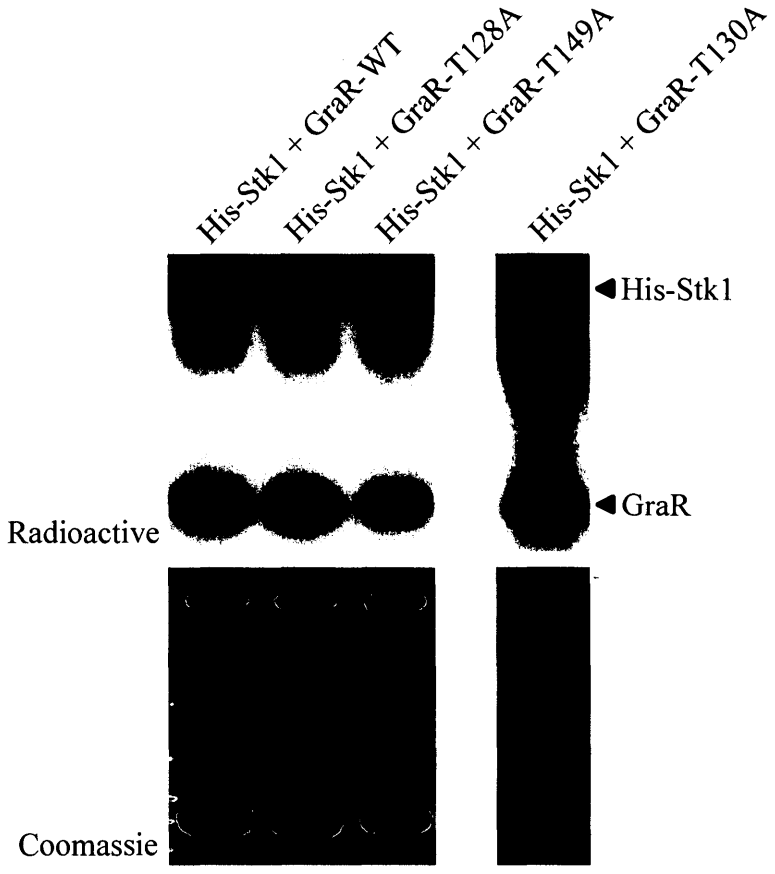

Figure 2.3.16 Phosphorylation of GraR single mutants by His-Stk1
His-Stk1 (5 μM) was incubated with GraR-WT (25 μM), GraR-T128A (25 μM), GraR-T130A (10 μM) and GraR-T149A (25 μM) with 20 μM [γ-^{32}P]-ATP (10 Ci/mmol) in PB at room temperature for 30 min. Proteins were separated by 15% SDS-PAGE. Gels were exposed to autoradiography cassette, which were scanned using TYPHOON Trio^{+} (GE Healthcare), and stained by Coomassie blue. Note GraR-T130A was run on separate gel on different day.

2.4 Discussion

Post-translational modification (PTM) in prokaryotes is an essential mechanism that allows modification of factors that ultimately govern the expression of other factors in order to maintain cellular equilibrium during stress. These stress responses, such as perturbations in the cell wall, are sensed and responded to by alterations in gene expression and protein activity. This is typically accomplished by two-component systems (TCS). The inherent properties of TCS to ensure bacterial survival prompted a lot of research in the field of signal transduction, in the hopes of exploiting these systems in order to decrease pathogenicity, resistance and virulence.

Briefly, upon sensing external stimuli a histidine kinase undergoes autophosphorylation at a histidine residue and transfers the phosphoryl group to the aspartic acid residue of a cognate response regulator. This phosphorylation event controls the activity of the response regulator by inducing conformational changes in the active site, or modifying protein-protein interaction. The end result is usually an alteration of gene expression to revert physiological equilibrium back to normal following the stress.

The majority of research in the field of prokaryotic signal transduction has focused on TCS, where the underlying theme is His/Asp phosphorylation. However, the discovery of Ser, Thr and Tyr phosphorylation in prokaryotes has propagated our understanding of the complex regulatory effects PTM can have on gene expression. A landmark study demonstrated the ability of *Bacillus subtilis* spores to exit dormancy by

sensing favorable conditions in the surrounding milieu (Shah et al., 2008). It was demonstrated that a *B. subtilis* STK was capable of binding peptidoglycan fragments, in turn signaling cells via PTM to come out of dormancy.

B. subtilis and *S. aureus* both contain one major STK, however, the latter does not form spores. Hence the function of the *S. aureus* STK, termed Stk1, is different then that of *B. subtilis*. Given the importance of Ser/Thr PTM and the lack of knowledge regarding Stk1 function in *S. aureus* this work aims to address the molecular mechanisms of Stk1 and cotranscribing Stp1 *in vitro*, focusing specifically on phosphorylation of new substrates.

Preliminary work by two independent groups paved the way for characterizing full length Stk1, and to a lesser extent, Stp1, functions *in vitro* (Beltramini et al., 2009; Debarbouille et al., 2009). However, it was necessary to establish our own protocols for working with these proteins. The Stk1 protein was expressed and purified as a His-tagged protein via Ni-NTA, whereas Stp1 was expressed and purified natively based on the protein's pI. Contrary to the above-mentioned papers our data suggest that His-Stk1 is capable of undergoing sufficient autophosphorylation with both magnesium and low-levels of manganese as cofactors. Furthermore, it was found that higher levels of manganese decreased autophosphorylation activity of His-Stk1. This observation corroborates the study by Donat et al., 2009, where the authors demonstrated a simlar pattern of phosphoryaltion.

Taken together, it is suggested that Stk1 autophosphorylation *in vivo* relies on

magnesium as a cofactor because excess amount of manganese is toxic to the cell (Jakubovics and Jenkinson, 2001). One group has demonstrated that *in vivo* survival of *S. aureus* depends on the manganese transport (Mnt) proteins (Horsburgh et al., 2002). It is interesting to propose that high-levels of manganese can upregulate the Mnt system, while simultaneously decreasing Stk1 activity, thus ensuring cellular ion balance is achieved prior to committing resources to upregulating virulence genes.

The versitility of phosphorylation depends on the reversibility of the reaction. In a prototypic TCS the histidine kinase is bifunctional and can catalyze both phosphorylation and dephosphorolation of its cognate response regulator (Laub and Goulian, 2007). Furthermore, the residues that undergo phosphorylation in TCSs, phosphohistidines and aspartyl-phosphates undergo rapid hydrolysis (Sickmann and Meyer, 2001; Stock et al., 1990). In contrast, phosphorylated Ser/Thr residues are less labile and have a much longer lifespan. Our data indicate that His-Stk1, following phosphorylation and removal of radioactive ATP, is stable for at least 30 min with no loss of signal.

This prompted us to investigate the phosphatase activity of Stp1 towards His-Stk1. As expected, Stp1 could completely dephosphorylate His-Stk1 *in vitro*, resulting in complete removal of radioactive signal. The phosphatase activity of Stp1 is necessary to quench the signaling cascade. Multiple studies have demonstrated that *S. aureus* strains with non-functional Stp1 become more resistant to vancomycin (Cameron et al., 2012; Cheung and Duclos, 2012; Renzoni et al., 2011). It was previously suggested that one

factor important for vancomycin resistance was cell wall thickening (Cui et al., 2003), a phentoype observed in the *S. aureus* Δ*stp1* strain (Beltramini et al., 2009). This phenotype likley arises from an "over-active" Stk1, where factors involved in cell wall synthesis, under the regulation of Stk1, are constitutively active. It cannot be ruled out that Stp1 is capable of dephosphorylating other targets besides Stk1.

As previously mentioned, other groups have identified targets of Stk1, such as the global transcription factors SarA and MgrA. However, a recent study in *Streptococcus agalactiae* identified a STK capable of phosphorylating a response regulator belonging to a TCS (Lin et al., 2009; Rajagopal et al., 2006). This observation was very intriguing because TCS pathways rarely cross talk at the level of phosphorylation with other systems.

The hallmark of this study was the discovery that His-Stk1 phosphorylates the response regulator GraR, which belongs to the GraSR TCS, *in vitro*. At the time of this writing, no peer-reviewed paper has established a connection between Stk1 and a response regulator of a TCS in *S. aureus*. Furthermore no *in vitro* study has confirmed GraR phosphorylation by its cognate histidine kinase (as a result of the inability to obtain an active form of the protein). Thus His-Stk1-mediated phosphorylation, and not GraS-mediated phosphorylation, of GraR will subsequently be referred to as GraR-P.

It was determined that Stk1 phosphorylated GraR in a time-dependent manner, where majority of phosphorylation occurred within 30 min. Furthermore, it was determined that Stp1 was capable of removing phosphorylation signal from GraR-P.

Taken together our *in vitro* kinase assays suggest Stk1/Stp1 are both involved in regulating GraR.

In order to address whether His-Stk1 phosphorylates GraR specifically we examined other *S. aureus* response regulators. It was determined that neither VraR nor WalR, under the conditions tested, could become phosphorylated in the presence of His-Stk1. VraR belongs to the NarL family of response regulators (Belcheva and Golemi-Kotra, 2008) and shares only 16% sequence similarity to GraR. WalR, on the other hand, shares 31% sequence similarity with GraR and both proteins belong to the OmpR family of response regulators (Okajima et al., 2008). We further investigated whether His-Stk1 could phosphorylate BceR, a response regulator from *B. subtilis*, which also belongs to the OmpR family and shares 56% sequence similarity to GraR. Interestingly, His-Stk1 could not phosphorylate BceR. Also, when GraR was thermo-denatured it was unable to undergo phosphorylation by His-Stk1. Together these results suggest that His-Stk1 specifically recognizes GraR at the molecular level, where unique structural folds determine recognition.

We attempted to quantify GraR phosphorylation by separating phospho species from nonphospho using Phos-tag gel. Our data indicates His-Stk1 phosphorylates <5% of GraR molecules under the conditions tested. The low level of phosphorylation could be due to suboptimal *in vitro* conditions, or another factor may be necessary to facilitate greater levels of phosphorylation. In order to speculate on the importance of phosphorylation levels *in vivo*, the total amount of GraR-P should be assessed by a more

accurate method such as mass spectrometry with an internal standard (Witze et al., 2007).

Response regulators typically consist of two unique domains, the N- and C-termini. The OmpR family of regulators are defined by their C-terminal amino acid sequence and three-dimensional structure (Itou and Tanaka, 2001; Martinez-Hackert and Stock, 1997). Given that GraR belongs to the OmpR family of response regulators and contains two unique domains, we were interested to determine which of these undergoes phosphorylation by His-Stk1. It was determined that phosphorylation was exclusive to the C-terminal domain, or DNA-binding domain, of GraR. It is beyond the scope of this work to dwell on the molecular effects phosphorylation could have on the C-terminal because no three dimensional structure of GraR exists. Needless to say these proteins tend to have flexible linkers, which allows for various dimer symmetries (Gao and Stock, 2009). Hence it remains to be determined whether phosphorylation enhances or represses DNA-binding or alters protein-protein interaction.

To confirm phosphorylation and determine the amino acids involved we sent $GraR^{C}$ and $GraR^{C}$-P for LC-MS/MS analysis. Mass spectrometry identified three phosphorylation sites on two different peptides: Thr128, Thr130 and Thr149. It should be noted some of these peptides were modified with both Thr128 and Thr130, suggesting these two residues can be simultaneously phosphorylated. Interestingly, when comparing BceR and GraR amino acid sequences the putative phosphorylation sites are located in the region that contains the most variability between the two proteins (Fig. 2.3.9).

To confirm these findings we collaborated with Dr. Siu's research group (Centre

for Research in Mass Spectrometry, York University), which analyzed the full length GraR by mass spectrometry. Findings from the full length GraR corroborated our initial data regarding the phosphorylation sites. As well, no phosphorylated residues were identified in the N-terminal domain.

To validate these results we opted for a mutagenesis approach, where single mutants of GraR, containing Thr to Ala mutations, were constructed. Despite the lack of a threonine residue, phosphorylation was attainable in all the GraR single mutants. There was a slight decrease in signal with the GarR-Thr149 mutant, but overall signal was not abolished. This result is contradictory to a recently published paper that described Stk1 phosphorylation of the global regulator CcpA (Leiba et al., 2012). It was observed that CcpA undergoes phosphorylation at two threonine sites: Thr18 and Thr33. However, when only a single Thr was mutated to Ala the entire phosphorylation signal was abolished. This is quite perplexing, as mutating one Thr should leave the other Thr intact and capable of phosphorylation.

We attempted to abolish phosphorylation by mutating all three Thr residues within GraR. We were able to clone the gene, however, when expressing the protein it became apparent that GraR-triple mutant was insoluble. It is very likely that simultaneously mutating three residues caused a deleterious affect on the three-dimensional structure. Various methods were employed to solubilize the protein, such as decreased IPTG concentrations and lower temperatures (Sorensen and Mortensen, 2005). However, the GraR-triple mutant remained insoluble and we were unable to obtain

protein for further investigation. Even if we could resolubilize the protein from the pellet portion, it is very likely this protein is aberrant and lack of phosphorylation is more the result of improper folding then residue specificity.

It should be noted that we observed phosphorylation of the penicillin-binding protein FmtA. It is unclear what the molecular mechanism or the significance of this phosphorylation is.

Cumulatively we provide strong evidence that His-Stk1 specifically phosphorylates GraR *in vitro*. More specifically, phosphorylation occurs on the GraR C-terminal domain on three threonine residues: Thr128, T130 and T149. Two separate mass spectrometry groups identified these residues. There was no evidence that other response regulators, regardless of family, were capable of undergoing phosphorylation by His-Stk1. The strongest data supporting our claim is that BceR, a homolog of GraR, was not phosphorylated by His-Stk1. Through sequence alignments we were able to demonstrate the amino acid discrepancy in and around the putative phosphorylation sites between BceR and GraR. In conclusion, the findings herein aim at progressing our understanding of signal transduction mechanisms within the complex regulatory network of the *S. aureus* pathogen.

References

Bakal, C.J., and Davies, J.E. (2000). No longer an exclusive club: eukaryotic signalling domains in bacteria. Trends Cell Biol *10*, 32-38.

Belcheva, A., and Golemi-Kotra, D. (2008). A close-up view of the VraSR two-component system. A mediator of Staphylococcus aureus response to cell wall damage. J Biol Chem *283*, 12354-12364.

Beltramini, A.M., Mukhopadhyay, C.D., and Pancholi, V. (2009). Modulation of cell wall structure and antimicrobial susceptibility by a Staphylococcus aureus eukaryote-like serine/threonine kinase and phosphatase. Infect Immun *77*, 1406-1416.

Brunskill, E.W., and Bayles, K.W. (1996). Identification and molecular characterization of a putative regulatory locus that affects autolysis in Staphylococcus aureus. J Bacteriol *178*, 611-618.

Cameron, D.R., Ward, D.V., Kostoulias, X., Howden, B.P., Moellering, R.C., Jr., Eliopoulos, G.M., and Peleg, A.Y. (2012). Serine/threonine phosphatase Stp1 contributes to reduced susceptibility to vancomycin and virulence in Staphylococcus aureus. J Infect Dis *205*, 1677-1687.

Chang, C., and Stewart, R.C. (1998). The two-component system. Regulation of diverse signaling pathways in prokaryotes and eukaryotes. Plant Physiol *117*, 723-731.

Cheung, A., and Duclos, B. (2012). Stp1 and Stk1: the Yin and Yang of vancomycin sensitivity and virulence in vancomycin-intermediate Staphylococcus aureus strains. J Infect Dis *205*, 1625-1627.

Cluzel, M.E., Zanella-Cleon, I., Cozzone, A.J., Futterer, K., Duclos, B., and Molle, V. (2010). The Staphylococcus aureus autoinducer-2 synthase LuxS is regulated by Ser/Thr phosphorylation. J Bacteriol *192*, 6295-6301.

Cui, L., Ma, X., Sato, K., Okuma, K., Tenover, F.C., Mamizuka, E.M., Gemmell, C.G., Kim, M.N., Ploy, M.C., El-Solh, N., *et al.* (2003). Cell wall thickening is a common feature of vancomycin resistance in Staphylococcus aureus. J Clin Microbiol *41*, 5-14.

Debarbouille, M., Dramsi, S., Dussurget, O., Nahori, M.A., Vaganay, E., Jouvion, G., Cozzone, A., Msadek, T., and Duclos, B. (2009). Characterization of a serine/threonine kinase involved in virulence of Staphylococcus aureus. J Bacteriol *191*, 4070-4081.

Didier, J.P., Cozzone, A.J., and Duclos, B. (2010). Phosphorylation of the virulence regulator SarA modulates its ability to bind DNA in Staphylococcus aureus. FEMS Microbiol Lett *306*, 30-36.

Donat, S., Streker, K., Schirmeister, T., Rakette, S., Stehle, T., Liebeke, M., Lalk, M., and Ohlsen, K. (2009). Transcriptome and functional analysis of the eukaryotic-type serine/threonine kinase PknB in Staphylococcus aureus. J Bacteriol *191*, 4056-4069.

Falord, M., Karimova, G., Hiron, A., and Msadek, T. (2012). GraXSR proteins interact with the VraFG ABC transporter to form a five-component system required for cationic antimicrobial peptide sensing and resistance in Staphylococcus aureus. Antimicrob Agents Chemother *56*, 1047-1058.

Fan, X., Liu, Y., Smith, D., Konermann, L., Siu, K.W., and Golemi-Kotra, D. (2007). Diversity of penicillin-binding proteins. Resistance factor FmtA of Staphylococcus aureus. J Biol Chem *282*, 35143-35152.

Gao, R., and Stock, A.M. (2009). Biological insights from structures of two-component proteins. Annu Rev Microbiol *63*, 133-154.

Horsburgh, M.J., Wharton, S.J., Cox, A.G., Ingham, E., Peacock, S., and Foster, S.J. (2002). MntR modulates expression of the PerR regulon and superoxide resistance in Staphylococcus aureus through control of manganese uptake. Mol Microbiol *44*, 1269-1286.

Ito, T., Katayama, Y., and Hiramatsu, K. (1999). Cloning and nucleotide sequence determination of the entire mec DNA of pre-methicillin-resistant Staphylococcus aureus N315. Antimicrob Agents Chemother *43*, 1449-1458.

Itou, H., and Tanaka, I. (2001). The OmpR-family of proteins: insight into the tertiary structure and functions of two-component regulator proteins. J Biochem *129*, 343-350.

Jakubovics, N.S., and Jenkinson, H.F. (2001). Out of the iron age: new insights into the critical role of manganese homeostasis in bacteria. Microbiology *147*, 1709-1718.

Kinoshita, E., and Kinoshita-Kikuta, E. (2011). Improved Phos-tag SDS-PAGE under neutral pH conditions for advanced protein phosphorylation profiling. Proteomics *11*, 319-323.

Kinoshita, E., Kinoshita-Kikuta, E., Takiyama, K., and Koike, T. (2006). Phosphate-binding tag, a new tool to visualize phosphorylated proteins. Mol Cell Proteomics *5*, 749-757.

Kuroda, M., Kuroda, H., Oshima, T., Takeuchi, F., Mori, H., and Hiramatsu, K. (2004). Two-component system VraSR positively modulates the regulation of cell-wall biosynthesis pathway in Staphylococcus aureus. Molecular Microbiology *49*, 807-821.

Kuroda, M., Ohta, T., Uchiyama, I., Baba, T., Yuzawa, H., Kobayashi, I., Cui, L., Oguchi, A., Aoki, K.-i., Nagai, Y., *et al.* (2001). Whole genome sequencing of meticillin-resistant Staphylococcus aureus. The Lancet *357*, 1225-1240.

Laub, M.T., and Goulian, M. (2007). Specificity in two-component signal transduction pathways. Annu Rev Genet *41*, 121-145.

Leiba, J., Hartmann, T., Cluzel, M.E., Cohen-Gonsaud, M., Delolme, F., Bischoff, M., and Molle, V. (2012). A Novel Mode of Regulation of the Staphylococcus aureus Catabolite Control Protein A (CcpA) Mediated by Stk1 Protein Phosphorylation. J Biol Chem *287*, 43607-43619.

Lin, W.J., Walthers, D., Connelly, J.E., Burnside, K., Jewell, K.A., Kenney, L.J., and Rajagopal, L. (2009). Threonine phosphorylation prevents promoter DNA binding of the Group B Streptococcus response regulator CovR. Mol Microbiol *71*, 1477-1495.

Liu, Q., Fan, J., Niu, C., Wang, D., Wang, J., Wang, X., Villaruz, A.E., Li, M., Otto, M., and Gao, Q. (2011). The eukaryotic-type serine/threonine protein kinase Stk is required for biofilm formation and virulence in Staphylococcus epidermidis. PLoS One *6*, e25380.

Lomas-Lopez, R., Paracuellos, P., Riberty, M., Cozzone, A.J., and Duclos, B. (2007). Several enzymes of the central metabolism are phosphorylated in Staphylococcus aureus. FEMS Microbiol Lett *272*, 35-42.

Martinez-Hackert, E., and Stock, A.M. (1997). Structural relationships in the OmpR family of winged-helix transcription factors. J Mol Biol *269*, 301-312.

Miller, M., Donat, S., Rakette, S., Stehle, T., Kouwen, T.R., Diks, S.H., Dreisbach, A., Reilman, E., Gronau, K., Becher, D., *et al.* (2010). Staphylococcal PknB as the first prokaryotic representative of the proline-directed kinases. PLoS One *5*, e9057.

Munoz-Dorado, J., Inouye, S., and Inouye, M. (1991). A gene encoding a protein serine/threonine kinase is required for normal development of M. xanthus, a gram-negative bacterium. Cell *67*, 995-1006.

Okajima, T., Doi, A., Okada, A., Gotoh, Y., Tanizawa, K., and Utsumi, R. (2008). Response regulator YycF essential for bacterial growth: X-ray crystal structure of the DNA-binding domain and its PhoB-like DNA recognition motif. FEBS Lett *582*, 3434-3438.

Paracuellos, P., Ballandras, A., Robert, X., Kahn, R., Herve, M., Mengin-Lecreulx, D., Cozzone, A.J., Duclos, B., and Gouet, P. (2010). The extended conformation of the 2.9-A crystal structure of the three-PASTA domain of a Ser/Thr kinase from the human pathogen Staphylococcus aureus. J Mol Biol *404*, 847-858.

Pullen, K.E., Ng, H.L., Sung, P.Y., Good, M.C., Smith, S.M., and Alber, T. (2004). An alternate conformation and a third metal in PstP/Ppp, the M. tuberculosis PP2C-Family Ser/Thr protein phosphatase. Structure *12*, 1947-1954.

Rajagopal, L., Vo, A., Silvestroni, A., and Rubens, C.E. (2006). Regulation of cytotoxin expression by converging eukaryotic-type and two-component signalling mechanisms in Streptococcus agalactiae. Mol Microbiol *62*, 941-957.

Rakette, S., Donat, S., Ohlsen, K., and Stehle, T. (2012). Structural analysis of Staphylococcus aureus serine/threonine kinase PknB. PLoS One *7*, e39136.

Renzoni, A., Andrey, D.O., Jousselin, A., Barras, C., Monod, A., Vaudaux, P., Lew, D., and Kelley, W.L. (2011). Whole genome sequencing and complete genetic analysis reveals novel pathways to glycopeptide resistance in Staphylococcus aureus. PLoS One *6*, e21577.

Shah, I.M., Laaberki, M.H., Popham, D.L., and Dworkin, J. (2008). A eukaryotic-like Ser/Thr kinase signals bacteria to exit dormancy in response to peptidoglycan fragments. Cell *135*, 486-496.

Sharma-Kuinkel, B.K., Mann, E.E., Ahn, J.S., Kuechenmeister, L.J., Dunman, P.M., and Bayles, K.W. (2009). The Staphylococcus aureus LytSR two-component regulatory system affects biofilm formation. J Bacteriol *191*, 4767-4775.

Sickmann, A., and Meyer, H.E. (2001). Phosphoamino acid analysis. Proteomics *1*, 200-206.

Sorensen, H.P., and Mortensen, K.K. (2005). Soluble expression of recombinant proteins in the cytoplasm of Escherichia coli. Microb Cell Fact *4*, 1.

Stock, A.M., Robinson, V.L., and Goudreau, P.N. (2000). Two-component signal transduction. Annu Rev Biochem *69*, 183-215.

Stock, J.B., Stock, A.M., and Mottonen, J.M. (1990). Signal transduction in bacteria. Nature *344*, 395-400.

Sun, F., Ding, Y., Ji, Q., Liang, Z., Deng, X., Wong, C.C., Yi, C., Zhang, L., Xie, S., Alvarez, S., *et al.* (2012). Protein cysteine phosphorylation of SarA/MgrA family transcriptional regulators mediates bacterial virulence and antibiotic resistance. Proc Natl Acad Sci U S A *109*, 15461-15466.

Tamber, S., Schwartzman, J., and Cheung, A.L. (2010). Role of PknB kinase in antibiotic resistance and virulence in community-acquired methicillin-resistant Staphylococcus aureus strain USA300. Infect Immun *78*, 3637-3646.

Truong-Bolduc, Q.C., Ding, Y., and Hooper, D.C. (2008). Posttranslational modification influences the effects of MgrA on norA expression in Staphylococcus aureus. J Bacteriol *190*, 7375-7381.

Ventura, C.L., Malachowa, N., Hammer, C.H., Nardone, G.A., Robinson, M.A., Kobayashi, S.D., and DeLeo, F.R. (2010). Identification of a novel Staphylococcus aureus two-component leukotoxin using cell surface proteomics. PLoS One *5*, e11634.

Witze, E.S., Old, W.M., Resing, K.A., and Ahn, N.G. (2007). Mapping protein post-translational modifications with mass spectrometry. Nat Methods *4*, 798-806.

Yang, S.J., Bayer, A.S., Mishra, N.N., Meehl, M., Ledala, N., Yeaman, M.R., Xiong, Y.Q., and Cheung, A.L. (2012). The Staphylococcus aureus two-component regulatory system, GraRS, senses and confers resistance to selected cationic antimicrobial peptides. Infect Immun *80*, 74-81.

Yarwood, J.M., McCormick, J.K., and Schlievert, P.M. (2001). Identification of a novel two-component regulatory system that acts in global regulation of virulence factors of Staphylococcus aureus. J Bacteriol *183*, 1113-1123.

Zhang, W., Munoz-Dorado, J., Inouye, M., and Inouye, S. (1992). Identification of a putative eukaryotic-like protein kinase family in the developmental bacterium Myxococcus xanthus. J Bacteriol *174*, 5450-5453.

CHAPTER THREE

ANALYSIS OF STK1-MEDIATED GRAR PHOSPHORYLATION *IN VIVO*

3.1 Introduction

Research on signal transduction in prokaryotes has primarily focused on two-component systems (TCS) (Capra and Laub, 2012). The reason these systems were appealing to study was the result of faithful flow of information. Following sensing an external cue, the histidine kinase undergoes autophosphorylation and becomes active. The enzyme is then capable of phosphorylating its cognate response regulator, usually a DNA-binding protein, and a response is elicited. The important part of this flow of information is that the kinase and response regulator selectively recognize each other. In other words, there is very little cross talk with other TCS. In *S. aureus* there are 16 TCS (Kuroda et al., 2001), thus it's vital to turn on pathways only when required.

Typically a single TCS is responsible for activating a very specific pathway, which makes *in vivo* investigation through knockouts a fairly straightforward task. For example, the *S. aureus* ΔvraSR mutant was found to be extremely sensitive towards many classes of antibiotics that act on the cell wall, such as fosfomycin, bacitracin, β-lactams and teicoplanin (Kuroda et al., 2004). The authors concluded that the VraSR system had a profound effect on cell-wall peptidoglycan synthesis. Many instances exist where a TCS

is inactivated, a loss of function is observed, and in hindsight the loss of function is assigned to that particular TCS. Although slightly off-topic, this approach was so elegantly described by Yuri Lazebnik that anyone studying signaling pathways, apoptosis in the authors case, should give it a read (Lazebnik, 2002).

Unfortunately this approach does not work so well with prokaryotic phosphorylation cascades involving Ser, Thr or Tyr residues, because kinases are promiscuous and multiple factors can be phosphorylated. In a recent review it was demonstrated that *Mycobacterium tuberculosis* has 11 kinases capable of Ser/Thr phosphorylation (Pereira et al., 2011), with a phosphoproteome containing over 300 targets (Prisic et al., 2010). Furthermore these factors themselves have significant global impacts that yield pleiotropic phenotypes.

Staphylococcus aureus strains contain one major STK (Stk1), however, in a subset of methicillin-resistant strains, such as MU50 and MW2, exists an atypical STK (Beltramini et al., 2009), termed Stk2 (SA0077 in N315). This second kinase does not traverse the membrane and thus contains no PASTA domains; it exists freely within the cytoplasm. Unpublished data suggests this second STK is active (Cheung and Duclos, 2012) but it remains unclear as to what its physiological roles or targets are. To date it is accepted that Stk1 carries out the majority of Ser/Thr phosphorylation in *S. aureus*.

Despite the presence of only one identified STK in the majority of *S. aureus* strains, the removal of this gene causes a profound alteration in global gene expression. A transcriptome profile of an *S. aureus* Δ*stk1* mutant demonstrated that of the 2,666 genes

evaluated expression of 72 ORFs were repressed and expression of 185 ORFs was increased (Donat et al., 2009). The authors concluded that the majority of these genes belong to nucleotide biosynthesis, cell wall metabolism, and central metabolic pathways. The important point here is that Stk1 plays a global regulatory role in *S. aureus*; hence it is not much of a surprise that multiple targets are phosphorylated. And the phosphorylation of factors by Skt1 could be an additional PTM to an already established layer of control. In *Myxococcus xanthus* it was found that a transcription factor can be under the control of a STK and a histidine kinase to control a single signaling event (Lux and Shi, 2005).

The points raised above are intended to remind the reader of the challenges associated with assigning specific functions to STKs. Nonetheless, the aim of the following study is to investigate *in vivo* the relevance of our *in vitro* work, which has demonstrated that Stk1 is capable of specifically phosphorylating GraR. Through complementation studies of an *S. aureus* Δ*graR* mutant, we aimed to understand the importance of the putative Stk1-mediated phosphorylation sites of GraR.

3.2 Materials and Methods

3.2.1 Materials and chemicals

Wizard® Genomic DNA Purification Kit for *S. aureus* genome extraction (Promega). QIAquick PCR Purification Kit was used to clean up DNA (Qiagen). Bacto™ Tryptic Soy Broth from BD (Becton, Dickson and Company) and Agar-Agar (granulated) from EMD (Millipore, USA). Vancomycin from Sigma Aldrich and chloramphenicol from EMD (Millipore, USA).

3.2.2 Generation of complementation plasmid pMK4

3.2.2.1 Construction of P_{native}:*graR* and insertion into pSTBlue-1

To construct the pMK4 complementation plasmid it was first necessary to separately amplify the DNA fragments of interest, ligate them together and insert into an intermediate plasmid pSTBlue-1. The promoter chosen was the native promoter (P_{native}, 175 bp) of the *graXRS* operon, which was amplified from *S. aureus* 6390 genome with primer set Dir 5'- GCTAGGATCCCGCTAACATTGAAATGAAATTTTC and Rev 5'- GCTACATATGCTAAAATACTCCTTTAAACTGTAAC. The fragments were separated with 1% agarose gel and visualized by staining with ethidium bromide. The restriction cut sites *BamHI* (Dir primer) and *NdeI* (Rev primer) are underlined.

The full-length *graR* gene (675 bp) was amplified from *S. aureus* 6390 genome with the primer set Dir 5'- GCTACATATGCAAATACTACTAGTAGAAGATGAC and

Rev 5'- GCTAGTCGACTTATTCATGAGCCATATATCCTT. The restriction cut sites *NdeI* (Dir primer) and *SalI* (Rev primer) are underlined. Following amplification the PCR products were cleaned up with PCR-clean up kit according to manufacturer recommendations, digested with *NdeI* and ligated at room temperature with T4 DNA ligase for 30 min. The resulting ligation product, designated P_{native}:*graR*, was amplified with P_{native} Dir and *graR* Rev primers to yield an 850 bp product. The P_{native}:*graR* product was cloned within the multiple cloning site of pSTBlue-1 vector using the Perfectly Blunt Cloning kit. The resulting clone was used to transform NovaBlue cells, which were sequenced for the correct insert at The Centre for Applied Genomics, The Hospital for Sick Children (Toronto, Canada).

3.2.2.2 Construction of pMK4-P_{native}:*graR*

The *E. coli-S. aureus* shuttle vector pMK4 (5.6 Kbp) was used for complementation studies where ectopic GraR expression was required. P_{native}:*graR*, 850 bp, was gel extracted from pSTBlue-1 following double digestion with *BamHI/SalI*. The vector pMK4 was digested with *BamHI/SalI*. The product and plasmid were cleaned up and ligated as described in 3.2.2.1. The resulting clone, pMK4-P_{native}:*graR*, was used to transform NovaBlue cells, which were sequenced for the correct insert at The Centre for Applied Genomics, The Hospital for Sick Children (Toronto, Canada).

3.2.2.3 Site-directed mutagenesis of Stk1-mediated phosphorylation sites in pMK4-P_{native}:*graR*

In order to study the importance of the putative Stk1-mediated phosphorylation sites of GraR, pMK4-P_{native}:*graR* mutants were prepared. Double mutants harboring threonine to alanine substitutions at either Thr128 (encoded by ACA), Thr130 (encoded by ACT), Thr149 (encoded by ACG) and a triple mutant containing all three mutations were generated with the QuikChange™ Site-Directed Mutagenesis method (Stratagene). The three possible variations for double mutants (*graR*-T128A/T130A, *graR*-T128A/T149A or *graR*-T130A/T149A) were generated via two rounds of amplification of the pMK4-P_{native}:*graR* plasmid. Alanine substitutions are highlighted in bold within the PCR primers. The primers used were T128A Dir 5'-CTGAAGAAAAACGT**GCA**TTGACTTGGCAAG and Rev 5'-CTTGCCAAGTCAA**TGC**ACGTTTTTCTTCAG, T130A Dir 5'- GAAAAA CGTACATTG**GCT**TGGCAAGATGC and Rev 5'- GCATCTTGCCA**AGC**CAA TGTACGTTTTTC and T149A Dir 5'-AAAGGTGATCAG**GCG**ATTTTC and Rev 5'-GAAAAT**CGC**CTGATCACCTTT. The triple mutant was constructed through three separate rounds of amplification with the above primers. Following each round of mutagenesis the constructs were digested with *DpnI* and transformed into NovaBlue cells. Given the high success rate of site-directed mutagenesis the constructs were sequenced once all desired mutations were introduced (The Centre for Applied Genomics, The Hospital for Sick Children, Toronto).

3.2.3 Introduction of pMK4-P_{native}:*graR* into 6390 and Δ*graR* mutant

Following the successful generation of pMK4-P_{native}:*graR* and the respective

mutants it was necessary to introduced these constructs into *S. aureus*. The pMK4-P_{native}:*graR* was electroporated with a time constant of 2.5 ms and voltage of 2 kV in a 1 mm gap cuvette into restriction deficient *S. aureus* RN4220 strain which was plated on Tryptic Soy Broth (TSB)-agar containing chloramphenicol (40 μg/mL) and incubated for 12-16 hrs at 37°C. Transformants were grown overnight in TSB supplemented with chloramphenicol (10 μg/mL) at 37°C and the plasmid was purified using the GeneJET Plasmid Miniprep kit (Thermo Scientific) with minor modifications. Briefly, lysostaphin (10 μg) was incubated with 4 mL overnight culture in resuspension buffer at 37°C for 40 min, followed by incubation at 80°C for 5 min and then chilled for 1 min on ice. Once the reaction warmed to room temperature the rest of the steps were carried out as per GeneJET Plasmid Miniprep kit (Thermo Scientific) instructions. The purified DNA was double-digested with *BamHI* and *SalI* to ensure the plasmid contained the insert of interest.

The purified pMK4-P_{native}:*graR* and respective mutants from *S. aureus* RN4220 were further electroporated into *S. aureus* 6390 wild-type and Δ*graR* (6390 background).

3.2.4 Growth curve of 6390, Δ*graR* and Δ*graR* complemented (Thr-Ala mutation) mutant strains

A growth curve was performed under optimal conditions in 250 mL glass flasks. To avoid the loss of plasmid strains containing pMK4 were always grown in Chloramphenicol (10 μg/mL). Overnight seed cultures were grown in TSB at 37°C, 200 rpm. The overnight culture was diluted into fresh 50 mL TSB medium to an OD_{600} of

0.05, this is considered time zero. Cultures were shaken at 37°C, 200 rpm and OD_{600} readings were obtained by UV-Visible Spectrophotometer (Varian Cary 100 Bio) every 60 min.

3.2.5 MIC of 6390, Δ*graR* and Δ*graR* complemented (Thr-Ala mutation) strains

Vancomycin minimum inhibitory concentration (MIC) determinations were carried out in 96-well microtiter plate (300 µL culture volume). To avoid loss of plasmid strains containing pMK4 were grown in Chloramphenicol (10 µg/mL). Overnight seed cultures were grown in TSB at 37°C, 200 rpm and the OD_{600} measured prior to starting experiment. Bacterial cultures were grown until mid-log phase in 50 mL TSB, initially adjusted to OD_{600} of 0.05, at 37°C for 180 min. Bacterial cultures were diluted 1000-fold with TSB and used to inoculate wells containing 2-fold increments of vancomycin concentrations, no Chloramphenicol was added at this step. Plates were incubated for 48 hours at 37°C with no shaking and the OD_{600} was read on a Synergy H4 plate reader (BioTek).

3.3 Results

3.3.1 Generation of complementation plasmid pMK4

To investigate the relevance of GraR phosphorylation by Stk1 we opted to use an *S. aureus* Δ*graR* strain (*graR* knockout) and complement with plasmids containing wild type and mutant versions of the *graR* gene. The mutant plasmids have the putative Stk1-mediated GraR phosphorylation sites, based on our *in vitro* data, mutated to alanines. In order to carry out the complementation experiment, it was first necessary to generate a plasmid to carry the gene of interest. The cloning strategy is illustrated in detail in Fig. 3.3.1.

In order for complementation to mimic physiological conditions we chose to use the native promoter (P_{native}) of the *graXRS* operon, which has been described in detail (Falord et al., 2011). In between the promoter of interest and the *graR* gene is located another gene, *graX*, hence it was necessary to separately amplify the two fragments by PCR (Fig. 3.3.2A). Following amplification the P_{native}, 175 bp, and *graR*, 675 bp, fragments were cleaned up with a PCR-clean up kit, to remove unwanted enzymes and buffer, and ligated with T4 DNA ligase to yield the product P_{native}:*graR*, 850 bp (Fig. 3.3.2B). Without the need for restriction digestion this construct was directly inserted into the linearized pSTBlue-1 vector using the Perfectly Blunt ® Cloning Kit (EMD Millipore).

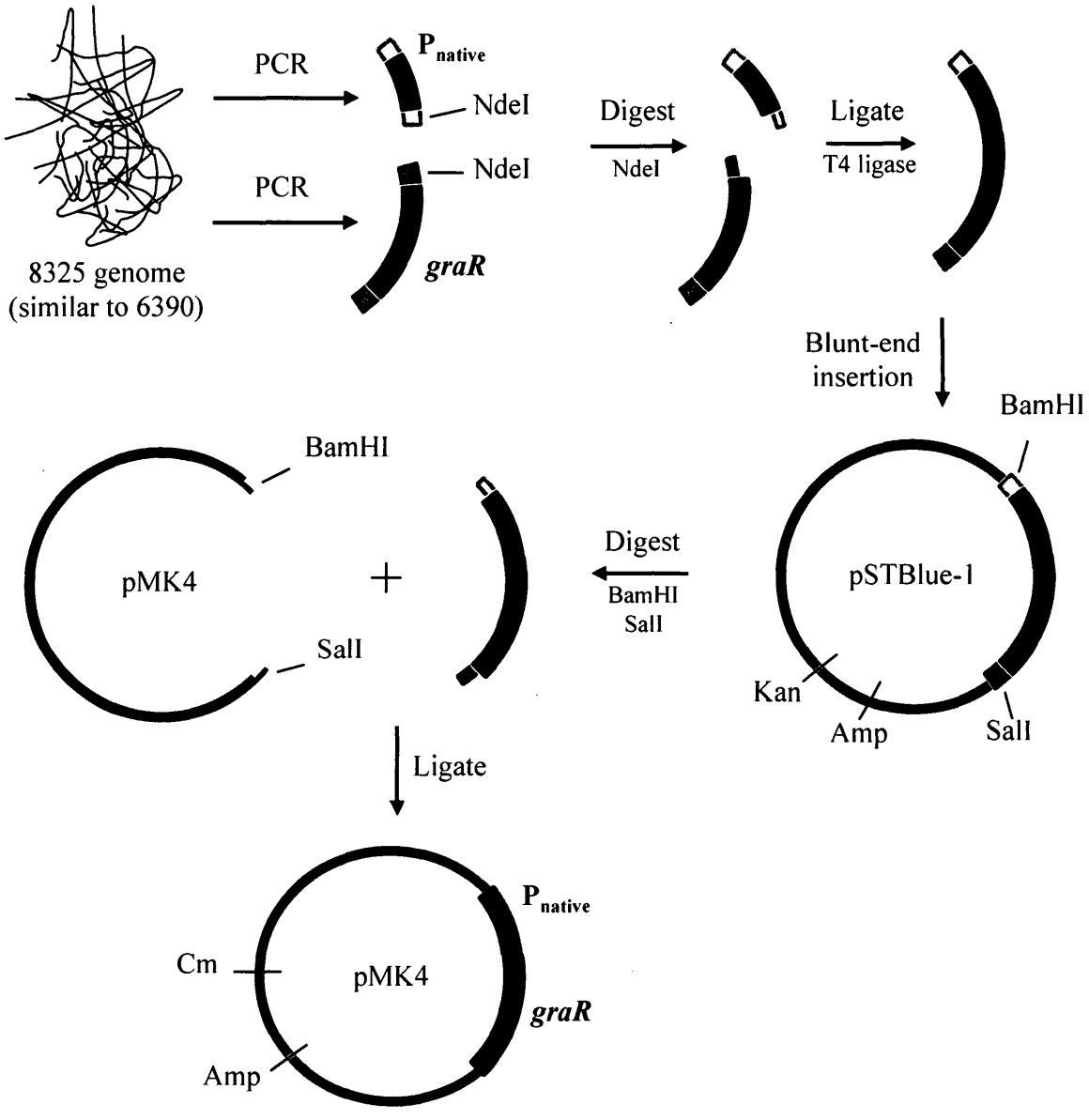

Figure 3.3.1 Cloning strategy for constructing pMK4-P_{native}:*graR*
A schematic depicting the cloning of the complementation plasmid pMK4 containing the native promoter (P_{native}) and the *graR* gene. The PCR products P_{native} and *graR* were separately amplified from *S. aureus* 8325 genome by PCR, digested with NdeI and ligated together to yield the product P_{native}:*graR*. The P_{native}:*graR* product was directly inserted into pSTBlue-1 as blunt end. P_{native}:*graR* was gel extracted from pSTBlue-1 following double digestion with BamHI/SalI. pMK4 plasmid was also double-digested with BamHI/SalI and the two products were ligated to yield the final construct pMK4-P_{native}:*graR*.

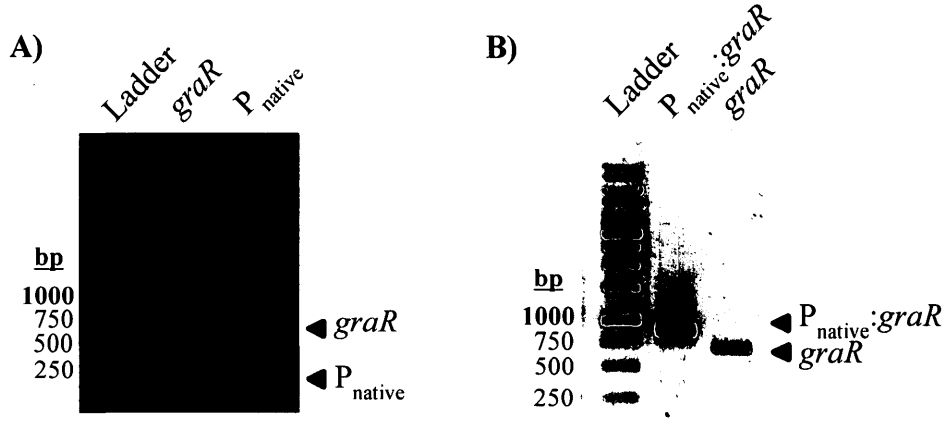

Figure 3.3.2 PCR amplification and ligation of P_{native} and *graR*
A) The promoter of the *graXRS* operon, termed P_{native} (175 bp), and the *graR* (675 bp) gene were separately PCR amplified from 8325 genome (similar to 6390). B) The fragments were digested with NdeI and ligated together to give the 850 bp product P_{native}:*graR*. The *graR* fragment was run as control. All fragments separated by 1% agarose and stained with ethidium bromide.

The pSTBlue-1-P_{native}:*graR* construct was transformed into NovaBlue cells and blue/white screening was performed to determine which colonies have the insert of interest. The white colonies were selected and double-digested to confirm insertion of P_{native}:*graR*. As seen in Fig. 3.3.3, ten colonies were screened and two contained inserts. The empty pSTBlue-1 vector was run alongside as a control. The colonies with inserts were sent for sequencing. The sequencing result for the chosen insert used in subsequent cloning steps can be found in Appendix D.

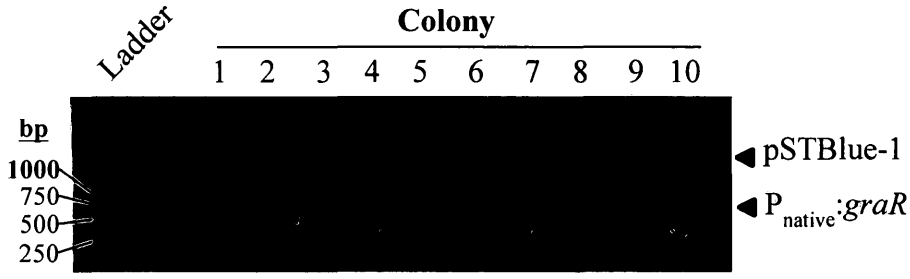

Figure 3.3.3 Screening pSTBlue-1 for the P_{native}:*graR* insert by double digestion
Following Blue/White screen ten white colonies were chosen; the pSTBlue-1 plasmid was isolated and double digested with BamHI and SalI. Colonies were considered positive for P_{native}:*graR* upon the release of a fragment 850 bp in size. Reactions were separated by 1% agarose gel and stained with ethidium bromide.

Following the successful sequencing of the pSTBlue-1 construct it was necessary to double digest in order to obtain P_{native}:*graR* for insertion into pMK4. The pMK4 plasmid was also double digested with *BamHI* and *SalI*. The two fragments were ligated together, and the newly constructed plasmid was inserted into *E. coli* cells. As can be see in Fig. 3.3.4, twelve colonies were screened and all contained the insert. Two colonies were selected and the pMK4-P_{native}:*graR* construct was sequenced. The sequencing result for these two colonies can be found in Appendix E.

Following the successful generation the pMK4-P_{native}:*graR* plasmid it was possible to proceed to mutating the putative Stk1-mediated threonine phosphorylation sites to alanines. Based on *in vitro* data it was suggested that mutating a single residue did not significantly abolish phosphorylation, thus we proceeded to making the three possible double mutants and a triple mutant. This was accomplished by using the Site-Directed Mutagenesis kit. All mutant constructs were sequenced.

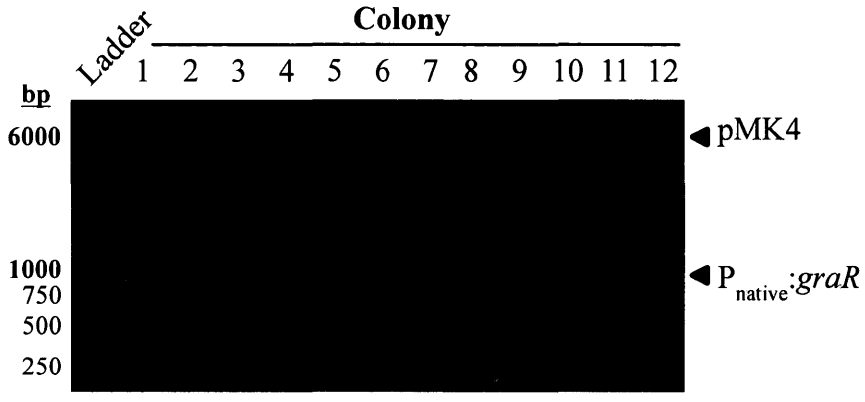

Figure 3.3.4 Screening *E. coli* pMK4 for the P_{native}:*graR* insert by double digestion
The pMK4 plasmid was isolated and double digested with BamHI and SalI. Colonies were considered positive for P_{native}:*graR* upon the release of a fragment 850 bp in size. Reactions were separated by 1% agarose gel and stained with ethidium bromide.

3.3.2 Electroporation of pMK4-P_{native}:*graR* into *S. aureus* strains

Following correct sequencing of pMK4-P_{native}:*graR* and respective mutants it was necessary to insert them into the *S. aureus* Δ*graR* strain. The Δ*graR* strain is a *graR* knockout strain that was generated from the wild type *S. aureus* strain 6390 by Dr. Ambrose Cheung's laboratory (Meehl et al., 2007). Given that pMK4-P_{native}:*graR* was isolated from *E. coli*, it is necessary to insert the DNA into a restriction-deficient strain of *S. aureus*, referred to as RN4220. The DNA was electroporated into RN4220 and grown on chloramphenicol plates. It was noticed that higher chloramphenicol concentrations (>20 μg/mL) were required in order to reduce the background growth. Several colonies were selected and the insertion of P_{native}:*graR* was confirmed by double digestion (Fig. 3.3.5).

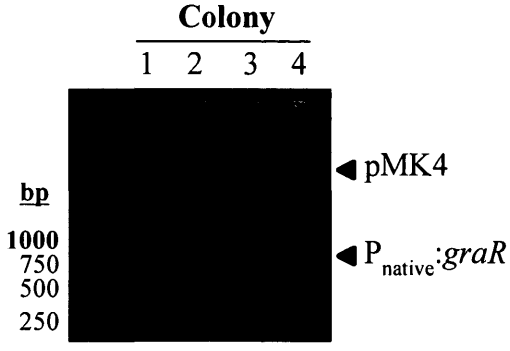

Figure 3.3.5 Screening *S. aureus* RN4220 pMK4 for the P_{native}:*graR* insert by double digestion
The pMK4 plasmid was isolated and double digested with BamHI and SalI. Colonies were considered positive for P_{native}:*graR* upon the release of a fragment 850 bp in size. Reactions were separated by 1% agarose gel and stained with ethidium bromide.

The pMK4- P_{native}:*graR* vector was isolated from RN4220 and inserted into Δ*graR* strain by electroporation and screened on TSB-agar plates containing 40μg/mL of chloramphenicol . For cloning purposes, as a control, 6390 was also electroporated with the pMK4-P_{native}:*graR* vector. This construct was not used for subsequent experiments given 6390 already contains the *graR* gene. The *S. aureus* 6390 and Δ*graR* strains were able to grow in the presence of chloramphenicol upon successful electroporation of pMK4 plasmid. In order to prevent loss of plasmid, 10 μg/mL of chloramphenicol was added to subsequent experiments where strains harboring the plasmids were used. It should be noted that 40 μg/mL of chloramphenicol is required for selection when selecting colonies from plates.

Although only the wild type pMK4-P_{native}:*graR* was described in detail, the same process of passaging through RN4220 was carried out for mutant derivatives of pMK4-

P_{native}:*graR* harboring the threonine to alanine mutations.

3.3.3 Growth curve of 6390 and Δ*graR* versus Δ*graR* complemented (Thr-Ala mutation) strains

An interesting observation of the Δ*graR* strain was that it reached stationary phase much quicker then wild type 6390. Furthermore, the number of cells at stationary phase, based on OD_{600}, was lower for Δ*graR* as compared to wild type 6390 (Fig. 2.3.6). Given this phenotype we tested whether Δ*graR* complemented with either pMK4-P_{native}:*graR* or pMK4-P_{native}:*graR*-mutants was capable of reverting the phenotype back to normal.

As can be observed in Fig. 3.3.6, all strains grew normally during early and mid exponential phase. Furthermore, the complemented strains all reverted the phenotype of the Δ*graR* mutant strain back to wild type. This is likely an indication that Stk1-mediated phosphorylation of GraR does not play a role in cell growth. Interestingly, the complemented Δ*graR* strains were capable of growing better then the wild type 6390. This is likely the result of multiple copies of the pMK4 plasmid within an individual *S. aureus* cell.

3.3.4 Vancomycin MIC of 6390 versus Δ*graR* complemented (Thr-Ala mutation) strains

Previous research by Meehl *et al.* has demonstrated that absence of *graR* sensitizes *S. aureus* strains towards vancomycin (Meehl et al., 2007). We tested this phenotype by assessing the MIC of the wild type 6390 strain against Δ*graR* and Δ*graR*

complemented strains. The results indicate that

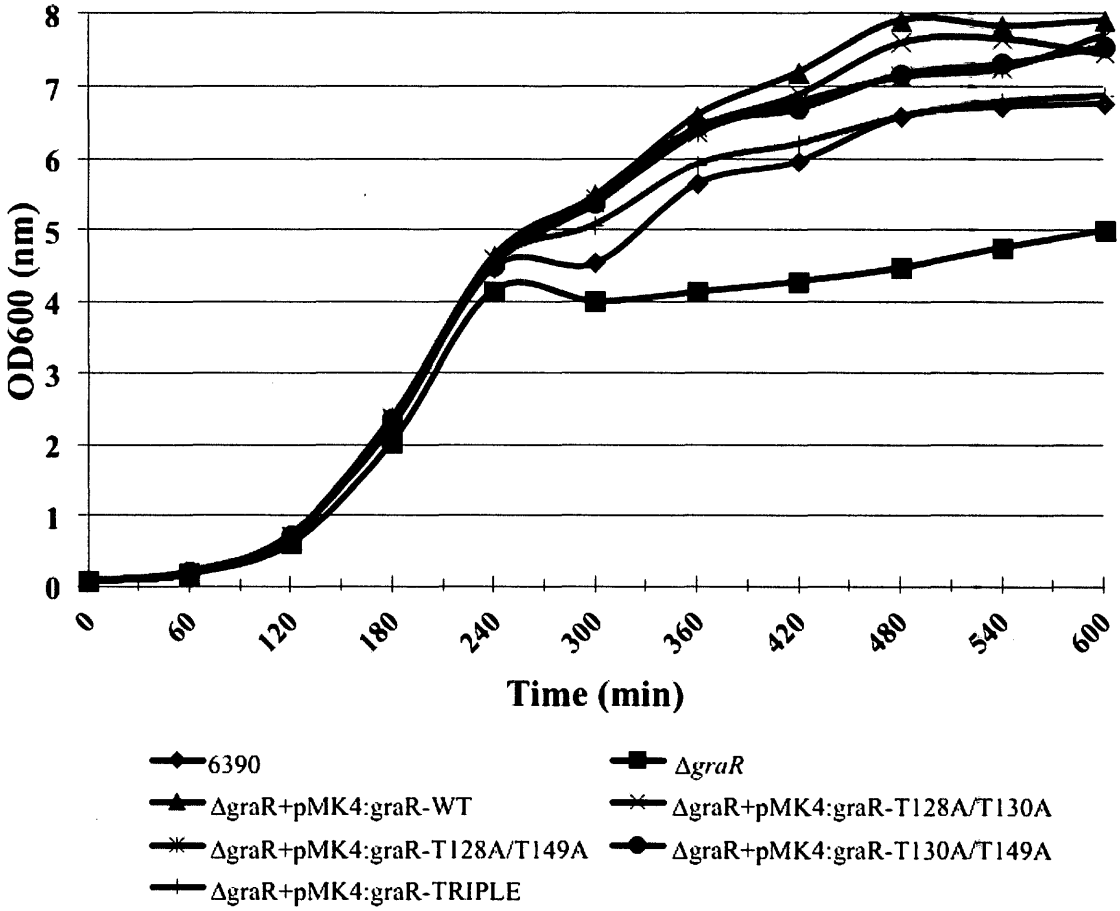

Figure 3.3.6 Growth curve of 6390 and ΔgraR versus ΔgraR complemented (Thr-Ala mutation) strains

Overnight seed cultures were diluted to an OD_{600} of 0.05 in TSB. The cultures were grown in flasks at 37°C, 200 rpm and readings were measured on a UV-Visible Spectrophotometer every 60 min. Chloramphenicol (10 μg/mL) added to cultures containing pMK4 plasmid.

6390 has an MIC of 1 μg/mL towards vancomycin, whereas Δ*graR* has an MIC of 0.5 μg/mL (Fig. 3.3.7). The values are based on growth, an elevated OD_{600}, in the particular well containing a given antibiotic concentration. If the OD_{600} is above baseline, depicted by a more intense blue color (raw data can be found in Appendix F), then that particular antibiotic concentration is unable to inhibit bacterial growth.

The lowest MIC value is determined by the well that contains no growth. All the Δ*graR*-complemented strains were able to revert the MIC back to 1 μg/mL, which suggest that Stk1-mediated phosphorylation sites likely do not play a role in vancomycin resistance.

Table 1 Vancomycin MICs of 6390, Δ*graR* and Δ*graR* complemented (Thr-Ala mutation) strains

Strain	Vancomycin MIC (μg/mL)
6390 [a]	1
Δ*graR* [a]	0.5
Δ*graR*+pMK4:*graR*-WT [a]	1
Δ*graR*+pMK4:*graR*-T128A/T130A [a]	1
Δ*graR*+pMK4:*graR*-T128A/T149A [b]	1
Δ*graR*+pMK4:*graR*-T130A/T149A [b]	1
Δ*graR*+pMK4:*graR*-TRIPLE [b]	1

Experiments were repeated at least [a]**three** times or [b]**two** times

3.4 Discussion

All living organisms, regardless of their location on the phylogenetic tree of life, must sense the constantly changing environment and respond accordingly. Multicellular organisms, in the classical sense, have specialized structures that relay information by converting it into a stimuli through nerve impulses. Prokaryotes on the other hand, such as *S. aureus*, depend upon two-component systems (TCS) for sensing and responding to environmental cues. Furthermore, it is becoming apparent that STKs, with their cognate STPs, also play an important role within this complex regulatory network. Together these systems respond and adapt to constantly changing environments.

The identification of STKs in prokaryotes has facilitated the need to understand their physiological roles. Unfortunately this was not a straightforward task, as STKs can phosphorylate multiple targets, which lead to complex pleiotropic phenotypes. Given this complexity many studies in *S. aureus* probing for targets of Stk1 have been carried out through *in vitro* kinase assays; such as the phosphorylation of MgrA (Truong-Bolduc et al., 2008), PurA (Donat et al., 2009) and SarA (Didier et al., 2010). These are very important discoveries that lay the foundations for future studies that will address their significance *in vivo.*

The discovery that Stk1 phosphorylates GraR *in vitro* has prompted us to investigate our findings *in vivo*. The goal was to complement an *S. aureus* Δ*graR* mutant strain with both wild type and mutant version of the *graR* gene, ectopically expressed on

a plasmid, and assess phenotypic differences. The plasmid chosen for complementation studies was the pMK4 vector, a pC194-fusion plasmid, which can replicate and yield chloramphenicol resistance in both *E. coli* and *S. aureus* (Sullivan et al., 1984). Majority of studies utilizing the pMK4 plasmid insert their gene of interest under the constitutively active P_{prot} promoter (Leimeister-Wachter et al., 1992). Due to high levels of expression that is achieved from P_{prot} we sought to express the *graR* gene under its native promoter, in order to mimic physiological conditions.

The native *graR* promoter regulates the entire *graXRS* operon (Falord et al., 2011). In between the promoter and *graR* lies the *graX* gene, thus we amplified the two fragments separately and ligated them together to yield P_{native}:*graR*. This fragments was inserted into the blunt end vector pSTBlue-1. Following sequencing the fragment was double digested from pSTBlue-1 and inserted directly into pMK4. The final product, pMK4-P_{native}:*graR* was passaged through *E. coli*, then the restriction-deficient *S. aureus* RN4220 and finally Δ*graR*. The Δ*graR* strain has an *S. aureus* 6390 background, which is very similar to RN4220, but contains digestive enzymes to protect against foreign DNA. Thus whenever electroporating DNA into *S. aureus* strains it is necessary to use RN4220 as an intermediate strain.

In order to investigate the importance of Stk1-mediated phosphorylation sites we generated mutant pMK4-P_{native}:*graR* plasmids where the Thr sites were mutated to Ala. The *in vitro* kinase assays demonstrated that mutating a single Thr to an Ala does not alter phosphorylation significantly, thus we chose to create either double mutations (two

threonines simultaneously mutated) or a triple mutant. All of these mutants were created through site-directed mutagenesis and ultimately inserted into the Δ*graR* strain.

Interestingly when working with *S. aureus* Δ*graR* it was observed that this strain has growth defects based on its growth pattern. Following four hours of growth it was observed that Δ*graR* plateaus much faster then all other strains, which is an indication that cells have reached stationary phase. In the wild type 6390 and all Δ*graR* complemented strains stationary phase was reached following seven-eight hours of growth. All complemented strains, expressing either wild type GraR or mutated GraR, could restore growth to normal. Thus, it was concluded that in the absence of the putative Stk1-mediated phosphorylation sites on GraR does not significantly alter its function in the context of cellular growth. Based on the growth pattern it was also observed that all complemented strains contained more cells then the wild type strain during stationary phase, which is likely the result of multiple copies within a single cell since pMK4 undergoes rolling circle mode of replication and thus yields multiple copies (Lindsay, 2008).

Previous research has suggested the absence of *graR* gene causes increased sensitivity towards vancomycin (Meehl et al., 2007), an antibiotic from the glycopeptide class (Moellering, 2006). To test whether the Stk1-mediated phosphorylation sites were important for activity of GraR we carried out MIC experiments towards vancomycin. It was observed that Δ*graR* strain had an MIC of 0.5 μg/mL, whereas the wild type 6390 strain had an MIC of 1 μg/mL. All the Δ*graR*-complemented strains were able to revert

the phenotype back to 1 μg/mL, Stk1 phosphorylation of GraR likely does not play a role in proper activity in the context of vancomycin resistance, given that ectopically expressed mutant version of GraR could restore Δ*graR* phenotype. Our *in vitro* data suggested that introducing three mutations at once causes the protein to misfold and aggregate. It was expected that when ectopically expressing the GraR-triple mutant in the Δ*graR* strain it should not be functional and phenotype should not be restored. However, given that the protein is expressed within its native cellular context it is likely chaperonin proteins and other factors aid in ensuring the protein is folded correctly.

Unfortunately our complementation studies did not deduce the role of GraR phosphorylation by Stk1 *in vivo.* A recent paper has suggested that although a given phosphorylation site does not yield immediate measurable effects on the target protein, it should not be ruled out as important (Cousin et al., 2013). Given that GraR plays an important role within the cell, relaxed substrate specificity could allow rapid adaptation to new environmental challenges. Alternatively, Stk1 phosphorylation could be a "last-resort" effort to counteract an unfavorable condition to which a TCS alone could not fully respond. Thus GraR could be part of a larger network of factors that Stk1 phosphorylates as a global response. It remains to be determined what is the precise role of this phosphorylation event. Nonetheless, exploiting these systems by synergistically targeting multiple signaling pathways could render the *S. aureus* pathogen unable to respond and adapt.

References

Beltramini, A.M., Mukhopadhyay, C.D., and Pancholi, V. (2009). Modulation of cell wall structure and antimicrobial susceptibility by a Staphylococcus aureus eukaryote-like serine/threonine kinase and phosphatase. Infect Immun *77*, 1406-1416.

Capra, E.J., and Laub, M.T. (2012). Evolution of two-component signal transduction systems. Annu Rev Microbiol *66*, 325-347.

Cheung, A., and Duclos, B. (2012). Stp1 and Stk1: the Yin and Yang of vancomycin sensitivity and virulence in vancomycin-intermediate Staphylococcus aureus strains. J Infect Dis *205*, 1625-1627.

Cousin, C., Derouiche, A., Shi, L., Pagot, Y., Poncet, S., and Mijakovic, I. (2013). Protein-serine/threonine/tyrosine kinases in bacterial signaling and regulation. FEMS Microbiol Lett.

Didier, J.P., Cozzone, A.J., and Duclos, B. (2010). Phosphorylation of the virulence regulator SarA modulates its ability to bind DNA in Staphylococcus aureus. FEMS Microbiol Lett *306*, 30-36.

Donat, S., Streker, K., Schirmeister, T., Rakette, S., Stehle, T., Liebeke, M., Lalk, M., and Ohlsen, K. (2009). Transcriptome and functional analysis of the eukaryotic-type serine/threonine kinase PknB in Staphylococcus aureus. J Bacteriol *191*, 4056-4069.

Falord, M., Mader, U., Hiron, A., Debarbouille, M., and Msadek, T. (2011). Investigation of the Staphylococcus aureus GraSR regulon reveals novel links to virulence, stress response and cell wall signal transduction pathways. PLoS One *6*, e21323.

Kuroda, M., Kuroda, H., Oshima, T., Takeuchi, F., Mori, H., and Hiramatsu, K. (2004). Two-component system VraSR positively modulates the regulation of cell-wall biosynthesis pathway in Staphylococcus aureus. Molecular Microbiology *49*, 807-821.

Kuroda, M., Ohta, T., Uchiyama, I., Baba, T., Yuzawa, H., Kobayashi, I., Cui, L., Oguchi, A., Aoki, K.-i., Nagai, Y., *et al.* (2001). Whole genome sequencing of meticillin-resistant Staphylococcus aureus. The Lancet *357*, 1225-1240.

Lazebnik, Y. (2002). Can a biologist fix a radio?--Or, what I learned while studying apoptosis. Cancer Cell *2*, 179-182.

Leimeister-Wachter, M., Domann, E., and Chakraborty, T. (1992). The expression of virulence genes in Listeria monocytogenes is thermoregulated. J Bacteriol *174*, 947-952.

Lindsay, J. (2008). Staphylococcus: Molecular Genetics 1edn (Caister Academic Press).

Lux, R., and Shi, W. (2005). A novel bacterial signalling system with a combination of a Ser/Thr kinase cascade and a His/Asp two-component system. Mol Microbiol *58*, 345-348.

Meehl, M., Herbert, S., Gotz, F., and Cheung, A. (2007). Interaction of the GraRS two-component system with the VraFG ABC transporter to support vancomycin-intermediate resistance in Staphylococcus aureus. Antimicrob Agents Chemother *51*, 2679-2689.

Moellering, R.C., Jr. (2006). Vancomycin: a 50-year reassessment. Clin Infect Dis *42 Suppl 1*, S3-4.

Pereira, S.F., Goss, L., and Dworkin, J. (2011). Eukaryote-like serine/threonine kinases and phosphatases in bacteria. Microbiol Mol Biol Rev *75*, 192-212.

Prisic, S., Dankwa, S., Schwartz, D., Chou, M.F., Locasale, J.W., Kang, C.M., Bemis, G., Church, G.M., Steen, H., and Husson, R.N. (2010). Extensive phosphorylation with overlapping specificity by Mycobacterium tuberculosis serine/threonine protein kinases. Proc Natl Acad Sci U S A *107*, 7521-7526.

Sullivan, M.A., Yasbin, R.E., and Young, F.E. (1984). New shuttle vectors for Bacillus subtilis and Escherichia coli which allow rapid detection of inserted fragments. Gene *29*, 21-26.

Truong-Bolduc, Q.C., Ding, Y., and Hooper, D.C. (2008). Posttranslational modification influences the effects of MgrA on norA expression in Staphylococcus aureus. J Bacteriol *190*, 7375-7381.

CHAPTER FOUR

GRAR REVISITED: *IN VIVO* INSIGHTS SUGGEST A MORE DIVERSE ROLE

4.1 Introduction

Prokaryotic signaling pathways have been extensively studied due to their roles in sensing and responding to unfavorable conditions. The *S. aureus* pathogen contains 16 two-component systems (TCS) that collectively allow the organism to respond to a plethora of stimuli (Ito et al., 1999; Kuroda et al., 2001). Briefly, a TCS is composed of a histidine kinase, a cytoplasmic membrane protein that undergoes autophosphorylation following an external stimuli and a response regulator, usually a transcription factor, which receives this message in the form of phosphorylation to ultimately control gene expression (Chang and Stewart, 1998; Laub and Goulian, 2007; Stock et al., 2000).

Some notable examples of TCSs include the VraSR system, where the VraS kinase senses perturbations in the cell wall and responds by phosphorylating VraR, which up regulates genes involved in the synthesis of new peptidoglycan (Kuroda et al., 2004; Yin et al., 2006). The HssSR system is involved in intracellular heme homeostasis, whereby phosphorylated transcription factor HssR binds within the *hrtAB* promoter and activates the expression of HrtAB, an efflux pump, in response to heme, hemin and hemoglobin (Stauff et al., 2007). In the context of bacterial adaptability these systems

play a vital role in responding to many different stimuli. It is beyond the scope of this work to understand all *S. aureus* TCS, hence subsequent discussion will focus only on the GraSR system, which is the focus of this study.

The GraSR, glycopeptide resistance associated, system is composed of a histidine kinase, GraS, and a response regulator, GraR. In the literature this system is also termed ApsSR, for antimicrobial peptide sensor, based on homology with *Staphylococcus epidermidis* (Li et al., 2007). Early studies suggested GraSR main role was to control the *dlt* and *vraFG* operons (Herbert et al., 2007; Meehl et al., 2007). The *dlt* operon encodes genes responsible for $_{D}$-alanylation of teichoic acids (Peschel et al., 1999) and *vraFG* operon encodes a pair of proteins comprising an ABC transporter responsible for CAMP sensing and signaling (Falord et al., 2012).

The genes controlled by GraSR help protect the *S. aureus* pathogen from human defense systems (Herbert et al., 2007). One important molecule that plays a role in suppressing bacterial infections is lysozyme, which acts as a cell wall lytic enzyme and a cationic antimicrobial peptide (CAMP). It is believed CAMPs act by disrupting bacterial membranes to allow free passage of ions, in turn disrupting homeostasis, which eventually leads to cell death (Sahl et al., 2005). The *S. aureus* pathogen has developed defense mechanisms to circumvent the actions of lysozyme. One of them is $_{D}$-alanylation of teichoic acids, which adds an overall positive charge to the cell wall to repel the positively charged CAMPs. In fact, it has been shown that *S. aureus* strains lacking the *dlt* operon were highly susceptible to the actions of the host immune system (Collins et al.,

2002).

Although strong evidence exists that GraSR is primarily involved in the host immune adaptability, it is suggested the GraSR system plays a global regulatory role that is not limited to sensing and responding to CAMPs. A recent report has linked the GraSR system to the *S. aureus* stress response, cell wall and pathogenesis pathways (Falord et al., 2011). Based on transcriptome analysis and *in silico* genome scanning the authors identified new potential regulons of the GraSR system. Many TCSs are specific in the types of stimuli they can sense and respond to, however, the GraSR TCS is hypothesized to play a more global role than previously expected. The objective of this study was to further characterize the involvement of GraSR TCS in biological processes by studying an *S. aureus* Δ*graR* mutant.

4.2 Materials and Methods

4.2.1 Materials and chemicals

QIAquick PCR Purification Kit was used to clean up DNA (Qiagen). Bacto™ Tryptic Soy Broth from BD (Becton, Dickson and Company) and Agar-Agar (granulated) from EMD (Millipore, USA). Vancomycin from Sigma Aldrich and chloramphenicol from EMD (Millipore, USA). Congo Red (certified by the Biological Stain Commission, BioXtra) from Sigma. Osmium tetroxide 4% aqueous sol. and all other chemicals for transmission electron microscopy obtained from Electron Microscopy Sciences (Cedarlane). Deuterium oxide "100%" (D, 99.96%) from Cambridge Isotope Laboratories, Inc.

4.2.2 Generation of pMK4-P_{native}:*graR*-D51N

The pMK4-P_{native}:*graR* plasmid was used as a template to mutate the Asp51 (encoded by GAT) to Asn51 via the QuikChange™ Site-Directed Mutagenesis method (Stratagene). Asparagine substitution is highlighted in bold within the PCR primers. The primers used were Dir 5'- CCTGAAATTGTTATATTGAATGTTCAATT **A**ACCTAAATATG and Rev 5'- CATATTTAGGTAATTGAACATTCAATA **T**TAACAATTTCAGG. Following amplification the product was digested with *DpnI* and transformed into NovaBlue cells. The construct was sequenced at The Centre for Applied Genomics, The Hospital for Sick Children, Toronto. Following sequencing the correct construct was first electroporated into RN4220, followed by electroporation into Δ*graR* as

section 3.2.3.

4.2.3 Growth curve of 6390 and ΔgraR complemented pMK4-P_{native}:*graR*-D51N

Growth curve were performed under optimal conditions in glass flasks. To avoid loss of plasmid, strains containing pMK4 were always grown in Chloramphenicol (10 μg/mL). Δ*dltA* and Δ*tarO* were used as controls. Overnight seed cultures were grown in TSB at 37°C, 200 rpm and the optical density at 600 nm (OD_{600}) measured prior to starting experiment in UV-Visible Spectrophotometer (Varian Cary 100 Bio). Bacterial cultures were grown in 50 mL TSB, initially adjusted to an OD_{600} of 0.05. The initial OD_{600} was recorded and is considered time zero. Cultures were shaken at 37°C, 200 rpm and OD_{600} readings were taken every 60 min.

4.2.4 CFU of 6390 and ΔgraR at stationary phase

Overnight seed cultures were grown in TSB at 37°C, 200 rpm and OD_{600} was measured prior to starting experiment in UV-Visible Spectrophotometer (Varian Cary 100 Bio). Bacterial cultures were grown in 50 mL TSB, adjusted to a starting OD_{600} of 0.05, at 37°C, 200 rpm for 480 min (corresponding to stationary phase). From each culture three separate biological replicates were removed and serially diluted (10^{-7}, 10^{-8} and 10^{-9}) in ddH_2O and 10 μL of each dilution in quadruplicates was spotted onto TSA plates. The plates were dried for 15 min at room temperature and incubated at 37°C for 12-16 hrs. The total sample size for each strain is 12.

4.2.5 TEM of 6390 and ΔgraR

Overnight seed cultures were grown in TSB at 37°C, 200 rpm. Cultures were diluted 100-fold and grown at 37°C, 200 rpm to OD_{600} of 0.5. Cells (2 mL) were spun down and suspended in 500 µL of 3.5% glutaraldehyde and 0.1 M sodium cacodylate pH 7.4 for 60 min. Mixtures were washed four times with 0.1 M sodium cacodylate pH 7.4 at room temperature with 15 min incubation in between each wash. Cells were post-fixed with 500 µL 1% osmium tetroxide in 0.3 M sodium cacodylate pH 7.4 for 60 min at room temperature. Cells were spun down, suspended in 0.1 M sodium cacodylate pH 7.4 and incubated at 4°C overnight. Subsequently cells were washed with 200 µL ethanol gradient of 30%, 50% and 80%, followed by 100% and incubated for 60 min. Fresh Spurr's resin was prepared based on the manufacturers instructions and mixed with ethanol in 1:1 ratio which was added to cell pellets. Mixture was left overnight at room temperature. The resin was removed and Fresh Spurr's resin was prepared, without ethanol, and added to the cell pellets. Mixture was incubated at 70°C for 48 hrs, or until matrix resin polymerized. The resin was cut into sections, stained with uranyl acetate followed by lead citrate and samples were examined using a Philips EM 210 transmission electron microscope at 80 kV with a SIA L3 camera (York University, Microscopy and Imaging Facility, Toronto).

4.2.6 Congo Red susceptibility

Overnight seed cultures were grown in TSB at 37°C, 200 rpm and OD_{600} was

measured prior to starting experiment in UV-Visible Spectrophotometer (Varian Cary 100 Bio). To avoid loss of plasmid, strains containing pMK4 were always grown in Chloramphenicol (10 μg/mL). Bacterial cultures were grown in 50 mL TSB, adjusted to a starting OD_{600} of 0.05, at 37°C, 200 rpm for 180 min (corresponding to mid-log phase). Cultures were serially diluted (10^{-2}, 10^{-3}, 10^{-4}, 10^{-5}, 10^{-6} and 10^{-7}) in sterile ddH_2O and 5 μL of each dilution was spotted onto Congo Red agar (CRA) plates and TSA plates. The plates were dried for 15 min at room temperature and incubated at 37°C for 12-16 hrs in the dark. Furthermore, the plates were incubated for 8-12 hrs at room temperature in the dark. Pictures were taken with a Canon Powershot G-12 camera. The experiments were performed three times, independently.

4.2.7 WTA analysis of 6390, ΔgraR and complemented strains

4.2.7.1 PAGE analysis of NaOH-extracted WTA

Overnight seed cultures, 10 mL, were grown in TSB at 37°C, 200 rpm. To avoid loss of plasmid, strains containing pMK4 were grown in Chloramphenicol (10 μg/mL). Cells were pelleted by centrifugation (2,000 xg, 10 min) and suspended in 30 mL of 50 mM 2-(N-morpholino)ethanesulfonic acid (MES), pH 6.5. Cells were pelleted as above, resuspended in 30 mL of 4% (wt/v) sodium dodecyl sulfate (SDS) in 50 mM MES, pH 6.5 and placed in boiling water bath for 60 min.

The samples were cooled, pelleted by centrifugation (10,000 xg, 10 min, room temperature) and resuspended in 1 mL of 4% SDS in 50 mM MES, pH 6.5. The cells

were transferred to 1.5 mL eppendorf tubes, pelleted by centrifugation (14,000 xg, 10 min, room temeprature) and resuspended with 4% SDS in 50 mM MES, pH 6.5, followed by 2% NaCl in 50 mM MES, pH 6.5 and lastly with 50 mM MES, pH 6.5.

The samples were treated with 1 mL containing 20 μg proteinase K in 20 mM Tris-HCl, pH 8.0, 0.5% SDS and incubated for 4 hrs at 50°C. Following incubation the samples were pelleted and resuspended once with 2% NaCl in 50 mM MES, pH 6.5 and three times with ddH_2O to remove SDS. Finally, the pellets were resuspended in 1 mL 0.1 M NaOH and shaken at room temperature for 16 hrs to hydrolyze WTA.

The hydrolyzed WTA samples were separated on a 20% acrylamide gel using the Bio-Rad Mini-PROTEAN system with a 0.75 mM-thick glass plate. The stacking gel contained 3% acrylamide. Crude WTA, mixed with 50% glycerol containing traces of bromophenol blue, was loaded to fresh gels and run at 4°C for 18 hrs in Tris-Tricine running buffer (0.1 MTris, 0.1 M Tricine, pH 8.2) with 16 mA as constant for two gels. WTA bands were visualized with the Alcian blue-silver stain method. Briefly, the gels were stained in 0.1% (wt/v) Alcian blue overnight and subsequently silver stained as per kit instructions (Bio-Rad).

4.2.7.2 NMR and PAGE of TCA-extracted WTA

Overnight seed cultures, 10 mL, were grown in TSB at 37°C, 200 rpm. To avoid loss of plasmid, strains containing pMK4 were grown in Chloramphenicol (10 μg/mL). Cultures were diluted 200-fold in 1 L of TSB and grown at 37°C, 200 rpm to mid-exponential phase. Cells were pelleted at 8,230 xg for 15 min, room temperature and

suspended in 10 mL of 2 M NaCl. Cells were softened in water bath for 1 min, sonicated for 2 min with 35% amplitude and collected by centrifugation (14, 000 xg, 5 min, 4°C). They were further resuspended in PBS, vortexed, centrifuged. The pellets were resuspended in 20 mL of 4% SDS and incubated for 4 hr at 37°C with shaking.

Cell walls were pelleted (14, 000xg, 5 min, 25°C) and washed by resuspending three times with ddH_2O by centrifugation. Covalently bound proteins and nucleic acids were removed by gentle stirring at 37°C overnight with 4 mL trypsin (0.2 mg/mL), RNaseI (0.1 mg/mL) and DNaseI (0.1 mg/mL, 20μL) in 50 mM Tris-HCl, pH 7.0, 5 mM $MgCl_2$. Cell walls were recovered by centrifugation (14,000 xg, 5 min, 4°C,) and washed by resuspending and centrifuging with 1 M Tris-HCl, pH 7.0 followed by 1 M Tris-HCl, 1 M NaCl pH 7.0, then with 1 M Tris-HCl, pH 7.0 and lastly three times with ddH_2O. Following last wash, the pellets were resuspended in ice-cold 10% Trichloroacetic acid (TCA) in glass vial and incubated for 48 hrs at 4°C with constant stirring.

The peptidoglycan was removed by centrifugation (5,300 xg, 45 min, 20°C) and the soluble portion (~4 mL) was mixed with ice-cold 95% ethanol (~20 mL) and solution was incubated for 5 days at 4°C. The precipitated WTA is recovered by washing precipitate with 5 mL 95% ethanol two times (spin 5,000xg, 30 min, room temperature). Following last wash, resuspend in 1 mL of ddH_2O and lyophilize overnight. At this stage pure WTA is observed as whitish powder, and for NMR analysis the WTA is suspended in D_2O at final concentration of 5-10 mg/mL. For PAGE analysis, 200 ng of WTA was resolved as described above, with exception of running gel for 10 hrs.

4.3 Results

4.3.1 Growth of 6390 and Δ*graR* versus Δ*graR*-D51N

As observed in section 3.3.3, Δ*graR* strains complemented with ectopically expressed GraR mutants harboring Thr to Ala mutations were capable of reverting the growth characteristics of Δ*graR* back to normal. This prompted us to investigate whether another post-translational modification was important for the growth phenotype. The *graR* gene is part of a two-component system termed GraSR. Although no *in vitro* work has confirmed GraS phosphorylation of GraR, recent *in vivo* work has suggested the aspartic acid at position 51 (D51) within the GraR N-terminal domain may be critical for activity (Falord et al., 2012). Through site-directed mutagenesis we generated a pMK4 vector harboring a point mutation, Asp51 to Asn51, in the *graR* gene.

When GraR-D51N was ectopically expressed from pMK4-P_{native}:*garR*-D51N in the Δ*graR* mutant, we did not observe a restoration of growth as compared to Δ*graR* complemented pMK4-P_{native}:*garR*-WT (Fig.4.3.1). This indicates that the D51 residue, likely through GraS signaling, is involved in proper cell growth.

It is well established that GraR controls the *dlt* operon, which is responsible for $_{D}$-alanylation of TA (adds positive charge). Furthermore the Δ*dltA* mutant strain has been suggested to play a role in cell growth (Tabuchi et al., 2010), thus it was used as a control because it grows abnormally. To test whether the OD_{600} corresponds to a lower amount of cells we carried out CFU to estimate the number of viable bacteria in the culture.

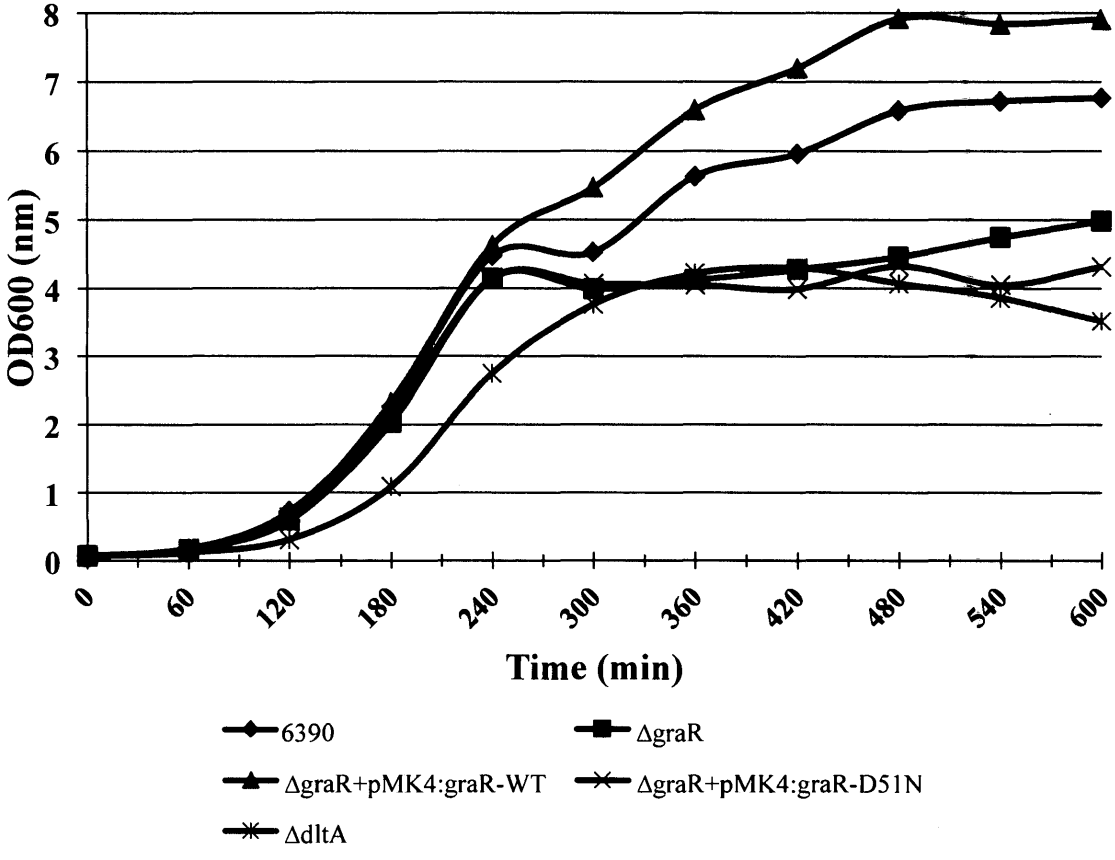

Figure 4.3.1 Growth curve of 6390 and Δ*graR* versus ectopically expressed GraR-WT and D51N

Overnight seed cultures were diluted to an OD600 of 0.05 in TSB. The cultures were grown in flasks at 37°C, 200 rpm and readings were measured on a UV-Visible Spectrophotometer every 60 min. Chloramphenicol (10 μg/mL) added to cultures containing pMK4 plasmid. Δ*dltA* was used as a control to show aberrant cell growth.

Cultures were harvested after 8 hrs of growth, which corresponds to stationary phase, serially diluted and spotted on TSA plates. As observed in Fig. 4.3.2, there are fewer viable Δ*graR* and Δ*dltA* cells as compared to the wild type 6390 strain. The number of cells in the 6390 wild type strain is three times more than Δ*graR* mutant strain.

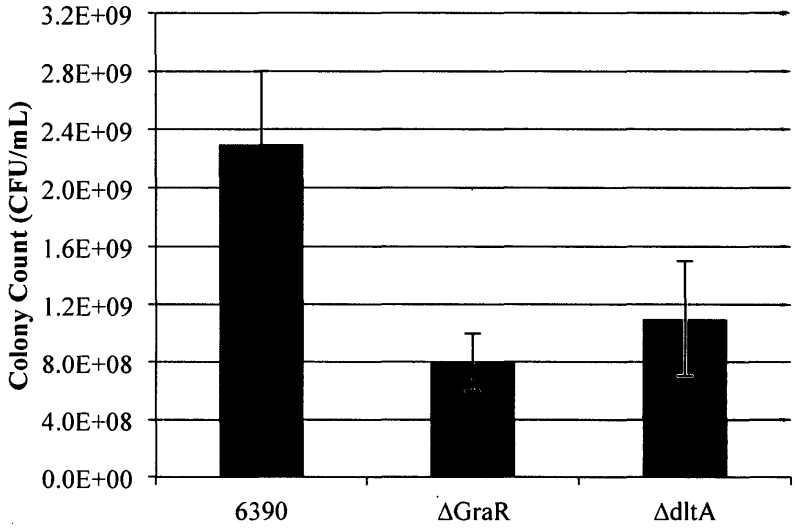

Figure 4.3.2 Viable cell count of 6390, Δ*graR* and Δ*dltA* after 8 hrs of growth
The number of bacterial cells for strains 6390 and ΔGraR was determined following 480 min of growth, at 37°C and 200 RPM, by counting the number of colony forming units from a 10μL drop of a 10^8 dilution. For each strain three biological replicates were removed and spotted in quadruplicates, giving a sample size of n=12 for each strain.

4.3.2 Transmission electron microscopy

The Δ*graR* strain was further examined by transmission electron microscopy. The results demonstrate that deletion of the *graR* gene had a profound effect on cell morphology (Fig. 4.3.3). As can be observed the Δ*graR* mutant strain contains a subpopulation of cells with aberrant septum positioning, where a second septa is parallel to an initiated or completed septum. This is very unusual given that septum positing in *S. aureus* is typically initiated at the end of daughter division and perpendicular to the fist plane of division (Turner et al., 2010). Examination of thousands of wild type 6390 cells did not reveal this phenotype; hence it is unique to the Δ*graR* strain. Furthermore we

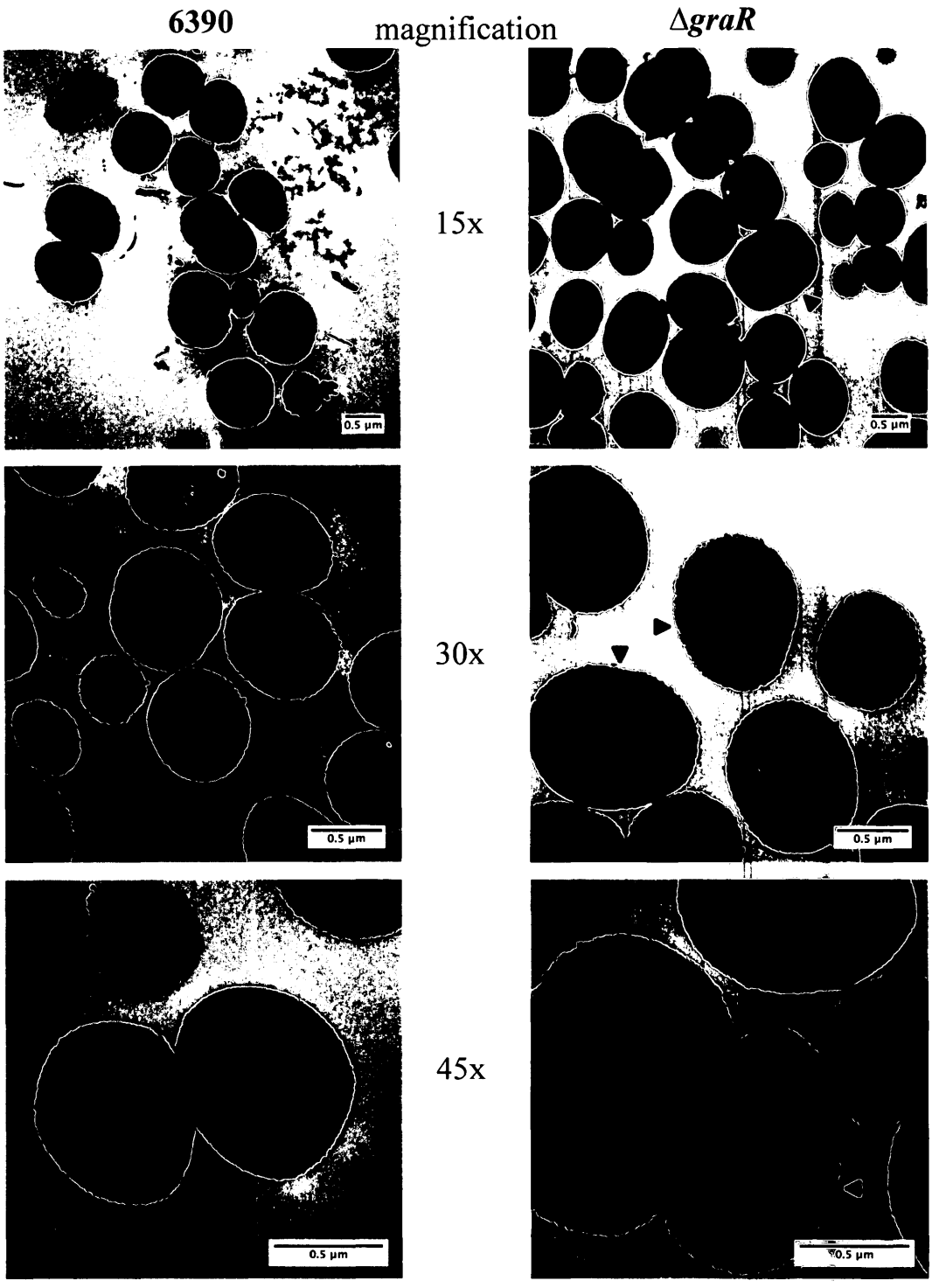

Figure 4.3.3 Transmission electron microscopy of 6390 and Δ*graR*

Overnight cultures were diluted 1/1000 and grown at 37°C, 200 RPM to OD_{600} of 1. Cells were harvested, fixed, immobilized in Spurr's resin and stained with heavy metal. No dual septa were observed in 6390 wild type, whereas only a subset of the population of Δ*graR* cells has dual septa (marked with arrow). Images are to scale with the corresponding magnification.

complemented the Δ*graR* strain with pMK4-P_{native}:*graR* ectopically expressing GraR-WT and less mutant cells were observed, although aberrant septa positioning still occurred in some cells.

4.3.3 Susceptibility towards Congo Red dye

Scanning the literature it was observed that *msrR* mutation in *S. aureus* also gives rise to dual septa (Hubscher et al., 2009). Furthermore, the *msrR* mutation renders *S. aureus* cells more susceptible towards Congo Red, an anionic azo dye. Through PCR we were able to confirm that Δ*graR* contains an intact copy of the *msrR* gene (Appendix G). Given the unique morphology between Δ*graR* and Δ*msrR* we decided to test Δ*graR* susceptibility towards Congo Red. It should be noted that MIC could not be carried out in 96-well microtiter plates due to the intense color of Congo Red. In order to assess bacterial turbidity the optical density is usually read at 600 nm, which corresponds to orange-red within the visible light spectrum. However, at various dilutions of Congo Red there will be variations in the light that passes through. Thus optical density will fluctuate not as a result of the bacterial density but more so the color of the dye.

To overcome this we opted to use a variation of the Miles and Misra method (Hedges et al., 1978) on agar plates containing varying concentrations of Congo Red.

This experiment was recently carried out to assess susceptibility of WTA-deficient *S. aureus* strains towards Congo Red (Suzuki et al., 2012). Briefly, bacterial cultures are serially diluted and each dilution is spotted on a control plate, containing just nutrients and agar, and on test plates, containing nutrients, agar and varying concentrations of Congo Red. A strain is considered not susceptible if the number of colonies for each dilution is similar between the control and test plates. However, at much higher concentrations of cells ($>10^2$) it is hard to distinguish between individual colonies, thus caution should be taken.

Congo Red susceptibility tests revealed that Δ*graR* was slightly sensitive towards Congo Red (Fig. 4.3.4) at concentrations >400 μg/mL. This is based on the observation that at 400 and 800 μg/mL Congo Red we expect Δ*graR* to yield 1000, 100 and 10 cells corresponding to 10^3, 10^2, and 10^1, respectively. Albeit a few colonies are observed, it is nowhere near the expected amount, thus these colonies likely form chance mutations resulting from stress. The wild type 6390 strain was capable of growing on all plates and was not considered sensitive towards Congo Red. As a control the *S. aureus* Δ*tarO* strain was included, a strain lacking WTA and as a result becomes sensitized towards Congo Red (Suzuki et al., 2012). This strain has an MIC of 4 μg/mL and could not grow on the plates containing 200, 400 or 800 μg/mL Congo Red. Furthermore, to showcase the sensitivity of this experiment, Δ*tarO* was grown on plates containing 10, 50 and 100 μg/mL Congo Red, and as can be seen in Appendix H on the 10 μg/mL Congo Red plate growth could only be observed when 10^6 cells are present.

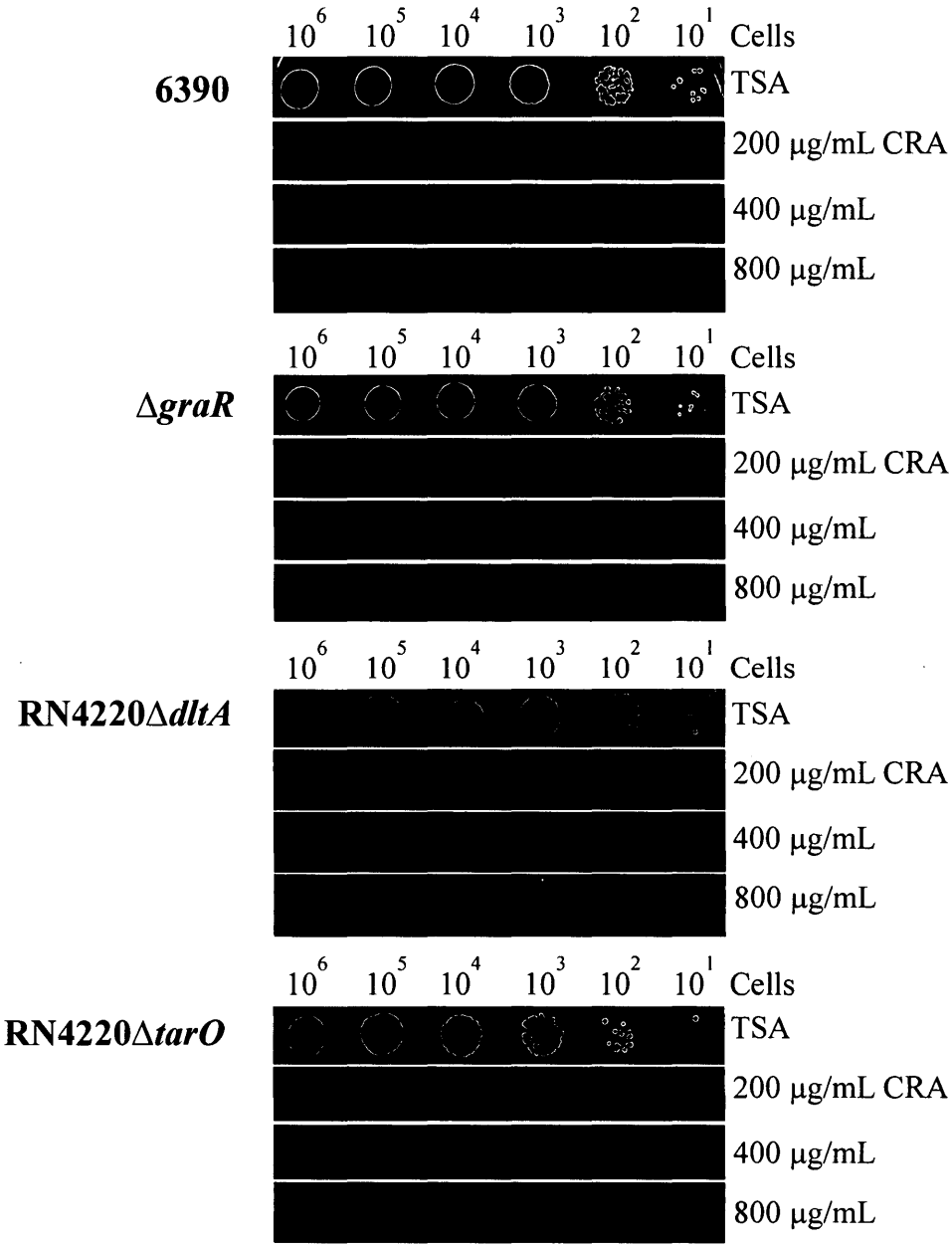

Figure 4.3.4 *S. aureus* 6390 wild-type, Δ*graR*, RN4220Δ*dltA* and RN4220Δ*tarO* susceptibility towards Congo Red

Cells in log phase were cultured, serially diluted, and 5 μL of each dilution was spotted onto either TSA or TSA plates containing 200, 400 or 800 μg/mL of Congo Red dye (termed CRA). Plates were incubated at 37°C in the dark for 12 hrs, and further another 8 hrs at room temperature. Congo Red is light sensitive. At higher concentration of Congo Red colonies turn black. Furthermore, colonies may also remain red and thus hard to observe against the red plate background. Expected colony number indicated at top.

The *dltA* gene, within the *dlt* operon, is responsible for adding a net postivie charge to TAs. Given that GraR controls *dlt* operon we examined whether Δ*graR* sensitivity is a result of charge variations. As observed in Fig. 4.3.4 the Δ*dltA* mutant strain (*dltA*-difficeint) was not sensitive towards Congo Red, due to the ability to grow on all tested concentrations. Hence it is suggested that Δ*graR* sensitivity towards Congo Red is not the result of charge differences.

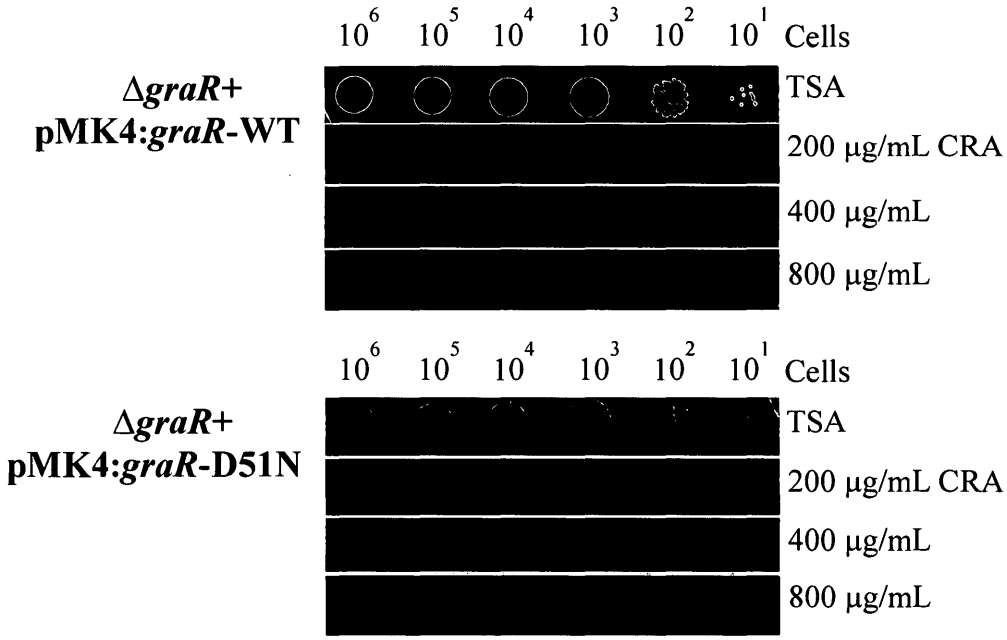

Figure 4.3.5 *S. aureus* Δ*graR* complemented with GraR-WT and GraR-D51N susceptibility towards Congo red
Cells in log phase were cultured, serially diluted, and 5 μL of each dilution was spotted onto either TSA or TSA plates containing 200, 400 or 800 μg/mL of Congo Red dye. Plates were incubated at 37°C in the dark for 12 hrs, and further another 8 hrs at room temperature. Congo Red is light sensitive. At higher concentration of Congo Red colonies turn black. Furthermore, colonies may also remain red and thus hard to observe against the red plate background. Expected colony number indicated at top.

We attempted to complement the Δ*graR* strain with the pMK4-P_{native}:*graR*-WT plasmid, however surprisingly, as can be obserevd in Fig. 4.3.5 the complemented strain remained sensitive twoards Congo Red. Likewise, so did the pMK4-P_{native}:*graR*-D51N complemented Δ*graR* strain. It is possible the plasmid was lost during cell growth and unable to fully complement as the plates did not contain chloramphenicol to maintain the plasmid.

4.3.4 PAGE analysis of WTA

The unique phenotypes observed for Δ*graR* suggest its involvement in cell growth and alterations in WTA composition and/or modification. WTA was extracted from *S. aureus* strains by both NaOH method and TCA method. Briefly, the NaOH is a relatively quick procedure, where cell wall is removed and WTA is hydrolyzed by NaOH. However a limitation of the NaOH method is that the $_D$-alanine ester group is labile at alkaline pH. The TCA method is quite laborious and time-consuming, but yields very pure WTA with the $_D$-alanyl group attached.

NaOH-extracted WTA was analyzed by 20% PAGE and as observed in Fig.4.3.6 the Δ*graR* WTA migrated faster as compared to the wild type 6390 WTA. The ability of WTA to migrate faster has previously been attributed to WTA lacking sugars (Meredith et al., 2008). The *S. aureus* K6 strain, which completely lacks sugar modifications on WTA, was used as a control. Although Δ*graR* WTA did not migrate as quickly as K6 WTA, it still migrated faster than wild strain 6390 WTA. It is possible that Δ*graR* produces WTA void of sugar modifications; however, it is also possible that faster

migration could be the result of Δ*graR* WTA polymer length.

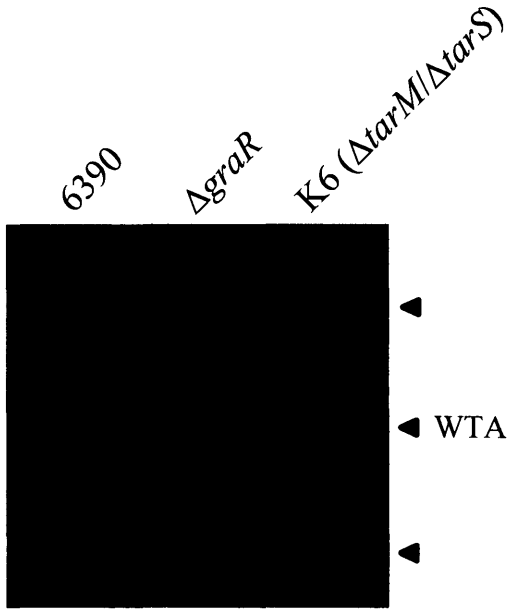

Figure 4.3.6 PAGE separation of NaOH-extracted WTA from 6390, Δ*graR* and K6
WTA from 6390, Δ*graR* and K6 was extracted at log phase following growth at 37°C, 200 rpm in TSB via the NaOH method. Crude WTA separated by 20% PAGE and run for 18 hrs and bands were visualized with the Alcian blue-silver stain method. *S. aureus* K6 WTA, completely lacks sugars, used as control.

When GraR-WT was ectopically expressed from pMK4-P_{native}:*garR*-WT in the Δ*graR* mutant, we observed a restoration of WTA migration identical to that of wild type 6390 (Fig.4.3.7). It should be noted that for this experiment WTA was extracted by the TCA method, and the PAGE gel was separated for 10 hrs, as opposed to 18 hrs. Had the gel been run longer the migration difference would have been more apparent. Nonetheless, ectopically expressed GraR complemented the Δ*graR* strain.

Interestingly, the GraR-D51N, ectopically expressed from pMK4-P_{native}:*garR*-D51N in Δ*graR*, could not restore WTA migration back to normal. This is indicative that the D51 residue is required for activation of the GraR protein, and given GraS is responsible for phosphorylation of GraR at that residue, it is suggested both proteins play a role in WTA synthesis and/or modification.

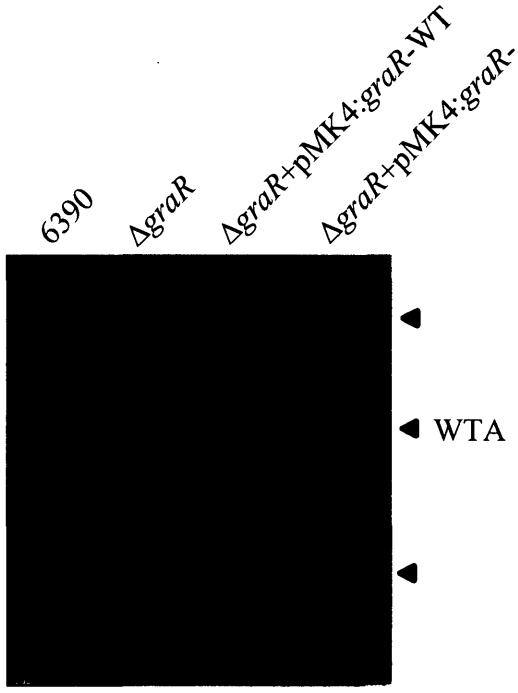

Figure 4.3.7 PAGE separation of TCA-extracted WTA from 6390, Δ*graR* and Δ*graR* complemented strains
WTA from 6390, Δ*graR* and Δ*graR* mutant complemented with GraR-WT and D51N was extracted at log phase following growth at 37°C, 200 rpm in TSB via the TCA method. WTA (2 μg) was separated by 20% PAGE, run for 10 hrs and bands were visualized with the Alcian blue-silver stain method.

4.3.5 NMR analysis of WTA

NMR analysis of TCA-extracted WTA was carried out to further investigate the differences between Δ*graR* mutant and 6390 wild type WTAs. This was done in collaboration with Dr. Hunter (The NMR Facility, York University). Both ^{1}H-NMR and 2D-HSQC were acquired, however only the ^{1}H-NMR will be discussed in detail. For the 2D-HSQC data refer to Appendix I and J.

Although not fully quantitative, the peak size of the $_{D}$-alanine methyl group, δ=1.542, can be compared to the methyl group of N-acetylglucosamine (GlcNAc), at δ=2.000. Upon closer inspection of the ^{1}H-NMR spectrum it was observed that Δ*graR* WTA (Fig. 4.3.8B) contains less $_{D}$-alanine esterification as compared to 6390 wild type WTA (Fig. 4.3.8A). This is expected given the regulatory role of GraR on the *dlt* operon. However, the $_{D}$-alanine peak in Δ*graR* does not fully diminish, suggesting either a basal level of *dlt* expression or compensation by another regulator.

Interestingly, when wild type GraR is ectopically expressed from pMK4-*graR*-WT in the Δ*graR* mutant the size of the methyl peak of $_{D}$-alanine returns to wild type levels (Fig. 4.3.9A). However, when GraR-D51N is ectopically expressed from pMK4-*graR*-D51N in the Δ*graR* mutant the methyl peak remains similar to that of Δ*graR* (Fig. 4.3.9B). This observation suggests the D51 residue is important for GraR function in decorating WTA with $_{D}$-alanine.

The GlcNAc group can be linked to the WTA poly-RboP backbone by an α-, δ=5.020, or β-, δ=4.643, glycosidic bond. The ^{1}H-NMR spectrum revealed that 6390 and

Δ*graR* WTA contain α and β-GlcNAc (Fig 4.3.8), albeit slightly less β-GlcNAc was observed in the Δ*graR* mutant WTA.

Lastly, an unassigned peak, δ=4.9, is present in both 6390 and Δ*graR* WTA, however, this peak is very pronounced in the Δ*graR* WTA (Fig. 4.3.8A and B). Of particular interest is that this peak is also present in the Δ*graR* strain ectopically expressing GraR-D51N, but not GraR-WT (Fig. 4.3.9A and B). It is unclear what this peak is and further investigation is necessary. However, it is suggested that enlargement of this peak is the result of the absence of GraR or the presence of a mutant GraR harboring a D51N mutation, which renders it unable to undergo phosphorylation by GraS.

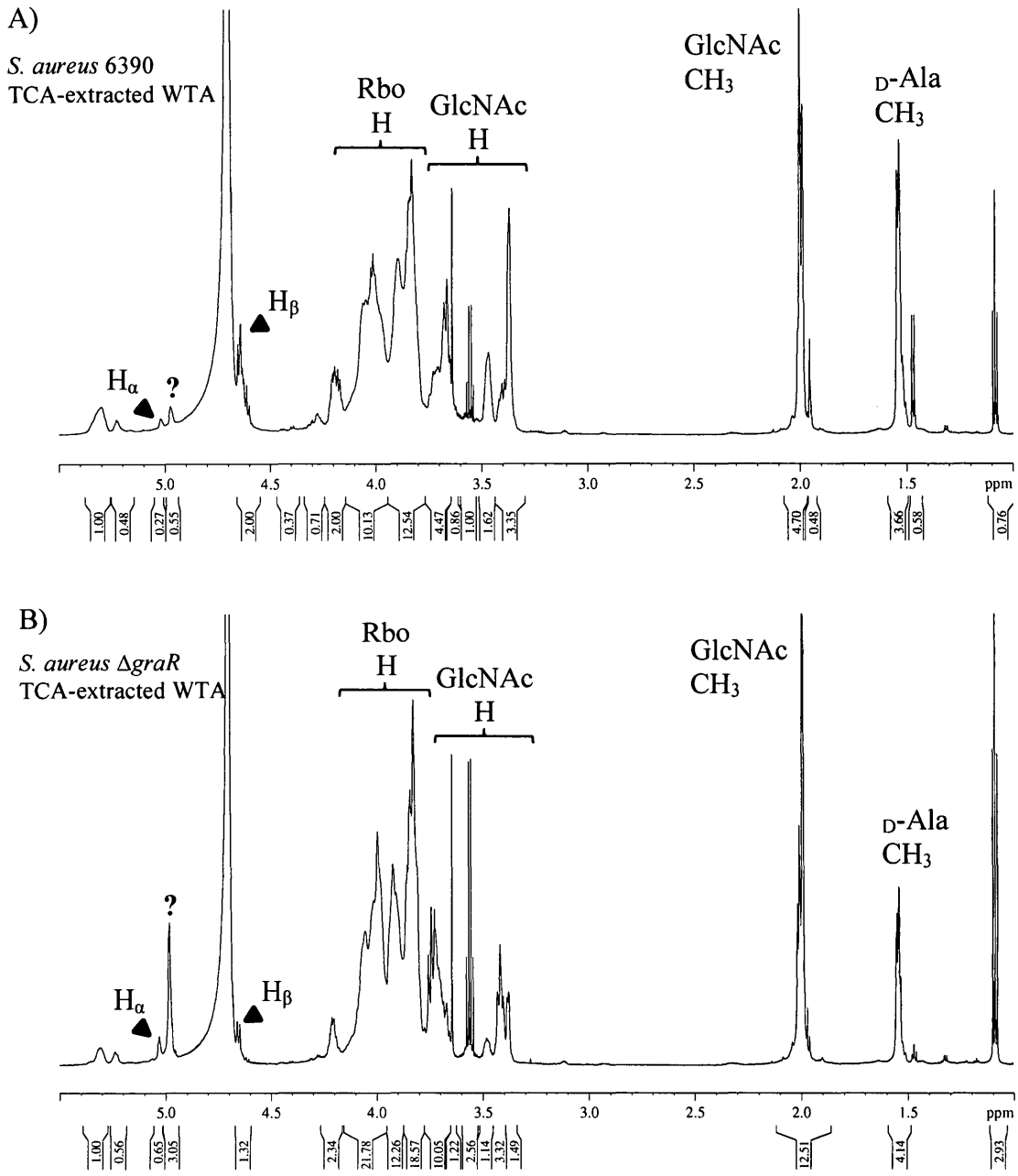

Figure 4.3.8 ^{1}H-NMR spectral data of TCA-extracted WTAs from 6390 and Δ*graR*
NMR spectral data of A) 6390 and B) Δ*graR* mutant. Abbreviations are as follows: H is hydrogen, Rbo is ribitol, GlcNAc is N-acetylglucosamine and D-Ala is alanine. Uncharacterized peak at ~4.9.

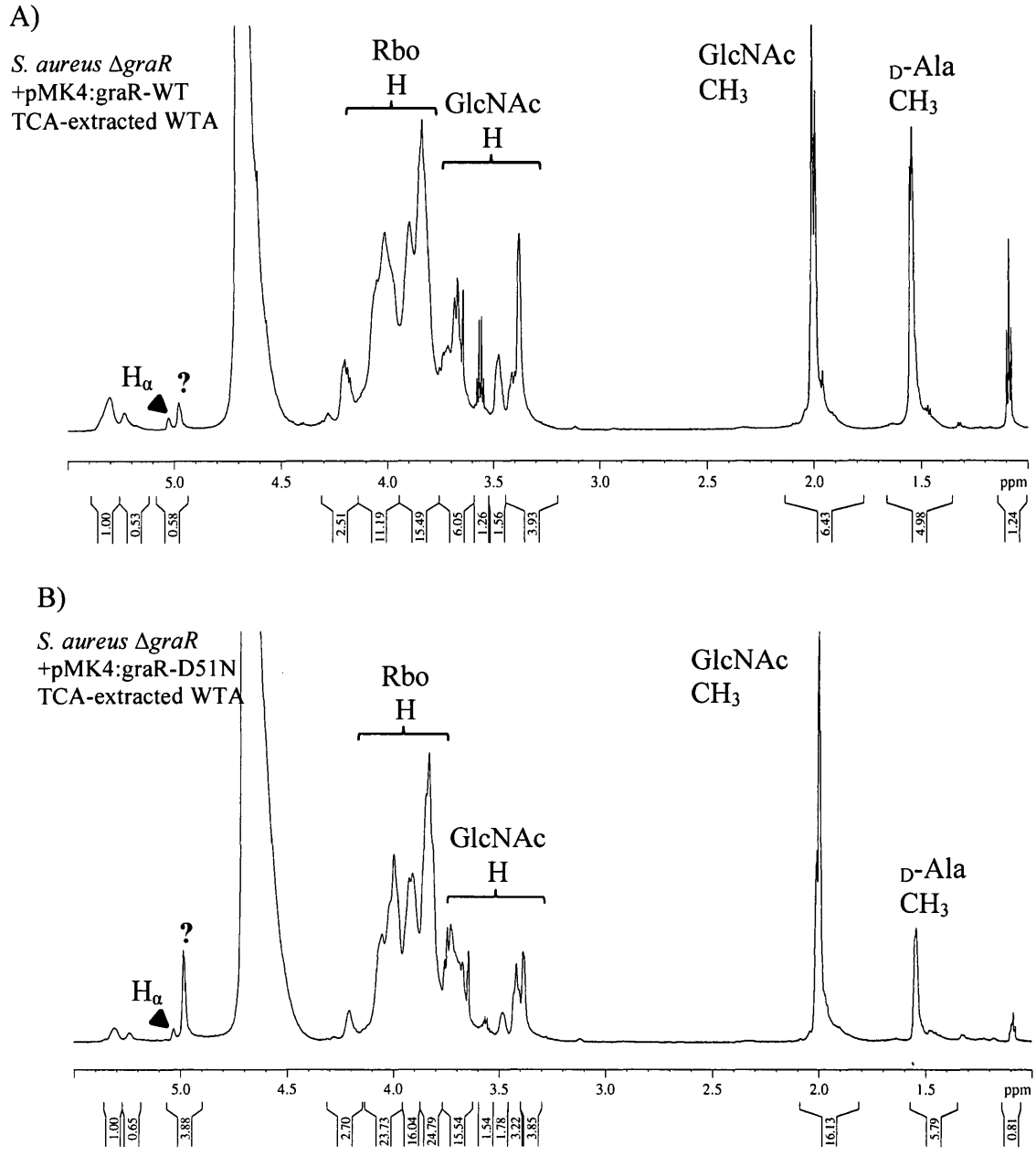

Figure 4.3.9 ^{1}H-NMR spectral data of TCA-extracted WTAs from Δ*graR* mutant complemented with GraR-WT and D51N

NMR spectral data of A) Δ*graR* + pMK4:*graR*-WT and B) Δ*graR* + pMK4:*graR*-D51N. Abbreviations are as follows: H is hydrogen, Rbo is ribitol, GlcNAc is N-acetylglucosamine and D-Ala is alanine. Uncharacterized peak at ~4.9. It should be noted H_β was not detected because the adjacent H_2O peak masked the signal.

4.4 Discussion

The identification of the first prokaryotic TCS in 1986 had a profound effect on the field of signal transduction (Nixon et al., 1986). At the time scientists were vigorously investigating phosphorylation events in eukaryotic system, and it was quickly becoming apparent that post-translational modification of proteins has a profound effect on gene expression and ultimately cellular physiology. Furthermore researcher realized that phosphorylation is not limited to eukaryotic systems and is widespread in prokaryotes as well (Cozzone, 1988). In prokaryotes such as *S. aureus* signal transduction typically involves TCSs, which are comprised of a sensor histidine kinase and a response regulator capable of binding DNA (Capra and Laub, 2012).

In *S. aureus* the GraSR TCS has been identified to be important in conferring resistance to antimicrobial peptides (Herbert et al., 2007) and as a consequence the majority of studies have focused on this particular response. It was widely accepted that GraSR controls the *dlt*, *mprF* and *vraFG* operons, whereby the genes upregulated are involved in either sensing or conferring resistance to CAMPs. However, a recent study has suggested that GraSR may in fact regulate many other genes involved in virulence, stress response and cell wall signal transduction (Falord et al., 2011). As a result of this study we hypothesized that certain phenotypes were previously overlooked. Hence the aim of this study was to investigate these newly identified characteristics of GraSR *in vivo*.

To investigate the GraSR system *in vivo*, we chose to work with an *S. aureus* Δ*graR* mutant. Although this mutant has an intact *graS* gene, the lack of the transcription factor *graR* renders this system inactive due to the inability to regulate gene expression. As was observed in section 3.3.3, the Δ*graR* mutant had growth defects, where stationary phase was reached quicker than 6390 wild type. Furthermore, all pMK4-P_{native}:*graR* constructs tested in section 3.3.3 could restore growth to wild type levels. This observation promoted us to investigate the GraS-mediated phosphorylation site, Asp51, within GraR.

Although no *in vitro* studies confirmed phosphotransfer, through *in vivo* studies the site on GraR that undergoes phosphorylation by GraS has been suggested to play an important role (Falord et al., 2012). Interestingly, the Δ*graR* strain complemented with ectopically expressed mutant GraR-D51N could not restore cellular growth to wild type levels, whereas the ectopically expressed GraR-WT could. This observation is strong evidence that the GraSR system is involved in cellular growth and the D51 site is important for proper function. It should be noted that growth defects were based on optical densities and it was determined that a lower optical density does indeed correlate with a lower viable cell count.

The *dlt* operon consists of four genes, but it is sufficient to inactive *dltA* gene, the ligase, in order to sufficiently decrease $_{D}$-alanylation of teichoic acids. It is suggested that Δ*graR* growth defect may be the result of decreased alanylation of teichoic acids. The *S. aureus* Δ*dltA* mutant was used as a control and had similar phenotype as Δ*graR*. This observation corroborates the study by Tabuchi et al., 2010, which also observed similar

defects in the Δ*dltA* strain. Taken together these results indicate that GraSR system is involved in proper cell growth, but further research would be required to determine if Δ*graR* defects are due to lowered *dltA* expression. Lowered $_{D}$-alanylation of WTA has been shown to increase magnesium ion binding to cell wall (Lambert et al., 1975). Although lucrative to speculate high concentrations of magnesium could explain Δ*graR* defects it is unlikely as high magnesium concentrations have been shown to have a positive effect on cellular growth (Bhat et al., 1994).

The morphology of Δ*graR* mutant was examined by thin-section transmission electron microscopy. Arguably the most important discovery of this study was that a subpopulation of Δ*graR* mutant cells contained aberrantly positioned septa. It is extremely uncommon for a cell that has initiated division to begin a second division plane parallel to an already initiated septum. Examination of thousands of *S. aureus* 6390 wild type cells did not reveal even one cell with this phenotype.

In nearly all prokaryotes, cell division is initiated with the polymerization of the tubulin-like protein FtsZ that forms the Z-ring at midcell (Adams and Errington, 2009). The Z-ring serves as a scaffold for the recruitment of cellular components required for cell division, collectively this is called the divisome, which is responsible for synthesis of new cell wall (Errington et al., 2003). This process is tightly regulated and can only occur after chromosome segregation in order to avoid bisection of the genomic content by the division apparatus. It has been demonstrated that the *S. aureus* nucleoid occlusion effector, Noc, determines the placement of the FtsZ ring (Veiga et al., 2011). It is unclear

what regions of DNA the Noc protein recognizes and binds, but it is suggested correct septum positioning heavily depends on this protein (Wu and Errington, 2012).

It is not apparently obvious what causes the dual septa formation in the Δ*graR* strain, as the *noc* gene was not identified to be under the control of the GraSR system (Cui et al., 2005; Falord et al., 2011). Furthermore it is not even clear if *noc* deficiency gives rise to such a phenotype, but it is a likely candidate. The dual septum phenotype has been previously identified in an *S. aureus* Δ*msrR* mutant, but the authors did not give a plausible explanation for this phenomenon (Hubscher et al., 2009). The msrR protein belongs to the LytR-CpsA-Psr (LCP) family of membrane proteins that have been implicated to play an important role in cell separation, autolysis, cell surface modification and virulence (Hubscher et al., 2008; Over et al., 2011). It is interesting that the *msrR* gene is one gene away from *mprF*, a gene that has been well established to be regulated by the GraSR system (Li et al., 2007). No GraR consensus binding sequence was found upstream of *msrR* (Falord et al., 2011), thus it remains to be determined whether GraSR can directly or indirectly regulate expression of this gene. It is also unclear if dual septa formation in Δ*graR* and Δ*msrR* is related or deficiencies in two unrelated mechanisms just happen to give rise to the same phenotype.

The similarities between Δ*graR* and Δ*msrR* strains prompted us to investigate other phenotypes. It was shown that an *S. aureus* ΔmsrR mutant strain is more sensitive towards Congo Red dye (Hubscher et al., 2009). Our data indicate that Δ*graR* is also sensitive towards Congo Red at concentrations > 400 μg/mL. Unexpectedly the Δ*graR*

strain complemented with ectopically expressed GraR-WT could not restore resistance to wild type levels. It is proposed that complemented cells may have lost the plasmid, as the plates contained no antibiotic for plasmid selection. We also cannot rule out the possibility that another mutation besides Δ*graR* exists within the *S. aureus* strain causing sensitivity towards Congo Red. This was the only instance in which the complemented strain was unable to restore a phenotype to wild type levels.

Congo Red mode of action towards *S. aureus* is unknown, but it was recently shown that cells lacking WTA, due to mutations in *tarO* gene, become extremely sensitive towards the dye (Suzuki et al., 2012). The authors concluded that WTA confers protection against Congo Red and other dyes of related structure. We sought to investigate whether decoration of WTA backbone is responsible for sensitizing cells towards Congo Red. Given that GraSR controls the *dlt* operon, and *dltA* is involved in $_{D}$-alanylation of teichoic acids (increased net positive surface charge), we hypothesized that charge could play a role in sensitizing Δ*graR* towards Congo Red. However, it was observed that *S. aureus* Δ*dltA* is comparable to wild type and is not sensitive towards Congo Red. Our data also corroborates that *S. aureus* ΔtarO mutant strain is very sensitive towards Congo Red. Taken together, we conclude that lack of *dltA*, which produces an overall negative charge on teichoic acid, does not sensitize *S. aureus* towards Congo Red. Thus Δ*graR* sensitivity towards Congo Red is not due to altered surface charge as a result of lowered *dltA* expression.

In addition to $_{D}$-alanylation, wall teichoic acids are also decorated with α- and β-

GlcNAc (Swoboda et al., 2010; Xia et al., 2010a). We hypothesized that sensitivity toward Congo Red could in part be due to sugar modifications within Δ*graR* WTAs. Our studies indicate that there are significant differences between Δ*graR* and wild type WTAs. PAGE analysis reveled that Δ*graR* WTA migrates faster than wild type WTA. It is proposed that Δ*graR* WTA contains less sugar modifications and thus migrates faster. This has previously been observed in an *S. aureus* mutant, K6, which completely lacks both α- and β- GlcNAc (Xia et al., 2010b). One could argue that Δ*graR* migrates faster as a result of charge differences, but we have isolated WTA by NaOH and TCA method and observed similar migration patterns. In the NaOH method the $_{D}$-alanine esters get hydrolyzed whereas in the TCA method they remain attached. Another possibility that cannot be excluded is that Δ*graR* WTA backbone is comprised of fewer polymer units, resulting in shorter WTA. The lack of higher molecular weight polymers in Δ*graR* WTA would give the impression of faster migration.

Closer examination of the Δ*graSR* transcriptome revealed that *tarM*, the gene that attaches α-GlcNAc units to WTA, is down regulated (Falord et al., 2011). Furthermore the authors identified *tarM* operon as one of 26 potential GraSR regulon members based on a highly conserved ten base pair palindromic sequence. Unfortunately the authors could not confirm DNA-binding *in vitro* because they were unable to get an active form of GraR. Although we did not test GraR binding to the *tarM* operon, based on NMR analysis of WTA it is suggested that indeed Δ*graR* contains alterations in WTA content. It is yet to be determined if these differences are indeed alterations in α- and/or β-

GlcNAc content within WTA.

In conclusion, the aim of this study was to uncover novel phenotypes of the GraSR system through *in vivo* investigations of an *S. aureus* Δ*graR* mutant strain. It is suggested that previous studies, primarily focusing on CAMP resistance, have overlooked other importance regulatory roles of the GraSR system. It was shown that 424 genes were differentially expressed in the Δ*graSR* mutant compared to wild type (Falord et al., 2011). Our studies, together with Falord et al., suggest a more global role for GraSR. In this study we have discovered defects in cellular growth and division, sensitivity towards Congo Red and alterations in WTA. This global regulation is substantiated by the large regulon size of the GraSR system. Thoroughly understanding TCSs such as GraSR allows us to develop targeted, small-molecule therapeutics to exploit these systems.

References

Adams, D.W., and Errington, J. (2009). Bacterial cell division: assembly, maintenance and disassembly of the Z ring. Nat Rev Microbiol *7*, 642-653.

Bhat, K.G., Joseph, K.M., and Shivananda, P.G. (1994). Effect of magnesium on the physiology of Staphylococcus aureus. Indian J Exp Biol *32*, 274-276.

Capra, E.J., and Laub, M.T. (2012). Evolution of two-component signal transduction systems. Annu Rev Microbiol *66*, 325-347.

Chang, C., and Stewart, R.C. (1998). The two-component system. Regulation of diverse signaling pathways in prokaryotes and eukaryotes. Plant Physiol *117*, 723-731.

Collins, L.V., Kristian, S.A., Weidenmaier, C., Faigle, M., Van Kessel, K.P., Van Strijp, J.A., Gotz, F., Neumeister, B., and Peschel, A. (2002). Staphylococcus aureus strains lacking D-alanine modifications of teichoic acids are highly susceptible to human neutrophil killing and are virulence attenuated in mice. J Infect Dis *186*, 214-219.

Cozzone, A.J. (1988). Protein phosphorylation in prokaryotes. Annu Rev Microbiol *42*, 97-125.

Cui, L., Lian, J.Q., Neoh, H.M., Reyes, E., and Hiramatsu, K. (2005). DNA microarray-based identification of genes associated with glycopeptide resistance in Staphylococcus aureus. Antimicrob Agents Chemother *49*, 3404-3413.

Errington, J., Daniel, R.A., and Scheffers, D.J. (2003). Cytokinesis in bacteria. Microbiol Mol Biol Rev *67*, 52-65, table of contents.

Falord, M., Karimova, G., Hiron, A., and Msadek, T. (2012). GraXSR proteins interact with the VraFG ABC transporter to form a five-component system required for cationic antimicrobial peptide sensing and resistance in Staphylococcus aureus. Antimicrob Agents Chemother *56*, 1047-1058.

Falord, M., Mader, U., Hiron, A., Debarbouille, M., and Msadek, T. (2011). Investigation of the Staphylococcus aureus GraSR regulon reveals novel links to virulence, stress response and cell wall signal transduction pathways. PLoS One *6*, e21323.

Hedges, A.J., Shannon, R., and Hobbs, R.P. (1978). Comparison of the precision obtained in counting viable bacteria by the spiral plate maker, the droplette and the Miles & Misra methods. J Appl Bacteriol *45*, 57-65.

Herbert, S., Bera, A., Nerz, C., Kraus, D., Peschel, A., Goerke, C., Meehl, M., Cheung, A., and Gotz, F. (2007). Molecular basis of resistance to muramidase and cationic antimicrobial peptide activity of lysozyme in staphylococci. PLoS Pathog *3*, e102.

Hubscher, J., Luthy, L., Berger-Bachi, B., and Stutzmann Meier, P. (2008). Phylogenetic distribution and membrane topology of the LytR-CpsA-Psr protein family. BMC Genomics *9*, 617.

Hubscher, J., McCallum, N., Sifri, C.D., Majcherczyk, P.A., Entenza, J.M., Heusser, R., Berger-Bachi, B., and Stutzmann Meier, P. (2009). MsrR contributes to cell surface characteristics and virulence in Staphylococcus aureus. FEMS Microbiol Lett *295*, 251-260.

Ito, T., Katayama, Y., and Hiramatsu, K. (1999). Cloning and nucleotide sequence determination of the entire mec DNA of pre-methicillin-resistant Staphylococcus aureus N315. Antimicrob Agents Chemother *43*, 1449-1458.

Kuroda, M., Kuroda, H., Oshima, T., Takeuchi, F., Mori, H., and Hiramatsu, K. (2004). Two-component system VraSR positively modulates the regulation of cell-wall biosynthesis pathway in Staphylococcus aureus. Molecular Microbiology *49*, 807-821.

Kuroda, M., Ohta, T., Uchiyama, I., Baba, T., Yuzawa, H., Kobayashi, I., Cui, L., Oguchi, A., Aoki, K.-i., Nagai, Y., *et al.* (2001). Whole genome sequencing of meticillin-resistant Staphylococcus aureus. The Lancet *357*, 1225-1240.

Lambert, P.A., Hancock, I.C., and Baddiley, J. (1975). Influence of alanyl ester residues on the binding of magnesium ions to teichoic acids. Biochem J *151*, 671-676.

Laub, M.T., and Goulian, M. (2007). Specificity in two-component signal transduction pathways. Annu Rev Genet *41*, 121-145.

Li, M., Cha, D.J., Lai, Y., Villaruz, A.E., Sturdevant, D.E., and Otto, M. (2007). The antimicrobial peptide-sensing system aps of Staphylococcus aureus. Mol Microbiol *66*, 1136-1147.

Meehl, M., Herbert, S., Gotz, F., and Cheung, A. (2007). Interaction of the GraRS two-component system with the VraFG ABC transporter to support vancomycin-intermediate resistance in Staphylococcus aureus. Antimicrob Agents Chemother *51*, 2679-2689.

Meredith, T.C., Swoboda, J.G., and Walker, S. (2008). Late-stage polyribitol phosphate wall teichoic acid biosynthesis in Staphylococcus aureus. J Bacteriol *190*, 3046-3056.

Nixon, B.T., Ronson, C.W., and Ausubel, F.M. (1986). Two-component regulatory systems responsive to environmental stimuli share strongly conserved domains with the nitrogen assimilation regulatory genes ntrB and ntrC. Proc Natl Acad Sci U S A *83*, 7850-7854.

Over, B., Heusser, R., McCallum, N., Schulthess, B., Kupferschmied, P., Gaiani, J.M., Sifri, C.D., Berger-Bachi, B., and Stutzmann Meier, P. (2011). LytR-CpsA-Psr proteins in Staphylococcus aureus display partial functional redundancy and the deletion of all three severely impairs septum placement and cell separation. FEMS Microbiol Lett *320*, 142-151.

Peschel, A., Otto, M., Jack, R.W., Kalbacher, H., Jung, G., and Gotz, F. (1999). Inactivation of the dlt operon in Staphylococcus aureus confers sensitivity to defensins, protegrins, and other antimicrobial peptides. J Biol Chem *274*, 8405-8410.

Sahl, H.G., Pag, U., Bonness, S., Wagner, S., Antcheva, N., and Tossi, A. (2005). Mammalian defensins: structures and mechanism of antibiotic activity. J Leukoc Biol *77*, 466-475.

Stauff, D.L., Torres, V.J., and Skaar, E.P. (2007). Signaling and DNA-binding activities of the Staphylococcus aureus HssR-HssS two-component system required for heme sensing. J Biol Chem *282*, 26111-26121.

Stock, A.M., Robinson, V.L., and Goudreau, P.N. (2000). Two-component signal transduction. Annu Rev Biochem *69*, 183-215.

Suzuki, T., Campbell, J., Kim, Y., Swoboda, J.G., Mylonakis, E., Walker, S., and Gilmore, M.S. (2012). Wall teichoic acid protects Staphylococcus aureus from inhibition by Congo red and other dyes. J Antimicrob Chemother *67*, 2143-2151.

Swoboda, J.G., Campbell, J., Meredith, T.C., and Walker, S. (2010). Wall teichoic acid function, biosynthesis, and inhibition. Chembiochem *11*, 35-45.

Tabuchi, Y., Shiratsuchi, A., Kurokawa, K., Gong, J.H., Sekimizu, K., Lee, B.L., and Nakanishi, Y. (2010). Inhibitory role for D-alanylation of wall teichoic acid in activation of insect Toll pathway by peptidoglycan of Staphylococcus aureus. J Immunol *185*, 2424-2431.

Turner, R.D., Ratcliffe, E.C., Wheeler, R., Golestanian, R., Hobbs, J.K., and Foster, S.J. (2010). Peptidoglycan architecture can specify division planes in Staphylococcus aureus. Nat Commun *1*, 26.

Veiga, H., Jorge, A.M., and Pinho, M.G. (2011). Absence of nucleoid occlusion effector Noc impairs formation of orthogonal FtsZ rings during Staphylococcus aureus cell division. Mol Microbiol *80*, 1366-1380.

Wu, L.J., and Errington, J. (2012). Nucleoid occlusion and bacterial cell division. Nat Rev Microbiol *10*, 8-12.

Xia, G., Kohler, T., and Peschel, A. (2010a). The wall teichoic acid and lipoteichoic acid polymers of Staphylococcus aureus. Int J Med Microbiol *300*, 148-154.

Xia, G., Maier, L., Sanchez-Carballo, P., Li, M., Otto, M., Holst, O., and Peschel, A. (2010b). Glycosylation of wall teichoic acid in Staphylococcus aureus by TarM. J Biol Chem *285*, 13405-13415.

Yin, S., Daum, R.S., and Boyle-Vavra, S. (2006). VraSR two-component regulatory system and its role in induction of pbp2 and vraSR expression by cell wall antimicrobials in Staphylococcus aureus. Antimicrob Agents Chemother *50*, 336-343.

CHAPTER FIVE

SUMMARY AND FUTURE DIRECTION

5.1 Summary

The goal of this study, primarily chapters 2 and 3, was to expand our knowledge on *S. aureus* Ser/Thr kinase, Stk1, and phosphatase, Stp1. Since their discovery a number of research groups have aimed to address the importance of these proteins, both through *in vitro* and *in vivo* studies. Several substrates were identified as phosphorylation targets of Stk1 *in vitro.* It has also been observed that Stk1/Stp1 knockout strains give rise to pleiotropic phenotypes. However, these phenotypes cannot be explained solely through the regulation of the identified substrates. This observation led us to postulate that other substrates exist.

We have successfully cloned, expressed and purified His-Stk1/Stp1 and through kinase assays demonstrated their enzymatic activity. Through *in vitro* kinase assays it was shown that His-Stk1 undergoes phosphorylation in a time dependent manner. Following phosphorylation His-Stk1 can remain phosphorylated for a prolonged period of time, or until Stp1 is added which can completely dephosphorylates His-Stk1. Analysis of Δ*graR* and Δ*Stk1* transcriptomes revealed that a number of genes are similarly regulated, which prompted us to investigate whether His-Stk1 can phosphorylate the response regulator GraR. It was shown that His-Stk1 could specifically phosphorylate GraR in a time-

dependent manner and Stp1 could dephosphorylate GraR.

To increase our confidence that His-Stk1 phosphorylation of GraR was specific we examined other transcription factors, either from same or different family as GraR. Our data suggest that BceR, a homolog of GraR which shares 56% sequence similarity, is unable to undergo phosphorylation by His-Stk1. Furthermore VraR and WalR, which share much less sequence similarity, also do not undergo phosphorylation by His-Stk1. The GraR protein is composed of two unique domains, and it was demonstrated that phosphorylation was exclusive to the C-terminal domain. The N-terminal domain did not undergo phosphorylation by His-Stk1. Mass spectrometry analysis of His-Stk1-phosphorylated C-terminal domain revealed that phosphorylation occurs on three threonine residues: Thr128, 130 and 149. We further collaborated with Dr. Siu's research group (Centre for Research in Mass Spectrometry, York University) and analyzed full length GraR. This group corroborated the putative phosphorylation sites and excluded any phosphorylation within the N-terminal domain.

Following identification of the phosphorylated sites, we created GraR mutant proteins. Through site-directed mutagenesis we generated three single mutants, where a threonine 128, 130 or 149 was mutated to an alanine. Following expression and purification these mutants were assessed for their ability to undergo phosphorylation by His-Stk1. Indeed all GraR mutants could undergo phosphorylation to similar levels as GraR wild type. We created a triple mutant harboring mutations in all three threonine sites simultaneously, but following generation of this mutant it was observed that the

protein becomes insoluble. We were unable to purify a structurally stable triple mutant of GraR. Lastly we attempted to employ a number of strategies to quantify the amount of phosphorylation. However, it was determined that phosphorylation was below the detectable range of the assay employed.

In chapter 3 we focused on translating our *in vitro* discovery that His-Stk1 phosphorylates GraR through *in vivo* studies. We first constructed a pMK4 plasmid that in *S. aureus* could ectopically express GraR wild type (cloned downstream of its native promoter). In addition, through site-directed mutagenesis we generated pMK4 variants of GraR that contained double mutations of the above-mentioned phosphorylation sites (T128A/T130A, T128A/T149A and T130A/T149A). We then introduced these vectors into *S. aureus* Δ*graR* (*graR* knockout strain) and assessed complementation towards vancomycin resistance and cell growth. It was observed that ectopically expressed GraR wild type and mutant proteins could revert cell growth and vancomycin resistance back to wild type levels (as compared to *S. aureus* 6390, this is the background strain from which Δ*graR* was generated).

Although in chapter 4 we focused on GraR, it was in an unrelated manner as chapters 2 and 3 and did not pertain to Stk1. We have noticed a gap in the field where GraR, and thus the GraSR system, has constantly been studied from the point of antimicrobial peptide resistance. Our goal was to investigate whether GraR was involved in other pathways that may have been overlooked. We examined *in vivo* the *S. aureus* Δ*graR* strain and discovered novel phenotypes that have not been previously reported. To

confirm GraR involvement, we complemented the Δ*graR* strain with a pMK4 ectopically expressing either a wild type or a mutant copy of GraR. The mutant copy was generated though site-directed mutagenesis, where the GraS-mediated phosphorylation site on GraR, aspartic acid residue 51, was mutated to asparagine; thus restricting the protein from receiving phosphorylation signals from GraS.

It was observed that Δ*graR*, under non-stressed conditions, reached stationary phase earlier as compared to the 6390 wild type strain. Furthermore it was observed that upon reaching stationary phase the Δ*graR* strain yielded three times less cells as compared to the wild type. This is an indication that absence of the *graR* gene leads to abnormal cell growth. Upon complementing the Δ*graR* strain with ectopically expressed GraR-WT cell growth was restored. However, when complementing with GraR-D51N cell growth remained abnormal. Thus ectopically expressed mutant GraR-D51N is not enough to revert the phenotype back to normal, it is also dependent on the aspartic acid residue at position 51.

The highlight of this thesis was the observation that Δ*graR* contains a subpopulation of cells that form dual septa. This morphological defect supports the notion that *graR* is involved in cell growth. It was also observed that Δ*graR* became more sensitive towards Congo Red dye. However, through complementation we were unable to revert resistance back to wild type levels. It was observed that Δ*dltA* was not sensitive towards Congo Red. Lastly, isolation of Δ*graR* wall teichoic acids revealed significant changes in composition. Analysis of wall teichoic acid by gel electrophoresis revealed

that Δ*graR* wall teichoic acid migrated faster than wild type 6390. Nuclear magnetic resonance analysis, in collaboration with Dr. Hunter (The NMR Facility, York University) suggested that Δ*graR* wall teichoic acids have alterations in sugar modifications within their backbone. It should be noted that complementing the Δ*graR* strain with ectopically expressed GraR wild type reverted wall teichoic acid composition back to normal, whereas complementation with GraR-D51N could not.

5.2 Future direction

The observation that His-Stk1 phosphorylates GraR *in vitro* is an interesting one. We have provided solid evidence that this phosphorylation event is specific, but it remains to be determined what the physiological role is. Future work will need to address if this phosphorylation event indeed occurs *in vivo*, which could be accomplished through mass spectrometry analysis of *S. aureus* specifically targeting the peptides containing the phosphorylation sites. Another strategy, if signal from *S. aureus* is below detectable range, is to express both Stk1 and GraR from same plasmid (pETDuet-1) in *E. coli*, and analyze phosphorylation states. As we were unable to show decreased phosphorylation through *in vitro* kinase assays with single mutants, it would be interesting to probe whether His-Stk1 can phosphorylate GraR double mutants that harbor two mutated sites. Given GraR is a transcription factor, future work should also address whether GraR affinity for DNA increases or decreases. However, this may be difficult until the signaling cascade of Stk1-GraR is characterized.

Our work has demonstrated that lack of *graR* gene leads to alterations in cell growth, division and wall teichoic acid maintenance. Future work should focus on the molecular mechanisms that govern these phenotypes. Of particular interest would be the examination of Δ*graR* and why subpopulations of cells form dual septa. Understanding why these cells form dual septa may shed light on the unusual growth patterns of Δ*graR*. It is also unclear whether alterations in wall teichoic acids play a role in cell growth and division. But, it is likely phosphorylation of GraR at aspartic acid 51 is important for proper activity and thus future studies should address DNA-binding of phosphorylated versus non-phosphorylated GraR. A gene that GraR may bind and regulate is *tarM*.

Lastly, Δ*graR* was observed to become more sensitive towards Congo Red but complementation studies were unable to revert resistance to wild type levels. Thus future studies should experiment with other Δ*graR* strains and address whether Congo Red sensitivity is reproducible.

Appendix A

LC-MS/MS of His-Stk1 prepared with Scaffold 3.6.1 and analyzed by liquid chromatography-mass spectrometry (LC-MS/MS) at the Advanced Protein Technology Centre, The Hospital for Sick Children (Toronto, Canada). Figure shows protein of interest, separated on 12.5% SDS-PAGE, belongs to His-Stk1.

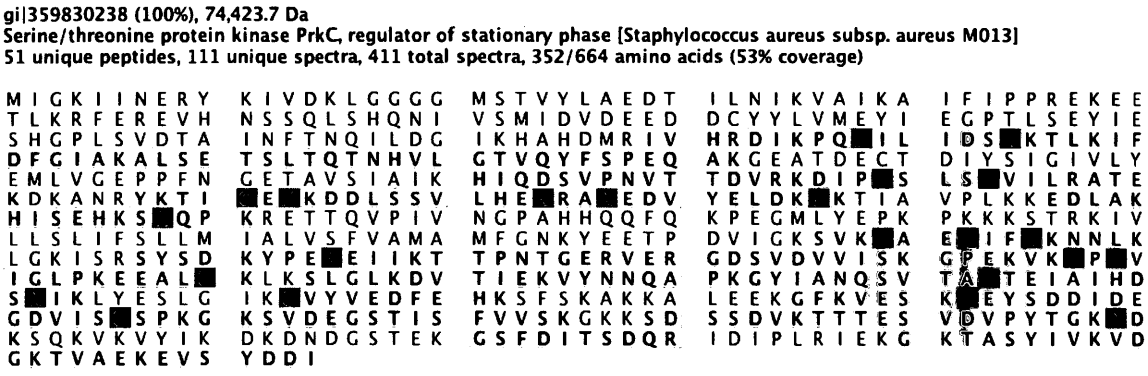

Appendix B

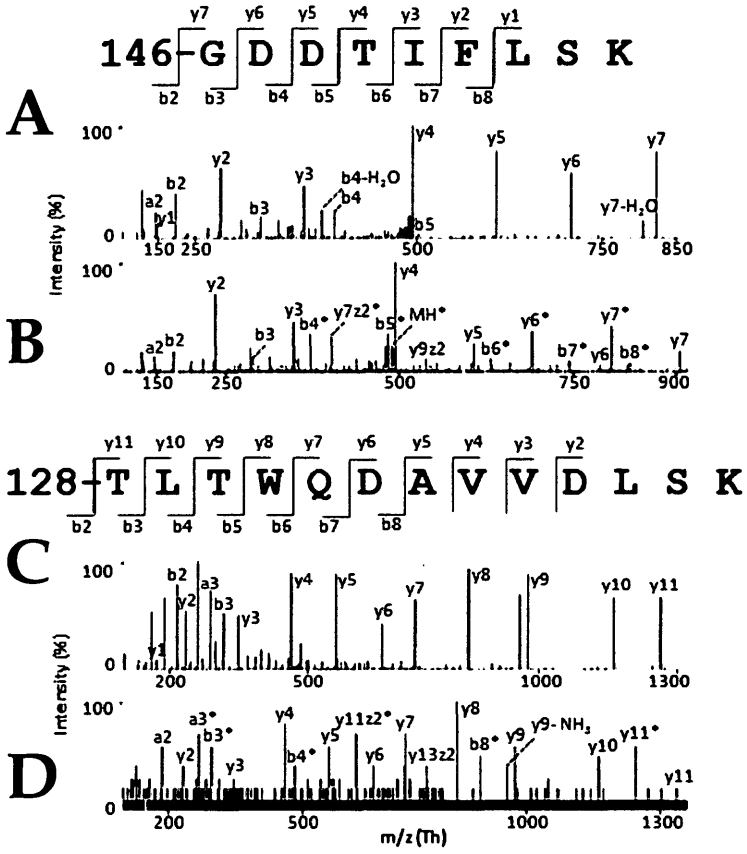

MS/MS spectra of tryptic GraR peptides containing the Stk1 phosphorylation sites

Sequence coverage illustrated by the labeling of fragment ions of each peptide according to Roepstorff–Fohlmann–Biemann nomenclature. (A) The MS/MS spectrum of the peptide 146-GDDTIFLSK-154 from untreated GraR. (B) The MS/MS spectrum of the phosphopeptide 146-GDDtIFLSK-154 from GraR incubated with ATP in the presence of Stk1. (C) The MS/MS spectrum of the peptide 128-TLTWQDAVVDLSK-140 from untreated GraR. (D) The MS/MS spectrum of the phosphopeptide 128-TLtWQDAVVDLSK-140 from GraR incubated with ATP in the presence of Stk1. (lowercase letters in description indicate the phosphoamino acids).

Appendix C

Expression of GraR-triple mutant, all gels resolved by 15% SDS-PAGE

25°C Overnight, 0.5 mM IPTG

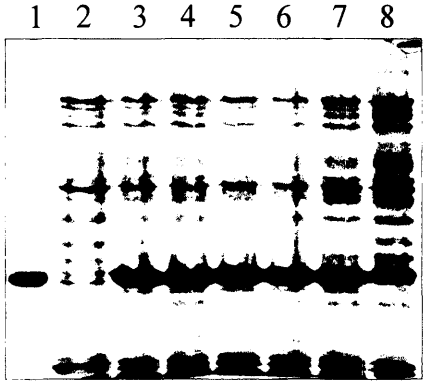

1 – GraR WT
2 – uninduced, 0 hr
3 – colony 1
4 – colony 2
5 – colony 3
6 – colony 4
7 – colony 5
8 – uninduced, overnight

25°C Overnight, 0.5 mM IPTG

Colony 1 2 3 4 5

P S P S P S P S P S

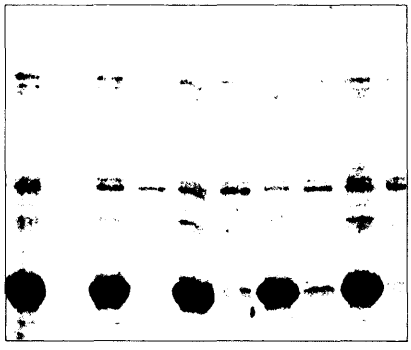

S = supernatant
P = pellet

18°C Overnight, varying IPTG

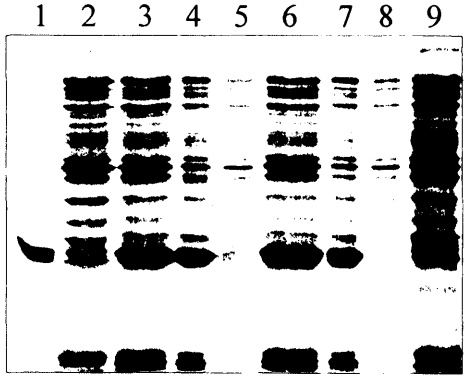

1 – grar WT
2 – uninduced 0 time
3 – 0.1 mM IPTG, total
4 – 0.1 mM IPTG, pellet
5 – 0.1 mM IPTG, supernatant
6 – 0.5 mM IPTG, total
7 – 0.5 mM IPTG, pellet
8 – 0.5 mM IPTG, supernatant
9 – uninduced, 18 hours

Appendix D

Sequencing result for pSTBlue-1 with insert P_{native}:*graR*

Colony F sequenced

gaccacacgtgtggtctagagctagcctaggctcgagaagcttgtcgacgaattcagatgcta*ggatcc*cgctaacaatgaaa
tgaaatttctacatctttgatactaactctacgtataatatgggccataaaaagcctccagtattttgaaatttaaaacatttgctactat
tataatatatatgtaactaaaaggtggagtaatatgttttttggttacagtttaaaggagtattttag**catatg**caaatactactagtag
aagatgacaatactttgtttcaagaattgaaaaaagaattagaacaatgggattttaatgttgctggtattgaagatttcggcaaagta
atggatacatttgaaagttttaatcctgaaattgttatattggatgttcaattacctaaatatgatgggttttattggtgcagaaaaatgag
agaagtttccaacgtaccaatattatttttatcatctcgtgataatccaatggatcaagtgatgagtatggaacttggcgcagatgatt
atatgcaaaaaccgttctataccaatgtattaattgctaaattacaagcgatttatcgtcgtgtctatgagtttacagctgaagaaaaac
gtacattgacttggcaagatgctgtcgttgatctatcaaaagatagtatacaaaaaggtgatcagacgattttcctgtccaaaacaga
aatgattatattagaaattcttattaccaaaaaaaatcaaatcgtttcgagagatacaattatcactgcattatgggatgatgaagcatt
tgttagtgataatacgttaacagtaaatgtgaatcgtttacgaaaaaaattatctgaaattagtatggatagtgcaatcgaaacaaaa
gtaggaaaaggatatatggctcatgaataa*gtcgac*tagcatcacgaattctggatccgatacgtaacgcgtct

Highlighted is the promoter region of the *graXSR* operon (P_{native})

NdeI (catatg) – contains ATG of GraR

In red is the 8325 *graR* gene

**Everything before and after the restriction sites flanking the promoter/gene is part of pSTBlue-1

Appendix E

Sequencing result for pMK4 with insert P_{native}:*graR*

Colony B sequenced

Gcctcttcgctattacgccagctggcgaaaggggatgtgctgcaaggcgattaagttgggtaacgccagggttttcccagtca
cgacgttgtaaaacgacggccagtgaattcccgg**ggatcc**cgctaacattgaaatgaaatttctacatctttgatactaactcta
cgtataatatgggccataaaaagcctccagtatttgaaatttaaaacatttgctactattataatatatatgtaactaaaaggtggagt
aatatgtttttggttacagtttaaaggagtatttagcatatgcaaatactactagtagaagatgacaatactttgtttcaagaattgaaa
aaagaattagaacaatgggattttaatgttgctggtattgaagatttcggcaaagtaatggatacatttgaaagttttaatcctgaaatt
gttatattggatgttcaattacctaaatatgatgggttttattggtgcagaaaaatgagagaagtttccaacgtaccaatattatttttatc
atctcgtgataatccaatggatcaagtgatgagtatggaacttggcgcagatgattatatgcaaaaaccgttctataccaatgtatta
attgctaaattacaagcgatttatcgtcgtgtctatgagtttacagctgaagaaaaacgtacattgacttggcaagatgctgtcgttga
tctatcaaaagatagtatacaaaaaggtgatcagacgattttcctgtccaaaacagaaatgattatattagaaattcttattaccaaaa
aaaatcaaatcgtttcgagagatacaattatcactgcattatgggatgatgaagcatttgttagtgataatacgttaacagtaaatgtg
aatcgtttacgaaaaaaattatctgaaattagtatggatagtgcaatcgaaacaaaagtaggaaaaggatatatggctcatgaataa
gtcgacctgcagccaagcttggcgtaatcatggtcatagctgtttcctgtgtgaaattgttatccgctcacaattccacacaacat
acgagcc

Highlighted is the promoter region of the *graXSR* operon (P_{native})

NdeI (catatg) – contains ATG of GraR

In red is the 8325 *graR* gene

**Everything before and after the restriction sites flanking the promoter/gene is part of pMK4

Appendix F

Raw data from vancomycin MIC experiment. The darker the box the higher the OD_{600}.

Vancomycin µg/mL	0	0.25	0.5	1	2	4
6390					0.052	0.051
Δ*graR*				0.051	0.05	0.05
Δ*graR*+pMK4:*graR*-WT					0.051	0.051
Δ*graR*+pMK4:*graR*-T128A/T130A					0.051	0.05
Δ*graR*+pMK4:*graR*-T128A/T149A					0.05	0.051
Δ*graR*+pMK4:*graR*-T130A/T149A					0.052	0.052
Δ*graR*+pMK4:*graR*-TRIPLE				0.421	0.052	0.051

Appendix G

PCR confirmation that Δ*graR* strain contains the *msrR* gene. Size of *msrR* product expected to be 738 bp. Truncated protein primers used. Cells used directly for PCR, thus variation in cell number could account for band intensity.

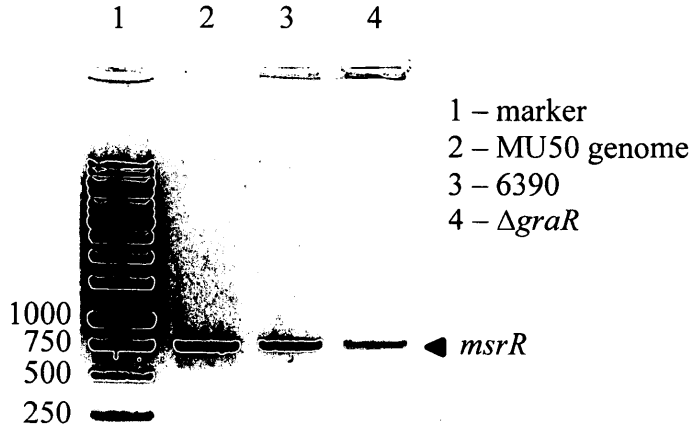

Appendix H

Congo Red susceptibility of Δ*tarO*. Δ*tarO* MIC towards Congo Red is 4μg/mL. At 10 μg/mL of Congo Red growth is observed only at 10^6 cells, likely because cells are growing on top of each other. Experiment showcases the sensitivity of the experiment.

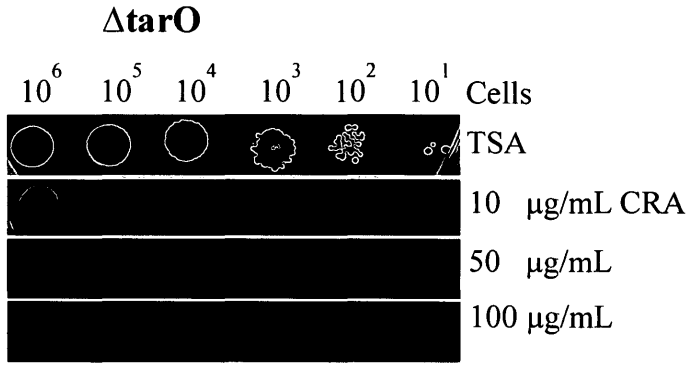

Appendix I

NMR 2D-HSQC of TCA-extracted WTA from 6390 and Δ*graR*

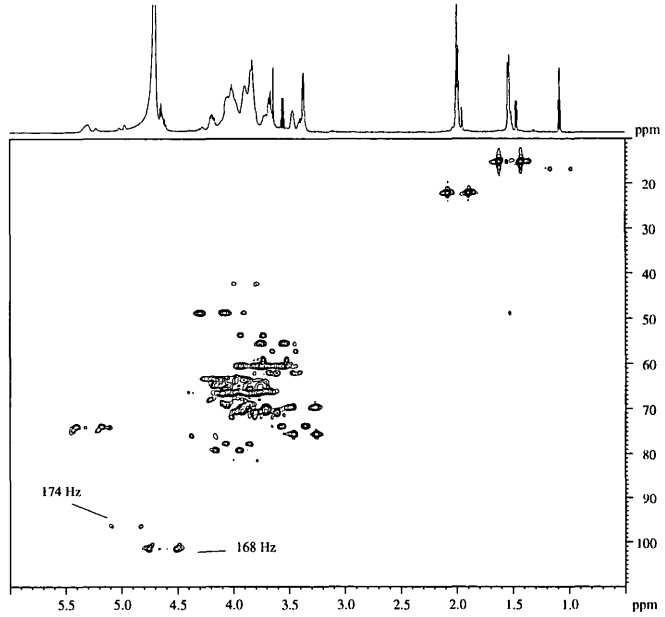

6390
(wild-type)

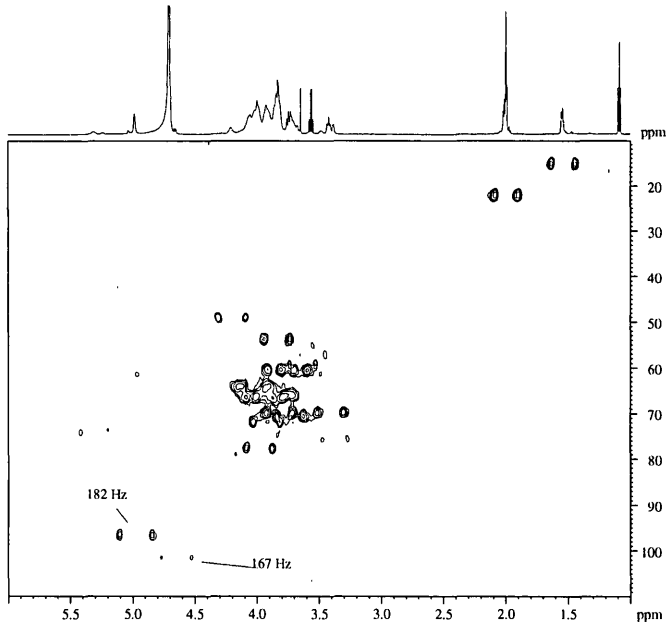

Δ*graR*

Appendix J

NMR 2D-HSQC of TCA-extracted WTA from Δ*graR* complemented with pMK4-GraR-WT or D51N

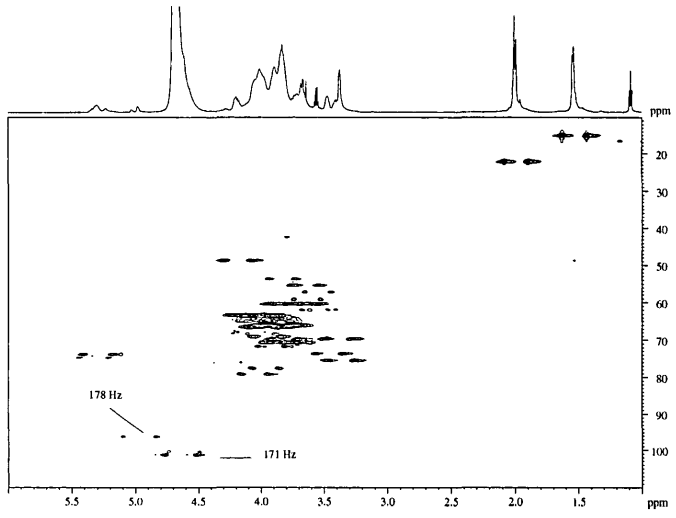

Δ*graR* pMK4-WT

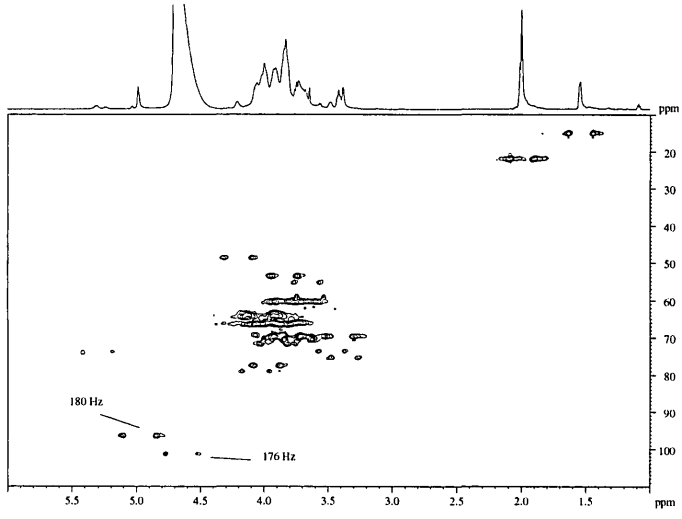

Δ*graR* pMK4-D51N